
**Title 40 CFR Part 191
Subparts B and C
Compliance Recertification
Application
for the
Waste Isolation Pilot Plant**

**Appendix MASS-2009
Performance Assessment
Modeling Assumptions**



**United States Department of Energy
Waste Isolation Pilot Plant**

**Carlsbad Field Office
Carlsbad, New Mexico**

**Appendix MASS-2009
Performance Assessment
Modeling Assumptions**

Table of Contents

MASS-1.0 Introduction..... MASS-1

MASS-2.0 Summary of Changes in Performance Assessment MASS-2

 MASS-2.1 FEPs Assessment MASS-3

 MASS-2.2 Monitoring MASS-3

 MASS-2.3 Experimental Activities MASS-4

 MASS-2.3.1 Magnesium Oxide Investigations MASS-4

 MASS-2.3.2 Actinide Investigations MASS-4

 MASS-2.4 Performance Assessment Models and Systems MASS-4

 MASS-2.5 PABC MASS-5

 MASS-2.5.1 Conceptual Model Changes MASS-5

 MASS-2.5.2 Recalculation of Culebra T Fields MASS-7

 MASS-2.5.3 Waste Inventory Update MASS-8

 MASS-2.6 CRA-2009 Changes MASS-8

 MASS-2.7 Operational Considerations MASS-8

MASS-3.0 General Assumptions in PA Models..... MASS-10

 MASS-3.1 Darcy’s Law Applied to Fluid Flow Calculated by BRAGFLO,
 MODFLOW-2000, and DRSPALL MASS-10

 MASS-3.2 Hydrogen Gas as Surrogate for Waste-Generated Gas Physical
 Properties in BRAGFLO and DRSPALL MASS-33

 MASS-3.3 Salado Brine as Surrogate for Liquid-Phase Physical Properties in
 BRAGFLO MASS-36

MASS-4.0 Model Geometries MASS-37

 MASS-4.1 Disposal System Geometry as Modeled in BRAGFLO MASS-37

 MASS-4.2 Change to Disposal System Geometry since the CCA MASS-37

 MASS-4.2.1 CCA to CRA-2004 Baseline Grid Changes..... MASS-39

 MASS-4.2.2 CRA-2004 Simplified Shaft Seal Model MASS-39

 MASS-4.2.3 CRA-2004 Implementation of Option D-Type Panel Closure . MASS-40

 MASS-4.2.4 Increased Segmentation of Waste Regions in Grid MASS-42

 MASS-4.2.5 CRA-2004 Redefined and Simplified Grid Flaring Method.... MASS-43

 MASS-4.2.6 CRA-2004 Refinement of the X-Spacing Outside the
 Repository MASS-43

 MASS-4.2.7 CRA-2004 Refinement of the Y-Spacing MASS-44

MASS-5.0 BRAGFLO Geometry of the Repository MASS-45

 MASS-5.1 Historical Context of the Repository Model MASS-45

 MASS-5.2 CRA-2009 Repository Model MASS-46

MASS-6.0 Creep Closure MASS-47

MASS-7.0 Repository Fluid Flow MASS-48

 MASS-7.1 Flow Interactions with the Creep Closure Model MASS-50

 MASS-7.2 Flow Interactions with the Gas Generation Model MASS-51

MASS-7.3 CRA-2009 Flow Interactions with the Gas-Generation Model Changes.....	MASS-51
MASS-8.0 Gas Generation	MASS-53
MASS-8.1 Historical Context of Gas Generation Modeling.....	MASS-53
MASS-9.0 Chemical Conditions	MASS-54
MASS-10.0 Dissolved Actinide Source Term.....	MASS-55
MASS-11.0 Colloidal Actinide Source Term.....	MASS-56
MASS-12.0 Shafts and Shaft Seals.....	MASS-57
MASS-13.0 Salado	MASS-58
MASS-13.1 High Threshold Pressure for Halite-Rich Salado Rock Units	MASS-59
MASS-13.2 Historical Context of the Salado Conceptual Model	MASS-60
MASS-13.3 The Fracture Model	MASS-60
MASS-13.4 Flow in the DRZ	MASS-61
MASS-13.5 Actinide Transport in the Salado	MASS-62
MASS-14.0 Geologic Units above the Salado.....	MASS-65
MASS-14.1 Historical Context of the Units above the Salado Model	MASS-66
MASS-14.2 Groundwater-Basin Conceptual Model	MASS-66
MASS-15.0 Flow Through the Culebra.....	MASS-67
MASS-15.1 Historical Context of the Culebra Model.....	MASS-67
MASS-15.2 Dissolved Actinide Transport and Retardation in the Culebra	MASS-67
MASS-15.3 Colloidal Actinide Transport and Retardation in the Culebra	MASS-68
MASS-15.4 Subsidence Caused by Potash Mining in the Culebra	MASS-68
MASS-16.0 Intrusion Borehole	MASS-69
MASS-16.1 Cuttings, Cavings, and Spallings Releases during Drilling.....	MASS-69
MASS-16.1.1 Historical Context of Cuttings, Cavings, and Spallings Models	MASS-70
MASS-16.1.2 Waste Mechanistic Properties.....	MASS-70
MASS-16.1.3 Mechanistic Model for Spall.....	MASS-71
MASS-16.1.4 Calculation of Cuttings, Cavings, and Spall Releases	MASS-72
MASS-16.2 Direct Brine Releases during Drilling	MASS-73
MASS-16.3 Long-Term Properties of the Abandoned Intrusion Borehole.....	MASS-74
MASS-17.0 Climate Change	MASS-75
MASS-18.0 Castile Brine Reservoir.....	MASS-76
MASS-18.1 Historical Context of the Castile Brine Reservoir Model.....	MASS-77
MASS-19.0 Option D Panel Closure	MASS-78

MASS-20.0 Summary of Clay Seam G Modeling Assumptions..... MASS-80

MASS-21.0 Evaluation of Waste Structural Impacts, Emplacement and Homogeneity.. MASS-81

MASS-22.0 References..... MASS-84

List of Figures

Figure MASS-1. Gas Viscosity as a Function of Mole Fraction H₂ at 7 MPa and 15 MPa Pressure MASS-35

Figure MASS-2. Gas Compressibility as a Function of Mole Fraction H₂ MASS-36

Figure MASS-3. Logical Grid Used for the CRA-2004 and 2009 PA BRAGFLO Calculations..... MASS-38

Figure MASS-4. Logical Grid Used for the CCA PA BRAGFLO Calculations MASS-40

Figure MASS-5. Comparison of the Simplified Shaft (CRA-2004 and CRA-2009) and the Detailed Shaft (CCA) Models MASS-41

Figure MASS-6. Logical Grid Representation of the Option D Panel Closures for the CRA MASS-42

Figure MASS-7. Schematic Comparison of the Representation of Panel Closures in the CCA PAVT and CRA-2004..... MASS-43

Figure MASS-8. Repository-Scale Horizontal BRAGFLO Mesh Used for DBR Calculations..... MASS-74

List of Tables

Table MASS-1. CRA-2009 PA Codes MASS-6

Table MASS-2. CRA-2009 PA Hardware..... MASS-6

Table MASS-3. Changes Incorporated in the CRA-2004 PABC MASS-7

Table MASS-4. Changes Incorporated in the CRA-2009 MASS-9

Table MASS-5. General Modeling Assumptions MASS-11

This page intentionally left blank.

Acronyms and Abbreviations

An	actinide
CCA	Compliance Certification Application
CCDF	complementary cumulative distribution function
CH-TRU	contact-handled transuranic
cm	centimeters
CPR	cellulosic, plastic, and rubber
CRA	Compliance Recertification Application
DBR	direct brine release
DOE	U.S. Department of Energy
DRZ	disturbed rock zone
EPA	U.S. Environmental Protection Agency
FEIS	Final Environmental Impact Statement
FEP	feature, event, and process
ft	foot
gal	gallon
in.	inch
INL	Idaho National Laboratory
km	kilometer
LHS	Latin hypercube sample
m	meter
MB	marker bed
MPa	megapascals
NIST	National Institute of Standards and Technology
OS	operating system
PA	performance assessment
PABC	Performance Assessment Baseline Calculation
PAVT	Performance Assessment Verification Test
PR	productivity ratio
QA	quality assurance
RH-TRU	remote-handled transuranic
RoR	rest of repository

SMC	Salado Mass Concrete
SNL	Sandia National Laboratories
T field	transmissivity field
TRU	transuranic
WIPP	Waste Isolation Pilot Plant

Elements and Chemical Compounds

CaCO_3	calcite
CH_4	methane
CO_2	carbon dioxide
H_2	hydrogen
H_2O	water
H_2S	hydrogen sulfide
$\text{Mg}(\text{OH})_2$	brucite, magnesium hydroxide
$\text{Mg}_5(\text{CO}_3)_4(\text{OH})_2 \cdot 4\text{H}_2\text{O}$	hydromagnesite
MgO	magnesium oxide

1 **MASS-1.0 Introduction**

2 This appendix presents supplementary information to Appendix PA-2009 regarding the
3 assumptions, simplifications, and approximations used in the models of the second recertification
4 performance assessment (PA) of the Waste Isolation Pilot Plant (WIPP) called the 2009
5 Compliance Recertification Application (CRA-2009) PA. Within this appendix, relevant issues
6 in the formulation or development of the various types of models (for example, conceptual,
7 mathematical, numerical, or computer code) used for the topic under consideration in each
8 section are discussed, and references to relevant historical information are included where
9 appropriate. The CRA-2009 PA is similar to the CRA-2004 PA used in the first recertification
10 of the WIPP. The technical baseline for the first recertification includes the modifications
11 required by the U.S. Environmental Protection Agency (EPA) during their review of the
12 CRA-2004 PA (Cotsworth 2005). These required modifications resulted in a PA called the
13 Performance Assessment Baseline Calculation (PABC), or the CRA-2004 PABC. The
14 CRA-2009 PA is not significantly different than the CRA-2004 PABC. The differences include
15 error corrections, updated parameters, and new software code versions. This appendix
16 references the Compliance Certification Application (CCA) (U.S. Department of Energy 1996)
17 and the CRA-2004 (U.S. Department of Energy 2004) when the information discussed has not
18 changed from past demonstrations of compliance with the EPA's disposal standards. Some of
19 the information important to PA methodology has been repeated from the CRA-2004, Appendix
20 PA, Attachment MASS for completeness.

21 Section MASS-2.0 contains a summary of changes in PA since the CRA-2004. Section MASS-
22 3.0 includes a discussion of general modeling assumptions applicable to the disposal system as a
23 whole, including a table of assumptions made in PA models, with cross-references. The
24 remainder of this appendix discusses assumptions specific to the conceptual models used in the
25 CRA-2009 PA. Historical development of the WIPP conceptual models that led to the PA used
26 in the CCA is documented in the CCA, Appendix MASS, Section MASS-2.0. Historical
27 development of the modeling assumptions for the CRA-2004 PA is documented in the
28 CRA-2004, Appendix PA, Attachment MASS.

1 **MASS-2.0 Summary of Changes in Performance Assessment**

2 Since the CCA, there have been changes to a number of the conceptual models and processes
3 important in assessing the performance of the WIPP. Changes for the first recertification were
4 discussed in the CRA-2004, Chapter 9.0, Section 9.3.1.3, and Appendix PA, Attachment MASS.
5 Other recertification-related, EPA-mandated changes were documented in the CRA-2004 PABC
6 (Leigh et al. 2005). The technical baseline used to demonstrate continued compliance with the
7 EPA's disposal standards was documented in these two documents. Since this time, ongoing
8 confirmatory experiments, monitoring results, and operational practices have generated
9 information relevant to the features, events, and processes (FEPs), modeling assumptions, and
10 conceptual models for PA, and provided additional support to the conceptual basis of PA. The
11 results of these investigations are included in a new PA for this recertification. Appendix
12 MASS-2009 has been updated to include the impacts of these ongoing investigations and results.
13 Included in the CRA-2009 PA are changes that have occurred since the CRA-2004 PA and new
14 information that is important to PA. These changes are

- 15 1. Reassessment of FEPs
- 16 2. Compliance monitoring
- 17 3. Experimental activities
- 18 4. Assessment of model and systems changes and updates
- 19 5. Incorporation of CRA-2004 PABC changes, including
 - 20 A. Parameter changes: solubility parameters; solubility uncertainty ranges; probability of
21 microbial cellulosic, plastic, and rubber (CPR) degradation
 - 22 B. Error corrections
 - 23 C. Inventory updates
 - 24 D. Changes to CPR degradation implementation
 - 25 E. New Culebra transmissivity fields (T fields)
- 26 6. Incorporation of CRA-2009 changes, including
 - 27 A. The parameter representing the maximum flow duration for direct brine releases (DBRs)
 - 28 B. The sampling method applied to the humid and inundated CPR degradation rates
 - 29 C. Additional chemistry parameters
 - 30 D. Capillary pressure and relative permeability models
 - 31 E. Updated drilling rate

1 F. Parameter corrections – emplacement material parameters, halite/disturbed rock zone
2 (DRZ) porosity, and fraction of the repository occupied by waste

3 G. Input file corrections

4 7. Operational considerations

5 A summary of each change is presented in this section. References to appropriate sections of
6 this appendix are provided for those changes that impact modeling assumptions. In addition,
7 references are provided to other sections of the CRA-2009 where implementation of the changes
8 is discussed.

9 **MASS-2.1 FEPs Assessment**

10 In the WIPP PA methodology (see Appendix PA-2009, Section PA-2.3), FEPs are elements used
11 to develop the conceptual models and modeling assumptions represented in PA. The process
12 used to develop and screen FEPs is outlined in Appendix SCR-2009, Section SCR-2.0. The
13 results of the CRA-2004 FEPs screening are documented in the CRA-2004, Appendix PA,
14 Attachment SCR. For the CRA-2009, a reassessment of the CRA-2004 baseline FEPs was
15 conducted to determine whether changes in WIPP activities and conditions affected the original
16 FEPs descriptions, bases, or screening decisions. This assessment also determined whether
17 additional FEPs should be included in the CRA baseline. The reassessment results are
18 documented in Appendix SCR-2009, Section SCR-3.0 and Section 32 of this application, Scope
19 of Performance Assessment. Changes to the baseline FEPs include updating screening
20 arguments with new information that has become available and separating general FEPs into
21 more descriptive FEPs. No changes to PA implementation or modeling assumptions were made
22 as a result of the FEPs reassessment because no FEPs that were previously screened out of PA
23 calculations have been screened in and no FEPs that were screened in have been screened out.

24 **MASS-2.2 Monitoring**

25 Monitoring activities have continued since the certification of the WIPP. These activities are
26 used to validate assumptions and PA parameters, and to detect substantial and detrimental
27 deviation from expected repository performance. Monitoring, as discussed here, applies to the
28 assurance requirement of 40 CFR § 191.14(b) (U.S. Environmental Protection Agency 1993) and
29 the monitoring criteria at 40 CFR § 194.42 (U.S. Environmental Protection Agency 1996).
30 Appendix MON-2009 details the monitoring program that meets these requirements. The
31 monitoring program was assessed to determine if the results indicate that changes should be
32 made to the monitoring program. The results did not indicate that changes were required
33 (Wagner 2008). The monitoring program did, however, lead to a change in one monitored
34 parameter used in PA: because of increased drilling in the Delaware Basin, the drilling rate
35 parameter value used in the CRA-2009 PA has increased (see Appendix DATA-2009, Section
36 DATA-2.0 for information on this parameter change).

37 In the CRA-2009 PA, the drilling rate has been changed to meet the requirements for 40 CFR
38 § 194.33 (U.S. Environmental Protection Agency 1996). The drilling rate for boreholes is

1 discussed in Section 33 of this application. No changes to modeling assumptions are necessary
2 to account for this parameter change.

3 **MASS-2.3 Experimental Activities**

4 The EPA requires the recertification documentation to include an update of “additional analyses
5 and results of laboratory experiments conducted by the Department or its contractors as part of
6 the WIPP program” (40 CFR § 194.15(a)(3); see also 40 CFR § 194.15, U.S. Environmental
7 Protection Agency 1996). The following sections discuss analyses and experiments conducted to
8 support compliance determinations. Only analyses with conclusions relevant to this
9 recertification are discussed here.

10 **MASS-2.3.1 Magnesium Oxide Investigations**

11 The EPA has approved a U.S. Department of Energy (DOE) change request to reduce the
12 magnesium oxide (MgO) excess factor from 1.67 to 1.2 times the quantity of MgO required to
13 consume all of the carbon dioxide (CO₂) that would be produced if microbes consumed all the
14 CPR materials in the emplaced waste at the WIPP (Reyes 2008 and Appendix MgO-2009,
15 Section MgO-6.2.4.6). Since PA assumes there is always enough MgO to maintain a favorable
16 chemical environment for actinide (An) solubilities, a reduction in the excess factor does not
17 change the modeling assumptions used to represent MgO in PA.

18 Experiments have been performed to support the implementation of MgO as an engineered
19 barrier. These experiments have characterized MgO and investigated the hydration and
20 carbonization of MgO to confirm its ability to sequester CO₂, buffer brine pH, and subsequently
21 help establish low An solubilities in the repository. These activities are described in detail in
22 Appendix MgO-2009. The results of these MgO investigations have not impacted the modeling
23 assumptions associated with MgO in PA (Appendix MgO-2009 and Appendix PA-2009, Section
24 PA-2.1.4.4).

25 **MASS-2.3.2 Actinide Investigations**

26 The DOE has continued to investigate An speciation and solubilities since the certification of the
27 WIPP. The current An experimental activities are described in Appendix SOTERM-2009,
28 Section SOTERM-3.0. The CRA-2009 PA uses the same An assumptions as the CRA-2004
29 PABC.

30 **MASS-2.4 Performance Assessment Models and Systems**

31 Changes have been made to the systems used to perform PAs. The PA hardware, operating
32 systems (OSs), and parameter database have been updated since the CRA-2004 and CRA-2004
33 PABC. These changes were necessary to replace obsolete hardware and OSs and to increase PA
34 capabilities.

35 Sandia National Laboratories (SNL) maintains the computational platforms used to execute the
36 WIPP PA modeling codes. A small number of modeling tasks that feed into compliance
37 calculations are performed on desktop PC workstations running the Microsoft[®] Windows[®] XP

1 OS, as well as PC-based workstations and clusters running the Red Hat[®] Linux[®] OS. The WIPP
2 PA parameter database is hosted on a PC-based server running Windows[®] 2000. However, the
3 vast majority of the WIPP PA modeling codes used directly in compliance calculations are run
4 on the WIPP PA Alpha Cluster composed of Hewlett Packard[®] (formerly Compaq[®])
5 AlphaServer[™] systems. AlphaServers[™] are built around the Alpha processor and run the
6 OpenVMS[™] OS.

7 The computer systems and OSs have been upgraded since the CRA-2004 because of increasing
8 obsolescence of the OS and hardware. The current hardware and software versions used in the
9 CRA-2009 PA calculations are shown in Table MASS-1 and Table MASS-2. Significant
10 changes include those made to the WIPP PA Alpha cluster, where older AlphaServers[™] were
11 replaced with newer machines and the OS for all servers was upgraded. The WIPP PA Alpha
12 cluster now consists of four ES47 AlphaServers[™] and four ES45 AlphaServers[™]. The OS on
13 these systems has been upgraded from OpenVMS[™] 7.3-1 to OpenVMS[™] 8.2. Regression
14 testing of all codes used in compliance calculations has been performed to verify that the codes
15 continue to perform correctly after the hardware and OS changes (Long 2006).

16 The PC-based Linux[®] clusters have also been upgraded since the CRA-2004, but the new
17 configurations have not been used in compliance calculations included in the CRA-2009.

18 All changes to these systems are performed under the quality assurance (QA) program per the
19 Carlsbad Field Office Quality Assurance Program Document, and include testing, validation, and
20 verification to ensure that there is no impact on PA implementation. A synopsis of the changes
21 and references to the QA documentation are found in Long (2006). It should be noted that the
22 codes identified in Table 2-1 of Long (2006) are those that have changed since the CRA-2004
23 PABC. Some code outputs from previous certification PAs continue to be used in this CRA-
24 2009 PA because these codes and their input parameters have not changed; therefore, the codes
25 do not need to be rerun. These outputs are identified in Long (2008) and include the outputs of
26 DRSPALL, MODFLOW, and SECOTP2D.

27 **MASS-2.5 PABC**

28 The EPA requested changes to the CRA-2004 PA during their review of the first recertification
29 (Cotsworth 2005). These changes were incorporated in the CRA-2004 PABC and Leigh et al.
30 (2005), and in the subsequent CRA-2009 PA. The changes were assessed by the EPA and
31 approved as the certified WIPP baseline in their recertification decision (U.S. Environmental
32 Protection Agency 2006). The CRA-2004 PABC changes are described in Table MASS-3.

33 **MASS-2.5.1 Conceptual Model Changes**

34 The CRA-2009 PA uses the same conceptual models used in the CRA-2004 PABC. No changes
35 were made to the conceptual models used in the CRA-2004 PABC. For the CRA-2004 PABC,
36 incorporation of the changes required by the EPA in Cotsworth (2005) led to several changes in
37 the conceptual models used in the CRA-2004 PABC. Specifically, the requirement to assume
38 that (1) microbial gas generation occurs for all vectors, and (2) the sequential consumption of
39 CPR via the nitrate-to-sulfate-to-methanogenesis reaction sequence is constrained to limit the
40

1

Table MASS-1. CRA-2009 PA Codes

Code	Version	Build Date
ALGEBRACDB	2.35	31-JAN-1996
BRAGFLO	6.0	12-FEB-2007
CCDFGF	5.02	13-DEC-2004
CUTTINGS_S	6.02	9-JUN-2005
DRSPALL	1.10	14-JAN-2004
EPAUNI	1.15A	3-JUL-2003
GENMESH	6.08	31-JAN-1996
GROPECDB	2.12	27-JUN-1996
ICSET	2.22	1-FEB-1996
LHS	2.42	18-JAN-2005
MATSET	9.10	29-NOV-2001
MODFLOW-2000	1.6	20-SEP-2002
NUTS	2.05C	24-MAY-2006
PANEL	4.03	25-APR-2005
POSTBRAG	4.00A	28-MAR-2007
POSTSECOTP2D	1.04	5-JUN-1997
POSTLHS	4.07A	25-APR-2005
PREBRAG	8.0	8-MAR-2007
PRECCDFGF	1.01	7-JUL-2005
PRELHS	2.30	27-NOV-2001
PRESECOTP2D	1.22	12-JUN-1997
RELATE	1.43	6-MAR-1996
SECOTP2D	1.41A	9-JUL-2003
STEPWISE	2.21	2-DEC-1996
SUMMARIZE	3.01	21-DEC-2005

2

3

Table MASS-2. CRA-2009 PA Hardware

Node	Hardware Type	CPU
CCR	HP AlphaServer™ ES45	Alpha EV68
TDN	HP AlphaServer™ ES45	Alpha EV68
BTO	HP AlphaServer™ ES45	Alpha EV68
CSN	HP AlphaServer™ ES45	Alpha EV68
GNR	HP AlphaServer™ ES47	Alpha EV7
MC5	HP AlphaServer™ ES47	Alpha EV7
TRS	HP AlphaServer™ ES47	Alpha EV7
TBB	HP AlphaServer™ ES47	Alpha EV7

4

1 consumption reaction to only nitrate and sulfate reduction, changed the chemical conditions and
 2 gas generation conceptual models for the CRA-2004 PABC. These changes are also
 3 incorporated in the CRA-2009 PA and are discussed further in the CRA-2004 PABC summary
 4 report sections listed in Table MASS-3.

5 **Table MASS-3. Changes Incorporated in the CRA-2004 PABC**

Changes Included in the Performance Assessment Baseline Calculation		
EPA-Mandated Change	Description of Change	Reference
Solubility Parameters	Organic ligand concentrations recalculated, brine composition changes, U(VI) solubility changes, and change to account for no nonmicrobial vectors	PABC Summary (Leigh et al. 2005, Section 2.5) PANEL Analysis Package (Garner and Leigh 2005)
Solubility Uncertainty Ranges	Updated uncertainty ranges used	PABC Summary (Leigh et al. 2005, Section 2.6)
Probability of Microbial Activity	Microbial activity in all vectors versus 50% previously	PABC Summary (Leigh et al. 2005, Section 2.2)
CPR Degradation	Parameters for humid and inundated rate-changed Removal of methanogenesis	PABC Summary (Leigh et al. 2005, Section 2.3) PABC Summary (Leigh et al. 2005, Section 2.4)
Inventory	Inclusion of waste emplacement CPR Correct inventory errors	PABC Summary (Leigh et al. 2005, Section 2.1) PABC Inventory Report (Leigh, Trone, and Fox 2005)
Error Corrections	Additional DRSPALL vectors sampled; LHS, CCDFGF, CUTTING_S, SUMMARIZE and PRECCDFGF code corrections	PABC Summary (Leigh et al. 2005, Section 2.8) PABC Summary (Leigh et al. 2005, Section 2.9)
Culebra T Fields	Mining modifications incorporated in new flow fields	PABC Summary (Leigh et al. 2005, Section 2.7) The CRA-2004, Appendix PA, Attachment TFIELD

6

7 **MASS-2.5.2 Recalculation of Culebra T Fields**

8 The CRA-2009 PA uses the CRA-2004 PABC T fields. No changes were made to the T field
 9 modeling assumptions for the CRA-2009 PA. Water level rises in the Culebra Dolomite
 10 Member of the Rustler Formation (hereafter referred to as Culebra) have continued over recent
 11 years, and the observed heads have exceeded the ranges of uncertainty established for the steady-
 12 state heads in many of the WIPP observation wells used in the calibration of the T fields
 13 described in the CCA (Sandia National Laboratories 2002). The DOE recalculated T fields for
 14 the CRA-2004 using new Culebra data and geologic information (see Appendix TFIELD-2009).
 15 Additionally, the treatment of potential potash mining was recalculated during the CRA-2004
 16 PABC. The areas affected by mining were modified, and new flow fields were generated in
 17 response to the EPA’s request for a PABC (Cotsworth 2005). (See also Leigh et al 2005, Section

1 2.7, and the CRA-2004, Appendix PA, Attachment TFIELD.) The DOE is continuing its field
2 observation program to investigate other potential causes for the water-level rises (Sandia
3 National Laboratories 2003). This program is discussed in Appendix HYDRO-2009.

4 **MASS-2.5.3 Waste Inventory Update**

5 The waste inventory used in the CCA was based on information contained in the Transuranic
6 Waste Baseline Inventory Database (see the CCA, Appendix BIR). No waste had been emplaced
7 in the repository at that time. Since 1996, waste has been emplaced in the repository and better
8 estimates have been made of the existing and projected waste streams at the generator sites.
9 Waste information in the CRA-2004 PA was updated to include the emplaced, currently stored,
10 and projected waste streams. This information was collected in the Transuranic Waste Baseline
11 Inventory Database, Rev 2.1, with the WIPP-specific information detailed in the CRA-2004,
12 Appendix DATA, Attachment F.

13 During the CRA-2004 PABC, the inventory information used in PA was again updated. Leigh,
14 Trone, and Fox (2005) summarizes these changes to the inventory. Changes include a correction
15 to the waste volumes reported by the Hanford Office of Richland Operations, the inclusion of
16 pre-1970 waste at Idaho National Laboratory (INL) as possible WIPP waste and a correction to
17 the volume and concentration of waste from Los Alamos National Laboratory.

18 The waste information used in the CRA-2009 PA is the same as in the CRA-2004 PABC
19 calculations, with the addition of cellulosic and plastic materials used for waste emplacement to
20 the inventory. Waste information in the CRA-2009 PA is discussed further in Leigh, Trone, and
21 Fox (2005).

22 **MASS-2.6 CRA-2009 Changes**

23 The CRA-2009 PA was updated based on new information since the CRA-2004 PABC.
24 Information on the implementation of these changes is contained in Clayton (2008, Section 2.1)
25 and is summarized in Table MASS-4.

26 **MASS-2.7 Operational Considerations**

27 No operational changes that would impact modeling assumptions have been made at the WIPP
28 since the 2006 recertification decision. As a result, no changes were made to modeling
29 assumptions for the CRA-2009 PA.

30 Shortly after submission of the CRA-2004 to the EPA, the DOE began using a new MgO
31 supplier, Martin Marrietta Magnesia Specialties, for the engineered barrier because the existing
32 vendor, Premier Chemicals, was no longer able to meet the stipulated MgO specifications. The
33 MgO specification did not change, and no associated change was made to modeling assumptions
34 as a result of the new vendor. Additional discussion of this operational change is found in
35 Appendix MgO-2009, Section MgO-2.2.

1

Table MASS-4. Changes Incorporated in the CRA-2009

WIPP Project Change	Summary of Change and Cross-Reference
DBR Parameters	The maximum DBR duration was decreased from 11 days to 4.5 days (Kirkes 2007).
CPR Degradation Rates	A conditional relationship was introduced between the inundated and humid gas generation rate to ensure that the inundated rate is the maximum rate (Kirchner 2008).
BRAGFLO Chemistry Capillary Pressure and Relative Permeability Model	New capillary pressure and relative permeability model for open cavities was added. Cut-off saturation is used, below which no chemical reactions occur (H ₂ O-required reactions) (Nemer and Clayton 2008).
Drilling Rate	Rate changed from 52.5 to 58.5 boreholes per square kilometer (km ²) over 10,000 years (Clayton 2008).
Parameter Error Corrections	Emplaced CPR Error Correction Halite/DRZ Porosity Error Correction Fraction of Repository Occupied by Waste Correction NUTS and DBR Calculation Input Files (Nemer 2007, Dunagan 2007, Ismail 2007a, Ismail 2007b, Clayton 2007).

2

1 **MASS-3.0 General Assumptions in PA Models**

2 A number of assumptions are applied generally to the disposal system through the conceptual
3 and mathematical models implemented in the CRA-2009 PA.

4 Table MASS-5, which lists modeling assumptions used in the PA, is a guide to general modeling
5 assumptions and provides guidance for integrating the assumptions with (1) the CRA-2004
6 chapters or CRA-2009 appendices in which they are discussed, and (2) the code(s) that
7 implement these assumptions.

8 The FEPs discussed in Appendix SCR-2009 that are relevant to these assumptions are also
9 indicated. The final column in the table indicates whether the DOE considers each assumption to
10 be reasonable or conservative. As discussed in the CRA-2004, Chapter 6.0, Section 6.5, the
11 DOE has not attempted to bias the overall results of PA toward a conservative outcome.
12 However, where data or models are impractical to obtain, or where effects on performance are
13 not expected to be significant enough to justify development of a more complicated model, the
14 DOE has chosen to use conservative assumptions. In all other cases, best unbiased conceptual
15 models and parameter values have been selected. The designator R (reasonable) in the final
16 column indicates that the DOE considers the assumption to be reasonable based on WIPP-
17 specific data or information, data or information considered analogous to the WIPP disposal
18 system, expert judgment, or other reasoning. The designator C (conservative) indicates the DOE
19 considers the assumption may overestimate a process or effect that may contribute to releases to
20 the accessible environment. The regulatory designator (Reg) indicates that the assumption is
21 based on regulations in 40 CFR Part 191, criteria in 40 CFR Part 194, or other regulatory
22 guidance.

23 **MASS-3.1 Darcy's Law Applied to Fluid Flow Calculated by BRAGFLO,** 24 **MODFLOW-2000, and DRSPALL**

25 A mathematical relationship expressing fluid flux as a function of hydraulic head gradients in a
26 porous medium, commonly known as Darcy's Law, is applied to geologic media for all fluid-
27 flow calculations. For details about the specific formulation of Darcy's Law used in these
28 calculations, refer to Appendix PA-2009, Section PA-4.2 for the disposal system and Section
29 PA-4.8 for the Culebra. Darcy's Law is not applied for flow up a borehole being drilled (see
30 Section MASS-16.2; the CRA-2004, Chapter 6.0, Section 6.4.7.1.1; and Appendix PA-2009,
31 Section PA-4.6 for more discussion of this topic).

32 Darcy's Law generally applies for flow models if certain conditions are satisfied: (1) the flow
33 occurs in a porous medium with interconnected porosity, (2) flow velocities are low enough that
34 viscous forces dominate inertial forces, and (3) a threshold hydraulic gradient is exceeded. In the
35 CCA, Appendix MASS, these conditions were shown to be valid for the WIPP PA.

36 Darcy's Law assumes laminar flow; that is, there is no motion of the fluid at the fluid/solid
37 interface and velocity increases with distance from the fluid/solid interface. For liquids, it is
38 reasonable to assume laminar flow under most conditions, including those found in and
39 surrounding the WIPP repository. For gases at low pressure, however, gas molecules near the
40 solid interface may not have intimate contact with the solid and may have finite velocity, not

1

Table MASS-5. General Modeling Assumptions

Chapter or Section	Assumption Number	Code	Modeling Assumption	Related FEP in Appendix SCR-2009	Assumption Considered ^a
MASS-3.0 Some General Assumptions in PA Models MASS-3.1 Darcy's Law Applied for Fluid Flow calculated by BRAGFLO, MODFLOW-2000, and SECOTP2D	1	BRAGFLO MODFLOW-2000	Flow is governed by mass conservation and Darcy's Law in porous media. Flow is laminar and fluids are Newtonian.	Saturated Groundwater Flow (N23) Unsaturated Groundwater Flow (N24) Brine Inflow (W40)	R
	2	BRAGFLO	Two-phase flow in the porous media is by simultaneous immiscible displacement.	Fluid Flow Due to Gas Production (W42)	R
	3	BRAGFLO	The Brooks-Corey or Van Genuchten/Parker equations represent interactions between brine and gas.	Fluid Flow Due to Gas Production (W42)	R
	4	BRAGFLO	The Klinkenberg effect is included for flow of gases at low pressures.	Fluid Flow Due to Gas Production (W42)	R
	5	BRAGFLO	Threshold displacement pressure for flow of gas into brine is constant.	Fluid Flow Due to Gas Production (W42)	R
	6	BRAGFLO MODFLOW-2000 SECOTP2D	Fluid composition and compressibility are constant.	Saturated Groundwater Flow (N23) Fluid Flow Due to Gas Production (W42)	R
MASS-3.2 Hydrogen Gas as Surrogate for Waste-Generated Gas Physical Properties in BRAGFLO	7	BRAGFLO DRSPALL	The gas phase is assigned the density and viscosity properties of hydrogen.	Fluid Flow Due to Gas Production (W42)	R
MASS-3.3 Salado Brine as Surrogate for Liquid Phase Physical Properties in BRAGFLO	8	BRAGFLO	All liquid physical properties are assigned the properties of Salado brine.	Saturated Groundwater Flow (N23)	R

^a R = Reasonable

C = Conservative

Reg. - Based on regulatory guidance

2 See above - Refers to assumptions 1 through 8 listed at the beginning of this table.

Table MASS-5. General Modeling Assumptions (Continued)

Chapter or Section	Code	Modeling Assumption	Related FEP in Appendix SCR-2009	Assumption Considered ^a
CRA-2004, Chapter 6.0, Section 6.4.2 Model Geometries MASS-4.0 Model Geometries CRA-2004, Chapter 6.0, Section 6.4.2.1 Disposal System Geometry MASS-4.1 Disposal System Geometry as Modeled in BRAGFLO	BRAGFLO	The disposal system is represented by a two-dimensional, north-south, vertical cross section.	Stratigraphy (N1) Physiography (N39)	R
	BRAGFLO	Flow in the disposal system is radially convergent or divergent centered on the repository, shaft, and borehole for disturbed performance.	Saturated Groundwater Flow (N23) Unsaturated Groundwater Flow (N24)	R
	BRAGFLO	Variable dip in the Salado is approximated by a 1 degree dip to the south.	Stratigraphy (N1)	R
	BRAGFLO	Stratigraphic layers are parallel.	Stratigraphy (N1)	R
	BRAGFLO	The stratigraphy consists of units above the Dewey Lake, the Forty-niner, the Magenta, the Tamarisk, the Culebra, the Los Medaños, and the Salado Formations (comprising impure halite, MB 138, anhydrites A and B [lumped together], and MB 139). The dimensions of these units are constant. A Castile brine reservoir is included in the BRAGFLO grid in all scenarios.	Stratigraphy (N1)	R
CRA-2004, Chapter 6.0, Section 6.4.2.2 Culebra Geometry MASS-4.3 Historical Context of Culebra Geometries as Modeled in MODFLOW-2000 and SECOTP2D	MODFLOW-2000 SECOTP2D	The Culebra is represented by a two-dimensional, horizontal geometry for groundwater flow and radionuclide transport simulation.	Stratigraphy (N1)	R
	MODFLOW 2000 PEST	Transmissivity varies spatially. There is no vertical flow to or from the Culebra.	Groundwater Recharge (N54) Groundwater Discharge (N53)	R
	SECOTP2D	The regional flow field provides boundary conditions for local transport calculations (see CRA-2004, Chapter 6.0, Section 6.4.10.2).	Advection (W90)	R

^a R = Reasonable

C = Conservative

Reg. - Based on regulatory guidance

See above - Refers to assumptions 1 through 8 listed at the beginning of this table.

Table MASS-5. General Modeling Assumptions (Continued)

Chapter or Section	Code	Modeling Assumption	Related FEP in Appendix SCR-2009	Assumption Considered ^a
CRA-2004, Chapter 6.0, Section 6.4.3 The Repository MASS-5.0 BRAGFLO Geometry of the Repository	BRAGFLO	The repository comprises five regions separated by panel closures: the waste panel, a north Rest of Repository (RoR), a south RoR and the access drifts (separated by panel closures), the operations region, and the experimental region. A single shaft region is also modeled, and a borehole region is included for a borehole that intersects the separate waste panel. The dimensions of these regions are constant (see the CRA-2004, Appendix MASS, Figure MASS-4).	Disposal Geometry (W1)	R-C
	BRAGFLO	Long-term flow up plugged and abandoned boreholes modeled as if all intrusions occur into a downdip (southern) panel.	Disposal Geometry (W1)	C
	BRAGFLO	For each repository region, the model geometry preserves design volume.	Disposal Geometry (W1)	R
	BRAGFLO	Pillars, individual drifts, and rooms are not modeled for long-term performance, and containers provide no barrier to fluid flow.	Disposal Geometry (W1)	C
	BRAGFLO	Long-term flow is radial to and from the borehole that intersects the waste disposal panel during disturbed performance.	Waste-Induced Borehole Flow (H32)	R
	BRAGFLO	DRZ provides a pathway to MBs.	—	R
	BRAGFLO	Grid and material properties are consistent with the Option D panel closure design.	—	R

^a R = Reasonable

C = Conservative

Reg. - Based on regulatory guidance

See above - Refers to assumptions 1 through 8 listed at the beginning of this table.

Table MASS-5. General Modeling Assumptions (Continued)

Chapter or Section	Code	Modeling Assumption	Related FEP in Appendix SCR-2009	Assumption Considered ^a
CRA-2004, Chapter 6.0, Section 6.4.3.1 Creep Closure MASS-6.0 Creep Closure Appendix PORSURF	SANTOS	Creep closure is modeled using a two-dimensional model of a single room. Room interactions are insignificant.	Salt Creep (W20) Changes in the Stress Field (W21) Excavation-Induced Changes in Stress (W19)	R
	SANTOS	The amount of creep closure is a function of time, gas pressure, and waste-matrix strength.	Salt Creep (W20) Changes in the Stress Field (W21) Consolidation of Waste (W32) Pressurization (W26)	R
	BRAGFLO	Porosity of operations and experimental areas is fixed at a value representative of consolidated material.	Salt Creep (W20)	R
CRA-2004, Chapter 6.0, Section 6.4.3.2 Repository Fluid Flow MASS-7.0 Repository Fluid Flow	BRAGFLO	General assumptions 1 to 8.	—	See above
	BRAGFLO	The waste disposal region is assigned a constant permeability representative of average consolidated waste without backfill.	Saturated Groundwater Flow (N23) Unsaturated Groundwater Flow (N24)	R
MASS-7.1 Flow Interactions with the Creep Closure Model	BRAGFLO	The experimental and operations regions are assigned a constant permeability representative of unconsolidated material and a constant porosity representative of consolidated material.	Saturated Groundwater Flow (N23) Unsaturated Groundwater Flow (N24) Salt Creep (N20)	C
MASS-7.2 Flow Interactions with the Gas Generation Model	BRAGFLO	For gas generation calculations, the effects of wicking are accounted for by assuming that brine in the repository contacts waste to an extent greater than that calculated by the Darcy Flow model used.	Wicking (W41)	R

^a R = Reasonable

C = Conservative

Reg. - Based on regulatory guidance

See above - Refers to assumptions 1 through 8 listed at the beginning of this table.

Table MASS-5. General Modeling Assumptions (Continued)

Chapter or Section	Code	Modeling Assumption	Related FEP in Appendix SCR-2009	Assumption Considered ^a
CRA-2004, Chapter 6.0, Section 6.4.3.3 Gas Generation MASS-8.0 Gas Generation CRA-2004 Appendix TRU WASTE	BRAGFLO	Gas generation occurs by anoxic corrosion of steel containers and Fe and Fe-base alloys in the waste, giving H ₂ , and by microbial consumption of cellulose and, possibly, plastics and rubbers, giving mainly CO ₂ and H ₂ S. Radiolysis, oxic reactions, and other gas generation mechanisms are insignificant. Gas generation is calculated using the average-stoichiometry model, and is dependent on brine availability.	Container Material Inventory (W5) Waste Inventory (W2) Degradation of Organic Material (W44) Gases from Metal Corrosion (W49)	R
	BRAGFLO	The anoxic corrosion rate is dependent on liquid saturation. Anoxic corrosion of steel continues until all the steel is consumed. Steel corrosion will not be passivated by microbially generated gases (CO ₂ or H ₂ S). The water in brine is consumed by the corrosion reaction.	Brine Inflow (W40) Gases from Metal Corrosion (W49) Degradation of Organic Material (W44)	R
	BRAGFLO	Laboratory-scale experimental measurements of gas generation rates at expected room temperatures are used to account for the effects of biofilms and chemical reactions.	Effects of Biofilms on Microbial Gas Generation (W48) Effects of Temperature on Microbial Gas Generation (W45) Chemical Effects of Corrosion (W51)	R

^a R = Reasonable

C = Conservative

Reg. - Based on regulatory guidance

See above - Refers to assumptions 1 through 8 listed at the beginning of this table.

Table MASS-5. General Modeling Assumptions (Continued)

Chapter or Section	Code	Modeling Assumption	Related FEP in Appendix SCR-2009	Assumption Considered ^a
	BRAGFLO	The rate of microbial gas production is dependent on the amount of liquid present. It is assumed that microbial activity neither produces nor consumes water. Significant microbial activity occurs in all the simulations. In 75% of the simulations, microbes may consume all of the cellulose but none of the plastics and rubbers. In the remaining 25% of the simulations, microbes may consume all of the cellulose and all of the plastics and rubbers. Microbial production will continue until all biodegradable CPR materials are consumed if brine is present. The MgO backfill will react with all of the CO ₂ and remove it from the gaseous phase.	Brine Inflow (W40) Degradation of Organic Material (W44) Waste Inventory (W2)	R
	BRAGFLO	Gas dissolution in brine is of negligible consequence.	Fluid Flow Due to Gas Production (W42)	R
	BRAGFLO	The gaseous phase is assigned the properties of hydrogen (General Assumption 7).	Fluid Flow Due to Gas Production (W42)	See above
CRA-2004, Chapter 6.0, Section 6.4.3.4 Chemical Conditions in the Repository SOTERM-2.0 Conceptual Framework of Chemical Conditions	NUTS PANEL	Chemical conditions in the repository will be constant. Chemical equilibrium is assumed for all reactions that occur between brine in the repository, waste, and abundant minerals, with the exceptions of gas generation and redox reactions.	Speciation (W56) Reduction-Oxidation Kinetics (W66)	R
	NUTS PANEL	Brine and waste in the repository will contain a uniform mixture of dissolved and colloidal species. All actinides have instant access to all repository brine.	Heterogeneity of Waste Forms (W3) Speciation (W56)	C

^a R = Reasonable

C = Conservative

Reg. - Based on regulatory guidance

See above - Refers to assumptions 1 through 8 listed at the beginning of this table.

Table MASS-5. General Modeling Assumptions (Continued)

Chapter or Section	Code	Modeling Assumption	Related FEP in Appendix SCR-2009	Assumption Considered ^a
	NUTS PANEL	No microenvironments that influence the overall chemical environment will persist.	Speciation (W56)	R
	NUTS PANEL	For the undisturbed performance and E2 scenarios, brine in the waste panels has the composition of Salado brine. For E1 and E1E2 (Appendix PA-2009, Section PA-2.3.2.2) scenarios, all brine in the waste panel intersected by the borehole has the composition of Castile brine.	Speciation (W56)	R
	NUTS PANEL	Chemical conditions in the waste panels will be reducing. However, a condition of redox disequilibrium will exist between the possible oxidation states of the An elements.	Reduction-Oxidation Kinetics (W66) Speciation (W56) Effects of Metal Corrosion (W64)	R
	NUTS PANEL	The pH and CO ₂ fugacity in the waste panels will be controlled by the equilibrium between Mg(OH) ₂ and Mg ₅ (CO ₃) ₄ (OH) ₂ ·4H ₂ O. (A result of this assumption is low CO ₂ fugacity and mildly basic conditions.)	Speciation (W56) Backfill Chemical Composition (W10)	R
CRA-2004, Chapter 6.0, Section 6.4.3.5 Dissolved Actinide Source Term SOTERM-3.3 The Fracture Matrix Transport Computer Code	NUTS PANEL	Radionuclide dissolution to solubility limits is instantaneous.	Dissolution of Waste (W58)	C
	NUTS PANEL	Of the 29 isotopes considered as inputs, 6 actinides (Th, U, Np, Pu, Am, and Cm) are used in PANEL for calculations of radionuclide transport of brine (up a borehole). Four actinides (Th, U, Pu, and Am) are explicitly considered in NUTS for calculations of radionuclide transport in brine (porous materials) (Leigh and Trone 2005a). Choice of radionuclides is discussed in Leigh and Trone (2005b), Leigh, Trone, and Fox (2005), and Leigh et al. (2005).	Waste Inventory (W2)	R

^a R = Reasonable

C = Conservative

Reg. - Based on regulatory guidance

See above - Refers to assumptions 1 through 8 listed at the beginning of this table.

Table MASS-5. General Modeling Assumptions (Continued)

Chapter or Section	Code	Modeling Assumption	Related FEP in Appendix SCR-2009	Assumption Considered ^a
	NUTS PANEL	The reducing conditions in the repository will eliminate significant concentrations of Np(VI), Pu(V), Pu(VI), and Am(V) species. Am and Cm will exist predominantly in the III oxidation state; while Th will exist in the IV oxidation state. It is assumed that the solubilities and $K_{d,s}$ of U, Np, and Pu will be dominated by one of the remaining oxidation states: U(IV) or U(VI), Np(IV) or Np(V), and Pu(III) or Pu(IV) (See Appendix SOTERM-2009, Table SOTERM-15).	Speciation (W56) Reduction-Oxidation Kinetics (W66)	R
	NUTS PANEL	For a given oxidation state, the different actinides have similar solubilities.	Speciation (W56)	R
	NUTS PANEL	For undisturbed performance and for all aspects of disturbed performance, except for cuttings and cavings releases, radionuclides in the waste are distributed evenly throughout the disposal panel.	Waste Inventory (W2) Heterogeneity of Waste Forms (W3)	R
	NUTS PANEL	Mobilization of actinides in the gas phase is negligible.	Dissolution of Waste (W58)	R
	NUTS PANEL	An concentrations in the repository will be inventory limited when the mass of an An becomes depleted such that the predicted concentrations cannot be achieved.	Dissolution of Waste (W58)	R
CRA-2004, Chapter 6.0, Section 6.4.3.6 Source Term for Colloidal Actinides	NUTS PANEL	Four types of colloids constitute the source term for colloidal actinides: microbes, humic substances, intrinsic colloids, and mineral fragments.	Colloid Formation and Stability (W79) Humic and Fulvic Acids (W70)	R
	NUTS PANEL	The only intrinsic colloids that will form are those of Pu.	Colloid Formation and Stability (W79)	R

^a R = Reasonable

C = Conservative

Reg. - Based on regulatory guidance

See above - Refers to assumptions 1 through 8 listed at the beginning of this table.

Table MASS-5. General Modeling Assumptions (Continued)

Chapter or Section	Code	Modeling Assumption	Related FEP in Appendix SCR-2009	Assumption Considered ^a
	NUTS PANEL	Concentrations of intrinsic colloids and mineral-fragment colloids are modeled as constants based on experimental observations. Humic and microbial colloidal An concentrations are modeled as proportional to dissolved An concentrations.	Colloid Formation and Stability (W79)	R
	NUTS PANEL	The maximum concentration of each An associated with each colloid type is constant.	Actinide Sorption (W61)	R
CRA-2004, Chapter 6.0, Section 6.4.4 Shafts and Shaft Seals MASS-12.0 Shafts and Shaft Seals	BRAGFLO	General Assumptions 1 to 8.	—	See above
	BRAGFLO	The four shafts connecting the repository to the surface are represented by a single shaft with a cross-section and volume equal to the total volume of the four real shafts and separated from the waste by less than the distance of the nearest real shaft.	Disposal Geometry (W1)	R
	BRAGFLO	The shaft seal system is represented by an upper and lower shaft region representing a composite of the actual materials in those regions.	Shaft Seal Geometry (W6) Shaft Seal Physical Properties (W7)	R
	BRAGFLO	The shaft is surrounded by a DRZ which heals with time. The DRZ is represented through the composite permeabilities of the shaft system itself, rather than as a discrete zone. The effective permeability of shaft materials are adjusted at 200 years after closure to reflect consolidation and possible degradation. Permeabilities are constant for the shaft seal materials through the Rustler formation.	Salt Creep (W20) Consolidation of Shaft Seals (W36) DRZ (W18) Microbial Growth on Concrete (W76) Chemical Degradation of Shaft Seals (W74) Mechanical Degradation of Shaft Seals (W37)	R
	BRAGFLO	Concrete shaft components of the lower shaft are modeled as if they degrade after emplacement.	Mechanical Degradation of Shaft Seals (W37)	C

^a R = Reasonable

C = Conservative

Reg. - Based on regulatory guidance

1 See above - Refers to assumptions 1 through 8 listed at the beginning of this table.

Table MASS-5. General Modeling Assumptions (Continued)

Chapter or Section	Code	Modeling Assumption	Related FEP in Appendix SCR-2009	Assumption Considered ^a
	NUTS	Radionuclides are not retarded by the seals.	Actinide Sorption (W61) Speciation (W56)	C
CRA-2004, Chapter 6.0, Section 6.4.5 The Salado MASS-13.0 Salado	BRAGFLO	General Assumptions 1 to 8.	—	See above
CRA-2004, Chapter 6.0, Section 6.4.5.1 Impure Halite MASS-13.1 High Threshold Pressure for Halite-Rich Salado Rock Units	BRAGFLO	Intact rock and hydrologic properties are constant.	Stratigraphy (N1)	R
CRA-2004, Chapter 6.0, Section 6.4.5.2 Salado Interbeds MASS-13.3 The Fracture Model	BRAGFLO	Interbeds have a fracture-initiation pressure above which local fracturing and changes in porosity and permeability occur in response to changes in pore pressure. A power function relates the permeability increase to the porosity increase. A pressure is specified above which porosity and permeability do not change.	Disruption Due to Gas Effects (W25)	R
	BRAGFLO	Interbeds have identical physical properties; they differ only in position, thickness, and some fracture parameters.	Saturated Groundwater Flow (N23)	R
CRA-2004, Chapter 6.0, Section 6.4.5.3 Disturbed Rock Zone MASS-13.4 Flow in the Disturbed Rock Zone	BRAGFLO	The permeability of the DRZ is sampled with the low value similar to intact halite and the high value representing a fractured material. The DRZ porosity is equal to the porosity of Salado halite to plus 0.29%.	Disturbed Rock Zone (DRZ) (W18) Roof Falls (W22) Gas Explosions (W27) Seismic Activity (N12) Underground Boreholes (W39)	C-R
CRA-2004, Chapter 6.0, Section 6.4.5.4 Actinide Transport in the Salado MASS-13.5 Actinide Transport in the Salado	NUTS	Dissolved actinides and colloidal actinides are transported by advection in the Salado. Diffusion and dispersion are assumed negligible.	Advection (W90) Diffusion (W91) Matrix Diffusion (W92)	R

^a R = Reasonable

C = Conservative

Reg. - Based on regulatory guidance

See above - Refers to assumptions 1 through 8 listed at the beginning of this table.

Table MASS-5. General Modeling Assumptions (Continued)

Chapter or Section	Code	Modeling Assumption	Related FEP in Appendix SCR-2009	Assumption Considered ^a
	NUTS	Sorption of actinides in the anhydrite interbeds, colloid retardation, colloid transport at higher than average velocities, coprecipitation of minerals containing actinides, channeled flow, and viscous fingering are not modeled.	Actinide Sorption (W61) Colloid Transport (W78) Colloid Filtration (W80) Colloid Sorption (W81) Fluid Flow Due to Gas Production (W42) Fracture Flow (N25)	R
	NUTS	Radionuclides having similar decay and transport properties have been grouped together for transport calculations as discussed in Leigh and Trone (2005a). See also assumptions for dissolved actinide source term.	Radionuclide Decay and Ingrowth (W12)	R
	NUTS	Sorption of actinides in the borehole is not modeled.	Actinide Sorption (W61)	C
CRA-2004, Chapter 6.0, Section 6.4.6 Units Above the Salado MASS-14.0 Geologic Units above the Salado	SECOTP2D	Above the Salado, lateral An transport to the accessible environment can occur only through the Culebra.	Saturated Groundwater Flow (N23) Unsaturated Groundwater Flow (N24) Solute Transport (W77)	R
CRA-2004, Chapter 6.0, Section 6.4.6.1 Los Medaños	MODFLOW-2000 BRAGFLO	The Los Medaños member of the Rustler Formation, Tamarisk, and Forty-niner are assumed to be impermeable.	Saturated Groundwater Flow (N23)	C
CRA-2004, Chapter 6.0, Section 6.4.6.2 The Culebra MASS-15.0 Culebra Appendix TFIELD	MODFLOW-2000 SECOTP2D	General Assumptions 1, 6, and 8.	—	See above
	MODFLOW-2000	For fluid flow, the Culebra is modeled as a uniform (single-porosity) porous medium.	Saturated Groundwater flow (N23)	R

^a R = Reasonable

C = Conservative

Reg. - Based on regulatory guidance

See above - Refers to assumptions 1 through 8 listed at the beginning of this table.

Table MASS-5. General Modeling Assumptions (Continued)

Chapter or Section	Code	Modeling Assumption	Related FEP in Appendix SCR-2009	Assumption Considered ^a
	MODFLOW-2000	The Culebra flow field is determined from the observed hydraulic conditions and estimates of the effects of climate change and potash mining outside the controlled area, and does not change with time unless mining is predicted to occur in the disposal system in the future.	Saturated Groundwater Flow (N23) Climate Change (N61) Precipitation (e.g., Rainfall) (N59) Temperature (N60) Changes in Groundwater Flow Due to Mining (H37)	R
	BRAGFLO	The Culebra is assigned a single permeability to calculate brine flow into the unit from an intrusion borehole.	Natural Borehole Fluid Flow (H31) Waste-Induced Borehole Flow (H32)	R
	MODFLOW-2000	Gas flow in the Culebra is not modeled. Gas from the repository does not affect fluid flow in the Culebra.	Saturated Groundwater Flow (N23) Fluid Flow Due to Gas Production (W42)	R
	BRAGFLO MODFLOW-2000 SECOTP2D	Different thicknesses of the Culebra are assumed for BRAGFLO, MODFLOW-2000, and SECOTP2D calculations, although the Ts are consistent.	Effects of Preferential Pathways (N27)	R
	PEST	Uncertainty in the spatial variability of the Culebra transmissivity is accounted for by statistically generating 100 T fields for PA.	Saturated Groundwater Flow (N23) Fracture Flow (N25) Shallow Dissolution (N16)	R
	MODFLOW-2000 BRAGFLO	Potentiometric heads are set on the edges of the regional grid to represent flow in a portion of a much larger hydrologic system.	Groundwater Recharge (N54) Groundwater Discharge (N53) Changes in Groundwater Recharge and Discharge (N56) Infiltration (N55)	R

^a R = Reasonable

C = Conservative

Reg. - Based on regulatory guidance

See above - Refers to assumptions 1 through 8 listed at the beginning of this table.

Table MASS-5. General Modeling Assumptions (Continued)

Chapter or Section	Code	Modeling Assumption	Related FEP in Appendix SCR-2009	Assumption Considered ^a
CRA-2004, Chapter 6.0, Section 6.4.6.2.1 Transport of Dissolved Actinides in the Culebra MASS-15.2 Dissolved Actinide Transport and Retardation in the Culebra	SECOTP2D	Dissolved actinides are transported by advection in high-permeability features and by diffusion in low-permeability features.	Solute Transport (W77) Advection (W90) Diffusion (W91) Matrix Diffusion (W92)	R
	SECOTP2D	Sorption occurs on dolomite in the matrix. Sorption on clays present in the Culebra is not modeled.	Actinide Sorption (W61) Changes in Sorptive Surfaces (W63)	C
	SECOTP2D	Sorption is represented using a linear isotherm model.	Actinide Sorption (W61) Kinetics of Sorption (W62)	R
	SECOTP2D	The possible effects on sorption of the injection of brines from the Castile and Salado into the Culebra are accounted for in the distribution of An K_d s.	Actinide Sorption (W61) Groundwater Geochemistry (N33) Changes in Groundwater Eh (N36) Changes in Groundwater pH (N37) Natural Borehole Fluid Flow (H31)	R
	SECOTP2D	Hydraulically significant fractures are assumed to be present everywhere in the Culebra.	Advection (W90)	C
CRA-2004, Chapter 6.0, Section 6.4.6.2.2 Transport of Colloidal Actinides in the Culebra MASS-15.3 Colloidal Actinide Transport and Retardation in the Culebra	SECOTP2D	An humic colloids are chemically retarded identically to dissolved actinides and are treated as dissolved actinides.	Advection (W90) Diffusion (W91) Colloid Transport (W78) Microbial Transport (W87)	R
	SECOTP2D	The concentration of intrinsic colloids is sufficiently low to justify elimination from PA transport calculations in the Culebra.	—	R

^a R = Reasonable

C = Conservative

Reg. - Based on regulatory guidance

See above - Refers to assumptions 1 through 8 listed at the beginning of this table.

Table MASS-5. General Modeling Assumptions (Continued)

Chapter or Section	Code	Modeling Assumption	Related FEP in Appendix SCR-2009	Assumption Considered ^a
	SECOTP2D	Microbial colloids and mineral fragments are too large to undergo matrix diffusion. Filtration of these colloids, which is modeled using an exponential decay approach, occurs in high-permeability features. Attenuation is so effective that associated actinides are assumed to be retained within the disposal system and are not transported in SECOTP2D.	Microbial Transport (W87) Colloid Sorption (W81)	R
CRA-2004, Chapter 6.0, Section 6.4.6.2.3 Subsidence Due to Potash Mining MASS-15.4 Subsidence Caused by Potash Mining in the Culebra	MODFLOW-2000	The effect of potash mining is to increase the hydraulic conductivity in the Culebra by a factor between 1 and 1,000.	Conventional Underground Potash Mining (H13) Changes in Groundwater Flow Due to Mining (H37)	Reg.
CRA-2004, Chapter 6.0, Section 6.4.6.3 The Tamarisk	MODFLOW-2000 BRAGFLO	The Tamarisk is assumed to be impermeable.	Saturated Groundwater Flow (N23)	R
CRA-2004, Chapter 6.0, Section 6.4.6.4 The Magenta	BRAGFLO	General Assumptions 1 to 8.	—	See above
	BRAGFLO	The Magenta permeability is set to the lowest value measured near the center of the WIPP site. This increases the flow into the Culebra.	Saturated Groundwater Flow (N23)	R
	NUTS	No radionuclides entering the Magenta will reach the accessible environment. However, the volumes of brine and actinides entering and stored in the Magenta are modeled.	Solute Transport (W77)	R

^a R = Reasonable

C = Conservative

Reg. - Based on regulatory guidance

See above - Refers to assumptions 1 through 8 listed at the beginning of this table.

Table MASS-5. General Modeling Assumptions (Continued)

Chapter or Section	Code	Modeling Assumption	Related FEP in Appendix SCR-2009	Assumption Considered ^a
CRA-2004, Chapter 6.0, Section 6.4.6.5 The Forty-niner	BRAGFLO	The Forty-niner is assumed to be impermeable.	Saturated Groundwater Flow (N23)	R
CRA-2004, Chapter 6.0, Section 6.4.6.6 Dewey Lake	BRAGFLO	General Assumptions 1 to 8.	—	See above
	NUTS	The sorptive capacity of the Dewey Lake is sufficiently large to prevent any release over 10,000 years.	Saturated Groundwater Flow (N23) Actinide Sorption (W61)	R
CRA-2004, Chapter 6.0, Section 6.4.6.7 Supra-Dewey Lake Units	BRAGFLO	General Assumptions 1 to 8.	—	See above
	BRAGFLO	The units above the Dewey Lake are a single hydrostratigraphic unit.	Stratigraphy (N1)	R
	BRAGFLO	The units are thin and predominantly unsaturated.	Unsaturated Groundwater Flow (N24) Saturated Groundwater Flow (N23)	R
CRA-2004, Chapter 6.0, Section 6.4.7 The Intrusion Borehole MASS-16.0 Intrusion Borehole CRA-2004 Section 6.4.7.1 Releases during Drilling	CUTTINGS_S BRAGFLO DRSPALL	Any actinides that enter the borehole during drilling are assumed to reach the surface.	—	C
MASS-16.1 Cuttings, Cavings, and Spall Releases during Drilling	BRAGFLO PANEL CUTTINGS_S DRSPALL	Future drilling practices will be the same as they are at present.	Oil and Gas Exploration (H1) Potash Exploration (H2) Oil and Gas Exploitation (H4) Other Resources (H8) Enhanced Oil and Gas Recovery (H9)	Reg.
	CUTTINGS_S DRSPALL	Releases of particulate waste material are modeled (cuttings, cavings, and spillings). Releases are corrected for radioactive decay until the time of intrusion.	Drilling Fluid Flow (H21) Suspension of Particles (W82) Cuttings (W84) Cavings (W85) Spallings (W86)	R
	CUTTINGS_S	Degraded waste properties are based on marine clays and surrogate materials.	Cavings (W85)	C

^a R = Reasonable

C = Conservative

Reg. - Based on regulatory guidance

1 See above - Refers to assumptions 1 through 8 listed at the beginning of this table.

Table MASS-5. General Modeling Assumptions (Continued)

Chapter or Section	Code	Modeling Assumption	Related FEP in Appendix SCR-2009	Assumption Considered ^a
	DRSPALL	A hemispherical geometry with one-dimensional spherical symmetry defines the flow field and cavity in the waste.	Spallings (W86)	C
	DRSPALL	Tensile strength, based on completely degraded waste surrogates, is felt to represent extreme, low-end tensile strengths because it does not account for several strengthening mechanisms.	Spallings (W86)	C
	DRSPALL	Shape factor is 0.1, corresponding to particles that are easier to fluidize and entrain in the flow.	Spallings (W86)	C
CRA-2004, Chapter 6.0, Section 6.4.7.1.1 Direct Brine Release During Drilling MASS-16.2 Direct Brine Releases during Drilling	BRAGFLO PANEL	Brine containing actinides may flow to the surface during drilling. DBR will have negligible effect on the long-term pressure and saturation in the waste panel.	Blowouts (H23)	R
	BRAGFLO	A two-dimensional grid (one degree dip) on the scale of the waste disposal region is used for DBR calculations.	Blowouts (H23)	R
	BRAGFLO CCDFGF	Calculation of DBR from several different locations provides reference results for the variation in release associated with location.	Blowouts (H23)	R
CRA-2004, Chapter 6.0, Section 6.4.7.2 Long-Term Releases Following Drilling MASS-16.3 Long-Term Properties of the Abandoned Intrusion Borehole	BRAGFLO CCDFGF	Plugging and abandonment of future boreholes are assumed to be consistent with practices in the Delaware Basin.	Natural Borehole Fluid Flow (H31) Waste-Induced Borehole Flow (H32)	Reg.
CRA-2004, Chapter 6.0, Section 6.4.7.2.1 Continuous Concrete Plug through the Salado and Castile	BRAGFLO CCDFGF	A continuous concrete plug is assumed to exist throughout the Salado and Castile. Long-term releases through a continuous plug are analogous to releases through a sealed shaft.	Natural Borehole Fluid Flow (H31) Waste-Induced Borehole Flow (H32)	Reg.-R

^a R = Reasonable

C = Conservative

Reg. - Based on regulatory guidance

See above - Refers to assumptions 1 through 8 listed at the beginning of this table.

Table MASS-5. General Modeling Assumptions (Continued)

Chapter or Section	Code	Modeling Assumption	Related FEP in Appendix SCR-2009	Assumption Considered ^a
CRA-2004, Chapter 6.0, Section 6.4.7.2.2 The Two-Plug Configuration	BRAGFLO	A lower plug is located between the Castile brine reservoir and underlying formations. A second plug is located immediately above the Salado. The brine reservoir and waste panel are in direct communication through an open cased hole.	Natural Borehole Fluid Flow (H31) Waste-Induced Borehole Flow (H32)	Reg.-R
	BRAGFLO	The casing and upper concrete plug are assumed to fail after 200 years, and the borehole is assumed to be filled with silty-sand-like material. At 1,200 years after abandonment, the permeability of the borehole below the waste panel is decreased by one order of magnitude as a result of salt creep.	Natural Borehole Fluid Flow (H31) Waste-Induced Borehole Flow (H32)	R
CRA-2004, Chapter 6.0, Section 6.4.7.2.3 The Three-Plug Configuration	BRAGFLO	In addition to the two-plug configuration, a third plug is placed within the Castile above the brine reservoir. The third plug is assumed not to fail over the regulatory time period.	Natural Borehole Fluid Flow (H31) Waste-Induced Borehole Flow (H32)	Reg.-R
CRA-2004 Section 6.4.8 Castile Brine Reservoir MASS-18.0 Castile Brine Reservoir	BRAGFLO	The Castile region is assigned a low permeability, which inhibits fluid flow. Brine occurrences in the Castile are bounded systems. Brine reservoirs under the waste panels are assumed to have limited extent and interconnectivity, with effective radii on the order of several hundred meters.	Brine Reservoirs (N2)	R
CRA-2004, Chapter 6.0, Section 6.4.9 Climate Change MASS-17.0 Climate Change	SECOTP2D	Climate-related factors are treated through recharge. A parameter called the Climate Index is used to scale the Culebra flux field.	Climate Change (N61) Temperature (N60) Precipitation (e.g., Rainfall) (N59)	R

^a R = Reasonable

C = Conservative

Reg. - Based on regulatory guidance

1 See above - Refers to assumptions 1 through 8 listed at the beginning of this table.

Table MASS-5. General Modeling Assumptions (Continued)

Chapter or Section	Code	Modeling Assumption	Related FEP in Appendix SCR-2009	Assumption Considered ^a
CRA-2004, Chapter 6.0, Section 6.4.10 Initial and Boundary Conditions for Disposal System Modeling CRA-2004, Chapter 6.0, Section 6.4.10.1 Disposal System Flow and Transport Modeling (BRAGFLO and NUTS)	BRAGFLO	There are no gradients for flow in the far-field of the Salado, and pressures are above hydrostatic but below lithostatic. Excavation and waste emplacement result in partial drainage of the DRZ.	Saturated Groundwater Flow (N23) Brine Inflow (W40)	R
	BRAGFLO	An initial water-table surface is set in the Dewey Lake at an elevation of 980 meters (m) (3,215 feet [ft]) above mean sea level. The initial pressures in the Salado are extrapolated from a sampled pressure in MB139 at the shaft and are in hydrostatic equilibrium. The excavated region is assigned an initial pressure of one atmosphere. The liquid saturation of the waste-disposal region is consistent with the liquid saturation of emplaced waste. Other excavated regions are assigned zero liquid saturation, except the shaft, which is fully saturated.	Saturated Groundwater Flow (N23)	R
	NUTS	Molecular transport boundary conditions are no diffusion or dispersion in the normal direction across far-field boundaries. Initial An concentrations are zero everywhere, except in the waste.	Radionuclide Decay and Ingrowth (W12) Solute Transport (W77)	R
CRA-2004, Chapter 6.0, Section 6.4.10.2 Culebra Flow and Transport Modeling (MODFLOW-2000, SECOTP2D)	MODFLOW-2000	Constant head and no-flow boundary conditions are set on the far-field boundaries of the flow model.	Saturated Groundwater Flow (N23)	R
	MODFLOW-2000	Initial An concentrations in the Culebra are zero.	Solute Transport (W77)	R

^a R = Reasonable

C = Conservative

Reg. - Based on regulatory guidance

See above - Refers to assumptions 1 through 8 listed at the beginning of this table.

Table MASS-5. General Modeling Assumptions (Continued)

Chapter or Section	Code	Modeling Assumption	Related FEP in Appendix SCR-2009	Assumption Considered ^a
CRA-2004, Chapter 6.0, Section 6.4.10.3 Initial and Boundary Conditions for Other Computational Models	NUTS PANEL BRAGFLO (DBR) CUTTINGS_S	Initial and boundary conditions interpolated from previously executed BRAGFLO calculation.	—	R
CRA-2004, Chapter 6.0, Section 6.4.12 Sequences of Future Events	CCDFGF	Each 10,000-year future (random sequence of future events) is generated by randomly and repeatedly sampling (1) the time between drilling events, (2) the location of drilling events, (3) the activity level of the waste penetrated by each drilling intrusion, (4) the plug configuration of the borehole, and (5) the penetration of a Castile brine reservoir, and by randomly sampling the occurrence of mining in the disposal system.	Oil and Gas Exploration (H1) Potash Exploration (H2) Oil and Gas Exploitation (H4) Other Resources (H8) Enhanced Oil and Gas Recovery (H9) Natural Borehole Fluid Flow (N31) Waste-Induced Borehole Flow (H32)	Reg.-R
CRA-2004, Chapter 6.0, Section 6.4.12.1 Active and Passive Institutional Controls in Performance Assessment Chapter 7.0	CCDFGF	Active institutional controls are effective for 100 years and completely eliminate the possibility of disruptive human activities (e.g., drilling and mining). No credit is taken for passive institutional controls.	—	Reg.-R
CRA-2004, Chapter 6.0, Section 6.4.12.2 Number and Time of Drilling Intrusions	CCDFGF	Drilling may occur after 100 years according to a Poisson process.	Loss of Records (H57) Oil and Gas Exploration (H1) Potash Exploration (H2) Oil and Gas Exploitation (H4) Other Resources (H8)	Reg.-R
CRA-2004, Chapter 6.0, Section 6.4.12.3 Location of Intrusion Boreholes	CCDFGF	The waste disposal region is discretized into 144 regions, each with an equal probability of being intersected. A borehole can penetrate only one region.	Disposal Geometry (W1)	R

^a R = Reasonable

C = Conservative

Reg. - Based on regulatory guidance

See above - Refers to assumptions 1 through 8 listed at the beginning of this table.

Table MASS-5. General Modeling Assumptions (Continued)

Chapter or Section	Code	Modeling Assumption	Related FEP in Appendix SCR-2009	Assumption Considered ^a
CRA-2004, Chapter 6.0, Section 6.4.12.4 Activity of the Intersected Waste Appendix TRU WASTE	CCDFGF	Six-hundred ninety waste streams are identified as contact-handled (CH) transuranic (TRU) (CH-TRU). All 77 remote-handled (RH) transuranic (TRU) (RH-TRU) waste streams were grouped (binned) together into one equivalent or average (WIPP-scale) RH-TRU waste stream.	Heterogeneity of Waste Forms (W3)	R
CRA-2004, Chapter 6.0, Section 6.4.12.5 Diameter of the Intrusion Borehole CCA Appendix DEL	CUTTINGS_S	The diameter of the intrusion borehole is constant at 12.25 inches (in.) (31.12 centimeters [cm]).	—	Reg.-R
CRA-2004, Chapter 6.0, Section 6.4.12.6 Probability of Intersecting a Brine Reservoir	CCDFGF	One brine reservoir is assumed to exist below the waste panels. The probability that a deep borehole intersects a brine reservoir below the waste panels is sampled uniformly from 0.01 to 0.60.	Brine Reservoirs (N2)	R
CRA-2004, Chapter 6.0, Section 6.4.12.7 Plug Configuration in the Abandoned Intrusion Borehole	CCDFGF	The two-plug configuration has a probability of 0.696. The three-plug configuration has a probability of 0.289. The continuous concrete plug has a probability of 0.015.	—	Reg.-R
CRA-2004, Chapter 6.0, Section 6.4.12.8 Probability of Mining Occurring in the Land Withdrawal Area	CCDFGF	Mining in the disposal system occurs a maximum of once in 10,000 years (a 10 ⁻⁴ probability per year).	—	Reg.-R
CRA-2004, Chapter 6.0, Section 6.4.13 Construction of a Single Complementary Cumulative Distribution Function (CCDF)	CCDFGF	Deterministic calculations are executed with BRAGFLO, NUTS, MODFLOW-2000, SECOTP2D, CUTTINGS_S, and PANEL to generate reference conditions. These reference conditions are used to estimate the consequences associated with random sequences of future events. These are, in turn, used to develop CCDFs.	—	R

^a R = Reasonable

C = Conservative

Reg. - Based on regulatory guidance

See above - Refers to assumptions 1 through 8 listed at the beginning of this table.

Table MASS-5. General Modeling Assumptions (Continued)

Chapter or Section	Code	Modeling Assumption	Related FEP in Appendix SCR-2009	Assumption Considered ^a
	CCDFGF	Ten thousand random sequences of future events are generated for each CCDF plotted.	—	R
CRA-2004, Chapter 6.0, Section 6.4.13.1 Constructing Consequences of the Undisturbed Performance Scenario	CCDFGF	A BRAGFLO and NUTS calculation with undisturbed conditions is sufficient for estimating the consequences of the undisturbed performance scenario.	—	R
CRA-2004, Chapter 6.0, Section 6.4.13.2 Scaling Methodology for Disturbed Performance Scenarios	CCDFGF	Consequences for random sequences of future events are constructed by scaling the consequences associated with deterministic calculations (reference conditions) to other times, generally by interpolation, but sometimes by assuming either similarity or no consequence.	—	R
CRA-2004, Chapter 6.0, Section 6.4.13.3 Estimating Long-Term Releases from the E1 Scenario	CCDFGF NUTS	Reference conditions are calculated or estimated for intrusions at 100, 350, 1,000, 3,000, 5,000, 7,000, and 9,000 years.	Waste-Induced Borehole Flow (H32)	R
CRA-2004, Chapter 6.0, Section 6.4.13.4 Estimating Long-Term Releases from the E2 Scenario	CCDFGF NUTS SECOT2D	The methodology is similar to the methodology for the E1 scenario. For multiple E1 intrusions into the same panel, the additional source term to the Culebra for the second and subsequent intrusions is assumed to be negligible.	Waste-Induced Borehole Flow (H32) Waste Inventory (W2)	R
CRA-2004, Chapter 6.0, Section 6.4.13.5 Estimating Long-Term Releases from the E1E2 Scenario	CCDFGF PANEL	The concentration of actinides in liquid moving up the borehole assumes homogeneous mixing within the panel.	Waste-Induced Borehole Flow (H32)	C
	PANEL	Any actinides that enter the borehole for long-term flow calculations reach the Culebra.	Waste-Induced Borehole Flow (H32)	C

^a R = Reasonable

C = Conservative

Reg. - Based on regulatory guidance

See above - Refers to assumptions 1 through 8 listed at the beginning of this table.

Table MASS-5. General Modeling Assumptions (Continued)

Chapter or Section	Code	Modeling Assumption	Related FEP in Appendix SCR-2009	Assumption Considered ^a
	CCDFGF PANEL	Reference conditions are calculated or estimated for intrusion at 100, 300, 1,000, 2,000, 4,000, 6,000 and 9,000 years.	Oil and Gas Exploration (H1)	—
CRA-2004, Chapter 6.0, Section 6.4.13.6 Multiple Scenario Occurrences	CCDFGF PANEL	The panels are assumed not to be interconnected for long-term brine flow.	Saturated Groundwater Flow (N23) Unsaturated Groundwater Flow (N24)	R
CRA-2004, Chapter 6.0, Section 6.4.13.7 Estimating Releases During Drilling for All Scenarios	CCDFGF PANEL NUTS	Repository conditions will be dominated by Castile brine if any borehole connects to a brine reservoir.	Brine Reservoirs (N2) Natural Borehole Fluid Flow (H31)	R
	CUTTINGS_S PANEL CCDFGF	Depletion of actinides in parts of the repository penetrated by boreholes is not accounted for in calculating the releases from subsequent intrusions at such locations.	Waste-Induced Borehole Flow (H32) Waste Inventory (W2)	C
CRA-2004, Chapter 6.0, Section 6.4.13.8 Estimating Releases in the Culebra and the Impact of the Mining Scenario	CCDFGF	Releases from intrusions at random times in the future are scaled from releases calculated at 100 years with a unit source of radionuclides in the Culebra.	—	R
	CCDFGF	Actinides in transit in the Culebra when mining occurs are transported in the flow field used for the undisturbed case. Actinides introduced subsequent to mining are transported in the flow field used for the disturbed case (i.e., the mined case).	—	R

^a R = Reasonable

C = Conservative

Reg. - Based on regulatory guidance

See above - Refers to assumptions 1 through 8 listed at the beginning of this table.

- 1
- 2 necessarily zero. This effect, which results in additional flux of gas above that predicted by
- 3 application of Darcy's Law, is known as the slip phenomenon, or Klinkenberg effect (Bear 1972,
- 4 p. 128). A correction to Darcy's Law for the Klinkenberg effect is incorporated into the
- 5 BRAGFLO model (see Appendix PA-2009, Section PA-4.2).
- 6 Darcy flow for one and two phases implies that values for principal fluid and rock parameters
- 7 must be specified. Fluid properties in the Darcy flow model used for the WIPP PA are density,
- 8 viscosity, and compressibility, while rock properties are porosity, permeability, and

1 compressibility (pore or bulk). In BRAGFLO, other parameters are required to describe the
2 interactions or interference between the gas and brine phases present in the model because those
3 phases can occupy the same pore space. In the WIPP application of Darcy flow models,
4 compressibility of both the liquid and rock are related to porosity through a dependence on
5 pressure. Fluid density, viscosity, and compressibility are functions of fluid composition,
6 pressure, and temperature. It is assumed in BRAGFLO that fluid viscosity is a function of
7 pressure, but its density and compressibility are held constant. Fluid composition for the
8 purposes of modeling flow and transport is assumed to be constant.

9 **MASS-3.2 Hydrogen Gas as Surrogate for Waste-Generated Gas Physical** 10 **Properties in BRAGFLO and DRSPALL**

11 Hydrogen gas is produced as a result of the corrosion of steel in the repository by water or brine.
12 As in the CCA, the gas phase in the BRAGFLO model is assigned the properties of hydrogen
13 because hydrogen will, under most conditions reasonable for the WIPP, be the dominant
14 component of the gas phase. The model for spillings, DRSPALL, also assigns the physical
15 properties of hydrogen to the gas phase. As discussed in the following text, the effect of
16 assuming flow of pure H₂ instead of a mixture of gases (including H₂, CO₂, H₂S, and CH₄), was
17 shown to be minor relative to the permeability variations in the surrounding formations.

18 Other gases may be produced by processes occurring in the repository. If microbial degradation
19 occurs, a significant amount of CO₂ and possibly methane (CH₄) will be generated by microbial
20 degradation of cellulose and, possibly, plastics and rubbers in the waste. The CO₂ produced,
21 however, will react with the magnesium-oxide (MgO) engineered barrier and cementitious
22 materials to form brucite (Mg(OH)₂), hydromagnesite (Mg₅(CO₃)₄(OH)₂·4H₂O), and calcite
23 (CaCO₃) thus resulting in very low CO₂ fugacity in the repository. Although other gases exist in
24 the disposal system, BRAGFLO calculations assume these gases are insignificant and they are
25 not included in the model.

26 With the average stoichiometry gas generation model, the total number of moles of gas generated
27 will be the same whether the gas is considered to be pure H₂ or a mixture of several gases,
28 because the generation of other gases is accounted for by specifying the stoichiometric factor γ
29 (see Appendix PA-2009, Section PA-4.2.5). Therefore, considering only the moles of gas
30 generated, the pressure buildup in the repository will be approximately the same because the
31 expected gases behave similarly to an ideal gas, even up to lithostatic pressures.

32 The effect of assuming pure H₂ instead of a mixture of gases (including H₂, CO₂, H₂S and CH₄)
33 on flow behavior, and its resulting impact on the WIPP repository pressure, is as follows:

34 Radial flow in a fully saturated rock with nonideal gas is described by Darcy's Law, which, for
35 the given problem, has a solution of the form (Amyx, Bass, and Whiting 1960, p. 78, Equation
36 2-33)

1
$$q_b = 1.988 \times 10^{-5} \left[\frac{T_b Z_b}{P_b} \frac{kh (P_e^2 - P_w^2)}{\mu_{avg} Z_{avg} \ln \left(\frac{r_e}{r_w} \right)} \right] \quad (\text{MASS.1})$$

2 which can be rewritten as

3
$$P_e^2 - P_w^2 = \frac{q_b P_b}{1.988 \times 10^{-5} T_b Z_b} \times \frac{\mu_{avg} Z_{avg}}{kh} \ln \left(\frac{r_e}{r_w} \right) \quad (\text{MASS.2})$$

4 where

- 5 q = gas flow rate (cubic feet per day at base (reference) conditions)
- 6 T = temperature (K)
- 7 P = pressure (pounds per square inch absolute)
- 8 k = permeability (millidarcys)
- 9 h = height (feet)
- 10 μ = viscosity (centipoises)
- 11 Z = gas compressibility factor (defined as the ratio of the actual molar volume of a gas to the
- 12 corresponding ideal gas volume RT/P at the same temperature and pressure)
- 13 r = radius (consistent units)
- 14 R = ideal gas constant
- 15 e = denotes external boundary (repository)
- 16 w = denotes internal boundary (wellbore)
- 17 b = denotes base or reference conditions for gas (temperature, pressure, compressibility
- 18 factor)
- 19 avg = denotes average properties between external and internal boundaries because u and z are
- 20 functions of pressure which change with time

21 This expression is useful for examining the effects of gas properties, specifically the viscosity (μ)

22 and the compressibility (Z) and rock properties (namely k), on the flow rate (q) and the pressure

23 (P).

24 To evaluate the effect of gas composition on q and P, SUPERTRAPP, a computer program

25 developed by the National Institute of Standards and Technology (NIST), was used (National

26 Institute of Standards and Technology 1992). SUPERTRAPP calculates gas properties for 116

27 pure fluids and mixtures of up to 20 components for temperatures to 1,000 K (726 °C, 1340 °F)

28 and pressures to 300 megapascals (MPa). Because such small quantities of H₂S are anticipated

29 at the WIPP, its impact is negligible.

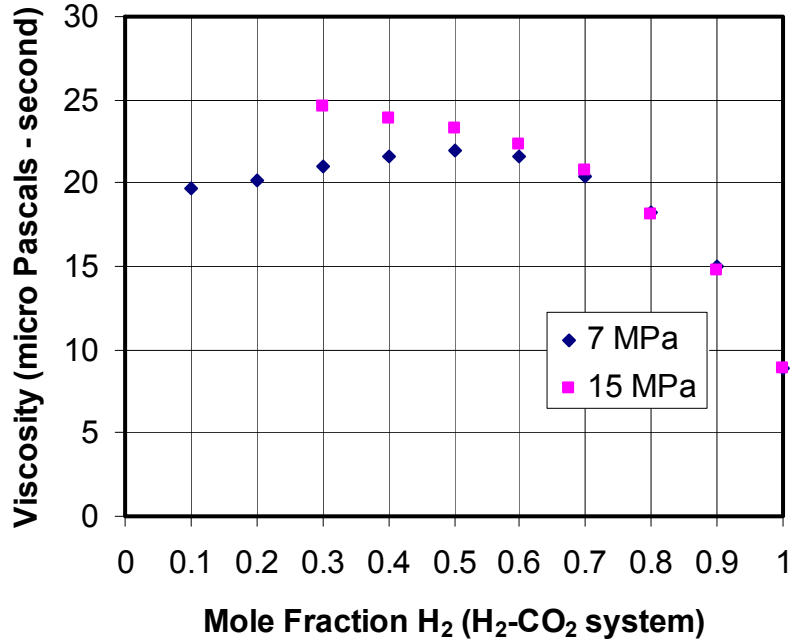
30 Figure MASS-1 shows the relationship between gas viscosity and composition of H₂-CO₂

31 mixtures for various mole fractions of H₂ at pressures of 7 MPa and 15 MPa, as determined from

32 SUPERTRAPP. The viscosity at 50% mole fraction H₂ is about 2.3 times greater than for 100%

33 mole fraction H₂. As shown in Equation (MASS.1), viscosity has an inverse relationship to flow

34 rate and, as shown in Equation (MASS.2), a direct relationship to the square of the repository



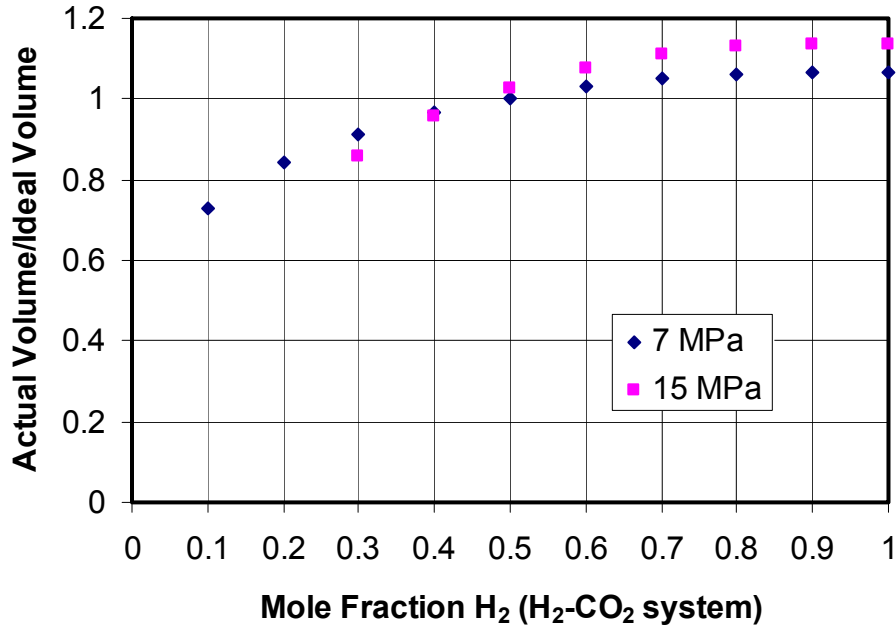
1
2 **Figure MASS-1. Gas Viscosity as a Function of Mole Fraction H₂ at 7 MPa and 15 MPa**
3 **Pressure**

4 pressure. Hence, viscosity differences that would result if gas properties other than those of
5 hydrogen were incorporated would result in a decrease in flow rate and potentially higher
6 pressures.

7 As shown in Figure MASS-2, the gas compressibility at 50% mole fraction H₂ is about 0.9 times
8 that of pure H₂. Like viscosity, the gas compressibility (actual volume/ideal volume) is inversely
9 related to flow rate and directly related to the square of the repository pressure. Therefore, the
10 impact of variation in gas compressibility caused by composition is considered minor and is not
11 considered.

12 The viscosity and compressibility calculations described above for H₂-CO₂ mixtures were
13 repeated for H₂-CH₄ mixtures for various mole fractions of H₂ at pressures of 7 MPa and 15 MPa
14 (Kanney 2003). The variability of viscosity with the composition for the H₂-CH₄ mixtures is
15 smaller than that observed for the H₂-CO₂ mixtures. For example, at 15 Mpa, the gas viscosity
16 of H₂-CH₄ at 50% mole fraction is only 1.6 times greater than the viscosity at 100% mole
17 fraction. The H₂-CH₄ mixtures are only slightly less compressible than the H₂-CO₂ mixtures.
18 For example, at 15 MPa, the gas compressibility of the H₂-CH₄ at 50% mole fraction is
19 approximately 0.94 times the compressibility at 100% mole fraction. Changing composition
20 from 100% to 50% H₂ would result in a slight increase in flow rate and a decrease in pressure.

21 The permeability of each component of the formation plays a significant role in determining both
22 flow rate and pressure. Because marker bed (MB) permeabilities and Salado impure halite
23 permeabilities vary over three to four orders of magnitude (see Fox 2008, Table 30 and Table
24 31), the permeabilities of these flow pathways will have a greater influence on pressure and flow
25 rate determinations than either uncertainty in viscosity or gas compressibility effects.



1
2 **Figure MASS-2. Gas Compressibility as a Function of Mole Fraction H₂**

3 Note that the BRAGFLO code includes a pressure-induced fracture model that will limit pressure
4 increases in the repository (Schreiber 1997). For example, at high repository pressures, the
5 factor of 1.5 pressure increase calculated here using the simplified Darcy’s Law model is
6 unlikely to be seen in the BRAGFLO results, since fracturing will lead to increased permeability,
7 effectively limiting pressure increases.

8 **MASS-3.3 Salado Brine as Surrogate for Liquid-Phase Physical Properties in**
9 **BRAGFLO**

10 BRAGFLO uses Salado Formation brine properties as the physical properties for all liquids.
11 However, liquid in the modeled region may consist of (1) brine originally in the Salado, (2)
12 liquid introduced in the excavation during construction, maintenance, and ventilation during the
13 operational phase, (3) a very small amount of liquid introduced as a component of the waste,
14 (4) liquid from overlying units, and (5) liquid from the Castile brine reservoir. However, for
15 BRAGFLO modeling, it is assumed that the properties of all of these liquids are similar enough
16 to Salado brine properties that the effect of any variation in properties resulting from liquids
17 mixing is negligible. The variations in chemical properties of brine are accounted for as
18 discussed in Appendix SOTERM-2009, Section SOTERM-2.0, Section SOTERM-2.3, and
19 Section SOTERM-5.0.

1 **MASS-4.0 Model Geometries**

2 This section presents supplementary information on the disposal system geometry.

3 **MASS-4.1 Disposal System Geometry as Modeled in BRAGFLO**

4 Overall, the conceptual model of the disposal system geometry represents the spatial effects of
5 process interactions in two dimensions. The geometry used to represent long-term fluid flow
6 processes in the Salado, flow between a borehole and overlying units and flow within the
7 repository (where processes coupled to fluid flow such as creep closure and gas generation
8 occur), is a vertical cross-section through the repository on a north-south axis shown in Figure
9 MASS-3 (see also Appendix PA-2009, Section PA-4.2.1). The dimension of this geometry in
10 the direction perpendicular to the plane of the cross-section varies so that spatial effects of
11 certain processes can be better represented.

12 For fluid flow and transport modeling in the Culebra, the geometry is a horizontal, two-
13 dimensional plane (see Appendix PA-2009, Section PA-4.8, Figure PA-32). For modeling brine
14 flow from the intruded panel to the borehole during drilling (DBR), the geometry is a two-
15 dimensional, horizontal representation of a waste panel as described in Section MASS-16.2 (see
16 also the CRA-2004, Chapter 6.0, Section 6.4.7.1).

17 Using a two-dimensional geometry to represent the three-dimensional Salado flow is based on
18 the assumption that brine and gas flow will converge upon and diverge from the repository
19 horizon. Grid flaring is used when flows can be represented as divergent and convergent from
20 the center of the flaring (see Section MASS-4.2.5). The impact of this conceptual model and its
21 implementation in a two-dimensional grid has been compared to a model that does not make the
22 assumption of convergent and divergent flow (see the CRA-2004, Appendix PA, Attachment
23 MASS, Attachment 4-1 for additional information). The conceptual model for the Salado also
24 includes the slight and variable dip of beds in the vicinity of the repository, which might affect
25 fluid flow.

26 Above and below the repository, it is assumed that any flow between the borehole or shaft (see
27 the CRA-2004, Chapter 6.0, Section 6.4.3) and surrounding materials will converge or diverge.
28 With respect to flow in units overlying the Salado, the only purpose of this conceptual model is
29 to determine the quantity (flux) of fluid leaving or entering the borehole or shaft. Fluid
30 movement through the units above the Salado is treated in a different conceptual model (see the
31 CRA-2004, Chapter 6.0, Section 6.4.6). Below the repository, the possible presence of a brine
32 reservoir is considered to be important, so a hydrostratigraphic layer representing the Castile and
33 a possible brine reservoir in it is included (see the CCA, Appendix MASS, Section MASS-4.2
34 for the disposal system geometry historical context prior to the CCA).

35 **MASS-4.2 Change to Disposal System Geometry since the CCA**

36 Changes have been made to the disposal system geometry since the first WIPP certification. The
37 disposal system geometry is specifically represented in BRAGFLO. This section describes the
38 methodology used to create the two-dimensional BRAGFLO computational grid used for the

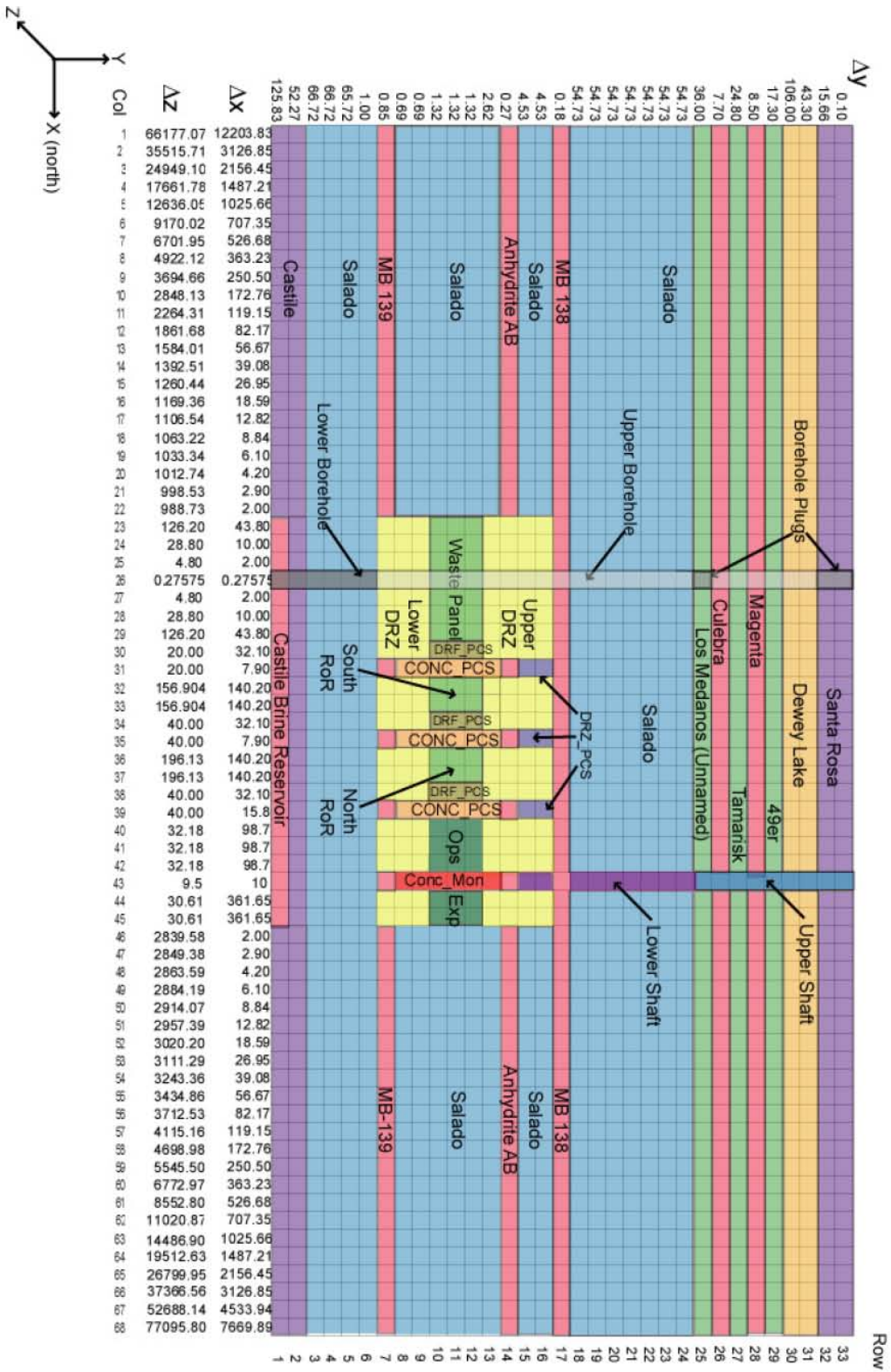


Figure MASS-3. Logical Grid Used for the CRA-2004 and 2009 PA BRAGFLO Calculations

1 CRA-2004 PA calculations. The CRA-2004 grid is similar to the CCA and the CCA
2 Performance Assessment Verification Test (PAVT) grids, except for the differences described
3 below. Since no changes have been made to the geometry since the CRA-2004 PABC, this grid
4 was used in the CRA-2009 PA.

5 The most important changes affecting the CRA-2004 BRAGFLO grid were the implementation
6 of the Option D panel closures and a simplified shaft seal model. Additional grid refinements
7 were also made to increase numerical accuracy and computational efficiency and to reduce
8 numerical dispersion. These changes modify the conceptual models. All conceptual model
9 changes were approved by the Salado Flow Peer Review Panel in February 2003 (Caporuscio,
10 Gibbons, and Oswald 2003). For completeness, all changes from the CCA PA/CCA PAVT grid
11 are described here. These changes were made and approved by the EPA in the 2004
12 recertification decision (U.S. Environmental Protection Agency 2006) and are repeated here for
13 completeness and to show the historical progression of the grid from the CCA to the CRA-2009
14 PA.

15 **MASS-4.2.1 CCA to CRA-2004 Baseline Grid Changes**

16 The baseline grid used in the CCA PA and the CCA PAVT had 33 cells in the x direction and 31
17 cells in the y direction, while the grid used for the CRA-2004 PA and later calculations has
18 dimensions 68 by 33 cells. The specific changes implemented in the CRA-2004 grid are listed
19 below and discussed in more detail in the following sections. Logical grids for the CCA PA, the
20 CCA PAVT, and the CRA-2004 and CRA-2009 PAs are shown in Figure MASS-3 and Figure
21 MASS-4.

22 The following changes have been implemented in the CRA-2004 grid:

- 23 1. A simplified shaft seal model is implemented.
- 24 2. Option D-type panel closures are implemented.
- 25 3. Segmentation of the waste regions is increased.
- 26 4. A grid-flaring method is redefined and simplified.
- 27 5. X spacing of the grid beyond the repository to the north and south is refined.
- 28 6. Layers above and below MB 139 have been made relatively thin (~1 m thick), and Y spacing
29 in the Salado has been changed.

30 **MASS-4.2.2 CRA-2004 Simplified Shaft Seal Model**

31 A shaft seal model is included in the CRA-2004 grid, but it is implemented in a simpler fashion
32 than that used for the CCA PA and the CCA PAVT. A detailed description of the parameters
33 used to define the simplified model is discussed in AP-094 (James and Stein 2002) and the
34 resulting analysis report (James and Stein 2003). The model used in the CRA-2004 PA is
35 described by Stein and Zelinski (2003a and 2003b), and was approved by the Salado Flow Peer
36 Review Panel (Caporuscio, Gibbons, and Oswald 2003).

CCA/PAVT Grid

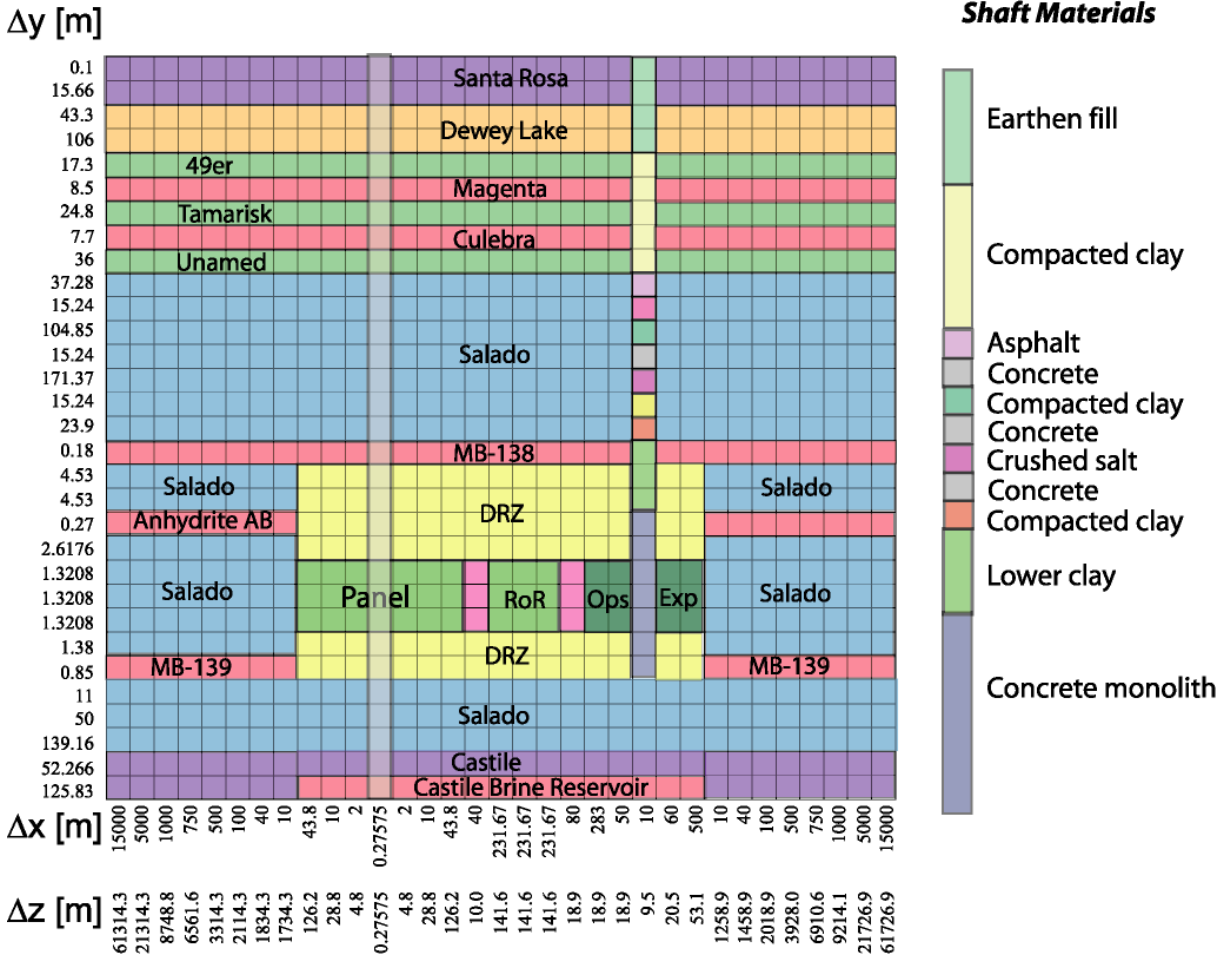
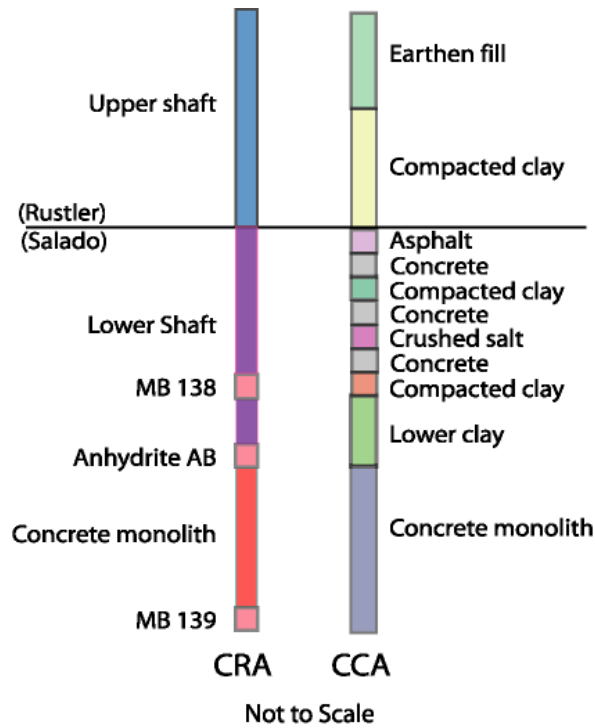


Figure MASS-4. Logical Grid Used for the CCA PA BRAGFLO Calculations

The new model does not alter the conceptual model of the shaft seal components as described in the CCA. Rather, it simplifies the representation of seal components in the repository system model. The CRA and CCA shaft models are graphically compared in Figure MASS-5. The simplified shaft model was tested in the AP-106 calculations (Stein and Zelinski 2003a and 2003b), which supported the Salado Flow Peer Review (see the CRA-2004, Chapter 9.0, Section 9.1.3.4). The results of this analysis demonstrated that brine flow through the simplified shaft model was comparable to brine flows through the detailed shaft model in the CCA PAVT calculations. The conclusion remains that the shaft seals are very effective barriers to flow throughout the 10,000-year regulatory period. The CRA-2004 PA shaft representation is used in the CRA-2009 PA.

MASS-4.2.3 CRA-2004 Implementation of Option D-Type Panel Closure

In the CCA, the DOE presented four options for panel closure designs (A through D). Upon reviewing the CCA, the EPA mandated the implementation of the Option D design. For the



1

2

3

Figure MASS-5. Comparison of the Simplified Shaft (CRA-2004 and CRA-2009) and the Detailed Shaft (CCA) Models

4

5

6

7

8

9

CRA-2004, the true cross-sectional area of the Option D panel closures was represented in the flow model. In addition, to appropriately represent the effect of Option D geometry on repository fluid flow, the segmentation of the waste regions was increased in the grid. This change is described fully in the CRA-2004, Appendix PA, Attachment MASS, Section MASS-4.2.4. The CRA-2009 PA continues to use the same panel closure representation as the CRA-2004 PA.

10

11

12

13

14

15

For CRA-2004, three sets of panel closures are included in the model domain. The southernmost set of closures represents a pair of closures separating a single waste panel from the other waste areas. The middle set of closures represents four panel closures that will be emplaced between the southern and northern extended panels. The northernmost set of panel closures represents two sets of four panel closures that will be emplaced between the waste regions and the shaft seals.

16

17

Each set of panel closures is represented in the CRA-2004 grid with four materials. Refer to Figure MASS-6.

18

19

1. CONC_PCS: This material represents the concrete monolith, which has properties of Salado Mass Concrete (SMC).

20

21

2. DRZ_PCS: This material represents the DRZ immediately above the concrete monolith that is expected to heal after the emplacement of the monolith.

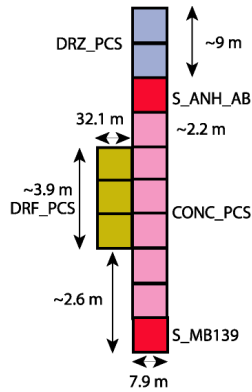


Figure MASS-6. Logical Grid Representation of the Option D Panel Closures for the CRA

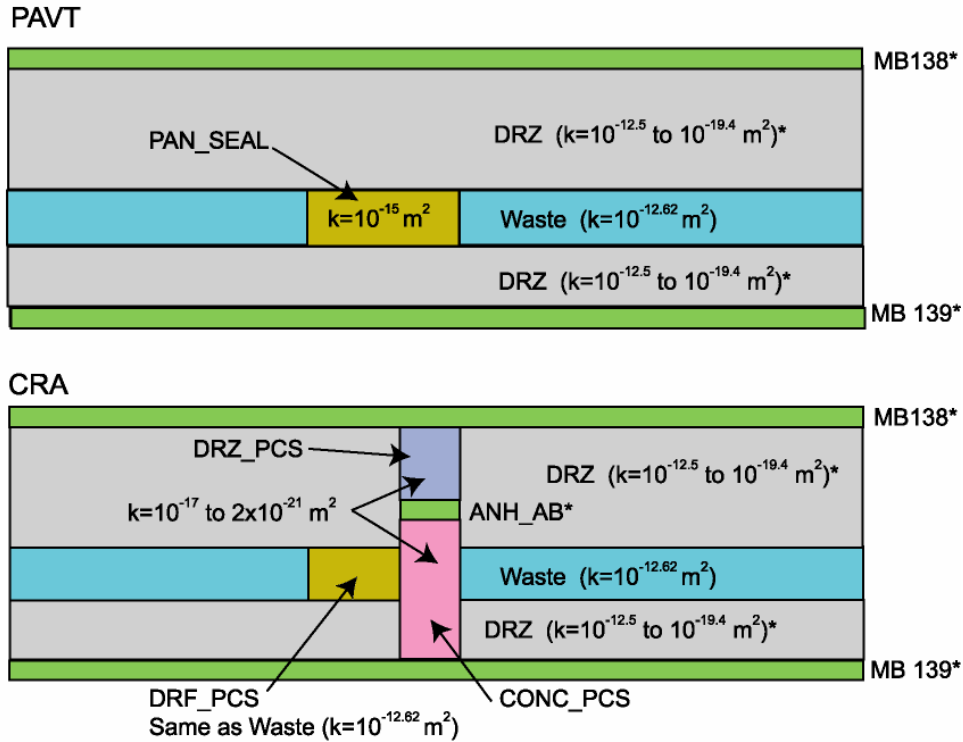
3. DRF_PCS: This material represents the empty drift and explosion wall portion of the panel closure. This material has the same properties as WAS_AREA (including creep closure).
4. MB materials S_ANH_AB and S_MB 139: These materials are the same as those used to represent the anhydrite MBs in other parts of the grid. MB materials were used because they have permeability ranges very close to the material CONC_PCS and in the case when pressures near the panel closures exceed the fracture initiation pressure of the MBs, fractures could extend around the concrete monolith out of the 2-D plane represented by the numerical grid. By using MB materials to represent the parts of the panel closures that intersect MBs, both the permeability of the closure and the potential fracture behavior of MB material near the closures are represented.

Figure MASS-7 is a schematic diagram comparing the panel closure implementation in the CCA and CRA-2004 grids. Permeability ranges are indicated for all materials. Figure MASS-6 shows the 13 grid cells used to represent each set of Option D panel closures in the CRA-2004 BRAGFLO grid.

MASS-4.2.4 Increased Segmentation of Waste Regions in Grid

The CCA PA/CCA PAVT grid divided the waste region into two regions: a single panel in the southern end of the repository referred to as the Waste Panel, and a larger region containing the other nine panels referred to as the RoR. The Waste Panel is intersected by an intrusion borehole and is used to represent conditions in any panel intersected by a borehole.

It is assumed that the Option D panel closures are effective at impeding flow between panels. Therefore, it was considered necessary to divide the rest of repository (RoR) into northern and southern blocks separated by a set of panel closures. The south RoR block represents conditions in a panel directly adjacent to an intruded panel. The north RoR block represents conditions in a nonadjacent panel far from the intruded panel (i.e., it has at least two panel closures between it and the intruded panel). This representation assumes that the effects of drilling intrusions will be damped in nonintruded panels, and the degree of damping will depend on the proximity of the drilling intrusion and the number of panel closures separating the intruded panel from other regions of the repository. The CRA-2009 PA uses the same segmentation of the waste regions as in the CRA-2004 PA. (See the CRA-2004, Appendix PA, Attachment MASS, Section MASS-4.2.4 for a description of waste-region segmentation.)



[* = allowed to fracture, permeability is pressure dependant above ~12.5 MPa]

1
2 **Figure MASS-7. Schematic Comparison of the Representation of Panel Closures in the**
3 **CCA PAVT and CRA-2004**

4 **MASS-4.2.5 CRA-2004 Redefined and Simplified Grid Flaring Method**

5 Grid flaring is a method to represent three-dimensional volumes in a two-dimensional grid.
6 Flaring is used when flows can be represented as divergent and convergent from the center of
7 flaring. The CCA PA/CCA PAVT grid used flaring at two different scales: locally around the
8 borehole and shaft, and regionally to the north and south of the excavated regions (around a point
9 in the northern end of the RoR). For the CRA-2004 PA, the local flaring around the borehole is
10 the same as in the CCA PA/CCA PAVT grid. The local flaring around the shaft was eliminated
11 because it had been demonstrated not to be a release pathway. Likewise, the manner in which
12 the regional flaring was calculated has been simplified. The CRA-2009 PA uses the same grid
13 flaring as in the CRA-2004 PA. (See the CRA-2004, Appendix PA, Attachment MASS, Section
14 MASS-4.2.5 for a description of grid flaring).

15 **MASS-4.2.6 CRA-2004 Refinement of the X-Spacing Outside the Repository**

16 The grid blocks to the north and south of the excavated region were refined in the x-direction
17 from the baseline grid. The x dimension of the grid cells immediately to the north and south of
18 the repository starts at 2 m and increases by a factor of 1.45.

1 Exceptions to this are made to ensure that the location of the Land Withdrawal Boundary and the
2 total extent of the grid matches that in the baseline grid. This CRA-2004 PA refinement factor
3 was chosen to reduce numerical dispersion caused by rapid increases in cell dimensions
4 (Anderson and Woessner 1992 and Wang and Anderson 1982). The CRA-2009 PA continues to
5 use this refinement.

6 **MASS-4.2.7 CRA-2004 Refinement of the Y-Spacing**

7 During the CRA-2004 PA, the y direction grid spacing within the layers representing the Salado
8 was changed from the CCA PA/CCA PAVT grid spacing. The Salado grid spacing used in the
9 CCA PA was dictated by the thickness of different shaft seal materials. Since the shaft is no
10 longer represented in the model domain, the y spacing in the Salado is now uniform. In addition,
11 two layers were added immediately above and below MB 139 to refine the grid spacing and
12 reduce numerical dispersion. These changes resulted in a total of 33 y divisions for the grid, and
13 increased the numerical accuracy of flow and transport calculations.

14 The x and y direction refinements used in the CRA-2004 PA grid are included in the CRA-2009
15 PA.

1 **MASS-5.0 BRAGFLO Geometry of the Repository**

2 The BRAGFLO code uses a grid to represent the conceptual model of the repository geometry
3 (see Figure MASS-3). As with the geometry of the disposal system discussed in the CRA-2004,
4 Chapter 6.0, Section 6.4.2.1 and earlier in this appendix, the principal process considered in
5 setting up the repository geometry is fluid flow. Several features considered to be important in
6 fluid flow are included in the conceptual model. The first is the overall dimension of the
7 repository along the north-south trend of the cross section, as well as the major divisions within
8 the repository (i.e., waste disposal region, operations region, and experimental region). The
9 second is the volume of a single panel, because fluid flow to a borehole penetrating the
10 repository may have direct access only to the volume in a waste panel. Access to other regions
11 of the repository may require flow through or around a panel closure. The third feature is the
12 physical dimensions of panel closures separating the single panel and the other major divisions
13 of the repository.

14 Notably absent from the conceptual model for the long-term performance of the repository are
15 pillars and individual drifts and rooms. These are excluded from the model for simplicity, and it
16 is assumed that they have either negligible impact on fluid-flow processes or, alternatively, that
17 including them in the conceptual model would be beneficial to long-term performance because
18 their presence could make flow paths more tortuous and decrease fluxes. This assumption
19 includes lumping four and five of the 10 panels into the south RoR and north RoR regions
20 respectively (see the CRA-2004, Appendix PA, Attachment MASS, Section MASS-4.2.4).

21 The BRAGFLO model of the WIPP disposal system is a two-dimensional array of three-
22 dimensional grid blocks. Each grid block has a finite length, width, height, volume, and surface
23 area for its boundaries with neighboring grid blocks. The BRAGFLO two-dimensional grid is
24 similar to any other two-dimensional grid used to treat flows, except that the grid-block
25 dimension in the z direction (perpendicular to the plane of the grid) varies from block to block as
26 a function of the x direction (the lateral direction) (see the CRA-2004, Appendix MASS, Section
27 MASS-4.2.5). This allows the BRAGFLO grid to treat important geometric aspects of the WIPP
28 disposal system, such as the very small intrusion borehole, the moderate-sized shaft, and the
29 larger controlled areas. The grid configurations used in the CCA PA and the CCA PAVT are
30 shown in Figure MASS-4, while the grid used for the CRA-2004 PA and the CRA-2009 PA is
31 shown in Figure MASS-3.

32 **MASS-5.1 Historical Context of the Repository Model**

33 Several early models of repository fluid-flow behavior—including models of radionuclide
34 migration pathways, gas flow from the disposal area to the shaft, Salado brine flow through
35 panel to borehole, effects of anhydrite layers on Salado brine flow through a panel, and flow
36 from a brine reservoir through a disposal room—are summarized in Rechar et al. (1990, pp.
37 153–60). In the preliminary PA of 1992, all waste was lumped into a single region (WIPP
38 Performance Assessment 1993). Because human intrusion boreholes were treated in detail for
39 the CCA PA, it was necessary to model a single waste panel with a borehole surrounded by two-
40 dimensional radial-flaring gridblocks. This approach is continued for the CRA-2009 PA. The
41 CCA PA treated the remainder of the waste area as a single RoR. For the CRA-2004 PA and
42 subsequent analyses, the RoR is divided into two areas separated by a panel closure system. As

1 discussed earlier, this change was made to more adequately simulate the effects of the Option D
2 closure in impeding fluid flow between panels.

3 **MASS-5.2 CRA-2009 Repository Model**

4 The repository model for the CRA-2009 PA is the same model used in the CRA-2004 PABC.
5 That model used the same features described for the CRA-2004 PA, with no changes to the
6 representation of the repository geometry or BRAGFLO grid.

1 **MASS-6.0 Creep Closure**

2 The creep closure model used in the CRA-2009 is the same used in the CRA-2004 and the CRA-
3 2004 PABC. The model used for creep closure of the repository is discussed in Appendix
4 PORSURF-2009. Historical information on creep closure modeling is also contained in
5 Appendix PORSURF-2009.

1 **MASS-7.0 Repository Fluid Flow**

2 Most repository fluid flow assumptions have not changed from those used in the CRA-2004
3 PABC. Those that did not change are discussed in Section MASS-7.1 and Section MASS-7.2
4 while those that did change are discussed in Section MASS-7.3. This model represents the long-
5 term flow behavior of liquid and gas in the repository and its interaction with other regions in
6 which fluid flow may occur, such as the Salado, shafts, or an intrusion borehole. This model is
7 not used to represent the interaction of fluids in the repository with a borehole during drilling.
8 Historical information on alternative conceptual models for brine inflow to the repository is
9 contained in the CCA, Appendix MASS, Section MASS-7.0).

10 The first principle in the conceptual model for fluid flow in the repository is that gas and brine
11 can both be present and mobile (two-phase flow), governed by conservation of energy and mass
12 and by Darcy's Law for their fluxes (see Appendix PA-2009, Section PA-4.2). Consistent with
13 typical concepts of two-phase flow, the phases can affect each other by impeding flow caused by
14 partial saturation (relative permeability effects) and by affecting pressure caused by capillary
15 forces (capillary pressure effects).

16 The flow of brine and gas in the repository is assumed to behave as two-phase, immiscible,
17 Darcy flow (see Appendix PA-2009, Section PA-4.2). BRAGFLO is used to simulate brine and
18 gas flow in the repository and to incorporate the effects of disposal-room closure and gas
19 generation. Fluid flow in the repository is affected by the following factors:

- 20 • The geometric association of pillars, rooms, and drifts; panel closure caused by creep; and
21 possible borehole locations
- 22 • The varied properties of the waste areas resulting from creep closure and heterogeneous
23 contents
- 24 • Flow interactions with other parts of the disposal system
- 25 • Reactions that generate gas

26 The geometry of the panel around the intrusion borehole is consistent with the assumption that
27 the fluid flow there will occur directly toward or directly away from the borehole. The geometry
28 represents a semicircular volume north of the borehole and a semicircular volume south of the
29 borehole (representing radial flow in a subregion of a two-dimensional representation of the
30 repository).

31 Approximating convergent and divergent flow around the intrusion borehole creates a narrow
32 neck in the otherwise fairly uniform width grid in the region representing the repository. In the
33 undisturbed performance scenario, and under certain conditions in other scenarios, flow in the
34 repository may pass laterally through this neck. In reality, this neck does not exist. Its presence
35 in the model is expected to have a negligible or conservative impact on model predictions
36 compared to predictions that would result from a more realistic model geometry. The time scale
37 involved and the permeability contrast between the repository and surrounding rock are
38 sufficient so that the lateral flow that may occur in the repository is restricted by the rate at which

1 liquid gets into or out of the repository, rather than by the rate at which it flows through the
2 repository.

3 Gas generation is affected by the quantity of liquid in contact with metal. However, the
4 distribution of fluid in the repository can only be approximated. For example, capillary action
5 can create wicking that would increase the overall region in which gas generation occurs, but
6 modeling this at the necessary resolution to simulate these processes would greatly increase the
7 time required to carry out the modeling (Appendix PA-2009, Section PA-4.2.6 and CRA-2004,
8 Section 6.4.3.3). Therefore, as a bounding measure for gas generation purposes, brine in the
9 repository is distributed to an extent greater than estimated by the Darcy flow models or by the
10 values of parameters chosen.

11 Option D panel closures and the surrounding rocks are represented by a group of materials,
12 including

13 1. SMC

14 2. A material representing the empty drift and explosion wall

15 3. A material representing healed DRZ

16 4. MBs

17 SMC and healed DRZ materials are assigned permeability values sampled independently from a
18 distribution ranging from 2×10^{-21} to 1×10^{-17} m². This value range is considered reasonable
19 because the shape of the Option D closure assumes a compressive state that maintains a concrete
20 permeability range similar to the CCA PAVT permeability. This range captures the uncertainty
21 in the long-term performance of the Option D panel closure design.

22 Modeling of flow within the repository is based on homogenizing the room contents into
23 relatively large computational volumes. The approach ignores heterogeneities in disposal room
24 contents that may influence gas and brine behavior by causing fluid flow among channels or
25 creating preferential paths in the waste, bypassing entire regions. Isolated regions could exist for
26 several reasons:

- 27 • They may be isolated by low-permeability regions of waste that serve as barriers.
- 28 • Connectivity with the interbeds may occur only at particular locations within the repository.
- 29 • The repository dip may promote preferential gas flow in the upper regions of the waste.

30 For the CCA, the adequacy of the repository homogeneity assumption was examined in
31 screening analyses DR-1 (Webb 1995) and DR-6 (Vaughn, Lord, and MacKinnon 1995a). These
32 analyses used an additional parameter in BRAGFLO to specify the minimum active (mobile)
33 brine flow saturation (pseudoresidual brine saturation). Above this saturation, the normal
34 descriptions of two-phase flow apply (i.e., either the Brooks and Corey or van Genuchten and
35 Parker relative permeability models). Below this minimum, brine is immobile, although it is
36 available for reaction and may still be consumed during gas-generation reactions. The

1 assumption of a minimum saturation limit was justified based on the presumed heterogeneity of
2 the waste and the slight dip in the repository. The minimum active brine saturation was treated
3 as an uncertain parameter and sampled uniformly between the values 0.1 and 0.8 during the
4 analysis. This saturation limit was applied uniformly throughout the disposal room to bound the
5 impact of heterogeneities on flow (Webb 1995 and Vaughn, Lord, and MacKinnon 1995a).
6 Results of this analysis showed that releases to the accessible environment in the baseline case
7 (homogenization) are consistently higher.

8 The experimental and operations regions were represented in the CCA PA by a fixed porosity of
9 18.0% and a permeability of 10^{-11} m². The combination of low porosity and high permeability
10 conservatively overestimated fluid flow through these regions and limited the capacity of these
11 regions to store fluids, potentially overestimating releases to the environment. This conclusion
12 was based on a screening analysis (Vaughn, Lord, and MacKinnon 1995b) that examined the
13 importance of permeability varying with porosity in closure regions (waste disposal region,
14 experimental region, and operations region). To perform this analysis, a model for estimating
15 the change in permeability with porosity in the closure regions was implemented in BRAGFLO.
16 A series of BRAGFLO simulations was performed to determine whether permeability varying
17 with porosity in the closure regions could enhance contaminant migration to the accessible
18 environment. Two basic scenarios were considered in the screening analysis: undisturbed
19 performance and disturbed performance. To assess the sensitivity of system performance on
20 dynamic permeability in the closure regions, CCDFs of normalized contaminated brine releases
21 were constructed and compared with the corresponding baseline conditional CCDFs. The
22 baseline model treated permeabilities in the closure regions as fixed values. Results of this
23 analysis showed that the inclusion of dynamic closure of the waste disposal region, experimental
24 region, and operations region in BRAGFLO resulted in computed releases to the accessible
25 environment that are essentially equivalent to the baseline case.

26 A separate analysis (Park and Hansen 2003) examined the possible effects of heterogeneity in
27 waste container and waste material strength on room closure. The analysis of room closure
28 found that the room porosity may vary widely depending on the type of waste container and the
29 emplacement of waste in the repository. However, analysis of a separate PA (Hansen et al.
30 2003) found that PA results are relatively insensitive to the uncertainty in room closure and room
31 porosity. The conclusions of the separate PA are summarized in Section MASS-21.0 of this
32 appendix.

33 **MASS-7.1 Flow Interactions with the Creep Closure Model**

34 The dynamic effect of halite creep and room consolidation on room porosity is modeled only in
35 the waste disposal region. Other parts of the repository, such as the experimental region and the
36 operations region, are modeled assuming fixed (invariant with time) properties. In these regions,
37 the permeability is held at a fixed high value representative of unconsolidated material, while the
38 porosity is maintained at relatively low values associated with highly consolidated material. This
39 combination of low porosity and high permeability is assumed to conservatively overestimate
40 flow through these regions and minimize the capacity of this material to store fluids, thus
41 maximizing the release to the environment. To examine the acceptability of this assumption, a
42 screening analysis (Vaughn, Lord, and MacKinnon 1995c) evaluated the effect of including
43 closure of the experimental region and operations region. In this analysis, consolidation of the

1 experimental region and operations region was implemented in BRAGFLO by relating pressure
2 and time to porosity using a porosity-surface method. The porosity surface for the experimental
3 region and operations region differs from the surface used for consolidation of the disposal room
4 and is based on an empty excavation (see Appendix PORSURF-2009). The screening analysis
5 showed that disregarding dynamic closure of the experimental region is acceptable because it is
6 conservative: lower releases occur when closure of the experimental region and operations
7 region is computed compared to simulations with time-invariant high permeability and low
8 porosity.

9 **MASS-7.2 Flow Interactions with the Gas Generation Model**

10 Gas generation affects repository pressure, which in turn is an important parameter in other
11 processes such as two-phase flow, creep closure, and fracturing of the interbeds and DRZ. Gas-
12 generation processes considered in PA calculations include anoxic corrosion and microbial
13 degradation. Radiolysis is excluded from PA calculations on the basis of laboratory experiments
14 and a screening analysis (Vaughn et al. 1995) that concluded that radiolysis does not
15 significantly affect repository performance.

16 In modeling gas generation, the effective liquid in a computational cell is the computed liquid in
17 that cell plus an adjustment for the uncertainty associated with wicking by the waste (see
18 Appendix PA-2009, Section PA-4.2.6). Capillary action (wicking) is the ability of a material to
19 carry a fluid by capillary forces above the level it would normally seek in response to gravity.
20 Because the current gas-generation model computes substantially different gas-generation rates
21 depending on whether the waste is wet or merely surrounded by water vapor, the physical extent
22 of wetting could be important. A screening analysis (Vaughn, Lord, and MacKinnon 1995d)
23 examined wicking and concluded that it should be included in PA calculations.

24 The baseline gas-generation model in BRAGFLO accounts for corrosion of iron and microbial
25 degradation of cellulose and possibly plastics and rubber. The net reaction rate of these
26 processes depends directly on brine saturation: an increase in brine saturation will increase the
27 net reaction rate by weighting the inundated portion more heavily and the slower humid portion
28 less heavily. To simulate the effect of wicking on the net reaction rate, an effective brine
29 saturation, which includes a wicking saturation contribution, is used to calculate reaction rates
30 rather than the actual brine saturation. To account for uncertainty in the wicking saturation
31 contribution, this contribution was sampled from a uniform distribution from 0.0 to 1.0 for each
32 BRAGFLO simulation in the analysis.

33 **MASS-7.3 CRA-2009 Flow Interactions with the Gas-Generation Model** 34 **Changes**

35 The assumptions for brine availability were changed in BRAGFLO Version 6.0 to account for
36 brine-consuming reactions. Brine-consuming reactions such as anoxic corrosion tend to dry out
37 the waste-filled regions of the repository. The former BRAGFLO code and underlying models
38 could not simulate completely dry cells in the grid. To accommodate brine-consuming reactions
39 and allow the code to run, BRAGFLO Version 6.0 includes a lower cut off in brine saturation for
40 waste-filled regions in the repository, representing a numerically dry condition. At this cut-off
41 saturation, biodegradation and iron corrosion ceases. This modification is explained fully in

- 1 Section 5.2.2 of Nemer and Clayton (2008). BRAGFLO version 6.0 was used in the CRA-2009
- 2 PA; older versions of the code were used in previous PAs.

1 **MASS-8.0 Gas Generation**

2 The gas generation model represents the possible generation of gas in the repository by corrosion
3 of steel and microbial degradation of CPR materials. The CRA-2009 uses the CRA-2004 PABC
4 gas generation modeling assumptions. Although the amount of the excess MgO engineered
5 barrier emplaced in the repository has been reduced from 1.67 to 1.2, the PA methodology does
6 not account for any excess material in the modeling assumption and therefore no changes to
7 these assumptions are necessary. Additional discussion of this topic may be found in Appendix
8 PA-2009, Section PA-4.2.5 and Appendix SCR-2009 (FEPs W44 through W48, W53, and N71)
9 and the CRA-2004, Chapter 6.0, Section 6.4.3.3.

10 **MASS-8.1 Historical Context of Gas Generation Modeling**

11 See the CCA, Appendix MASS, Section MASS-8.1 for historical information on the
12 development of the CCA gas-generation conceptual model.

1 **MASS-9.0 Chemical Conditions**

- 2 The chemical conditions modeling assumptions have not changed from those in the CRA-2004
3 PABC. The models used for chemical conditions in the repository are discussed in Appendix
4 MgO-2009 and Appendix SOTERM-2009.

1 **MASS-10.0 Dissolved Actinide Source Term**

2 The dissolved An source term modeling assumptions have not changed from those in the CRA-
3 2004 PABC. The models used for the dissolved An source term in the repository are discussed
4 in Appendix SOTERM-2009, Section SOTERM-4.0 and Section SOTERM-5.0.

1 **MASS-11.0 Colloidal Actinide Source Term**

- 2 The colloidal An source term modeling assumptions have not changed from those in the CRA-
3 2004 PABC. The models used for the colloidal An source term are discussed in Appendix
4 SOTERM-2009, Section SOTERM-3.8.

1 **MASS-12.0 Shafts and Shaft Seals**

- 2 The shafts and shaft seals modeling assumptions have not changed from those in the CRA-2004
3 PABC. The models used for shafts and shaft seals are discussed in the CRA-2004, Appendix
4 PA, Attachment MASS, Section MASS-12.0.

1 **MASS-13.0 Salado**

2 The far-field Salado modeling assumptions used in the CRA-2009 are the same as those used in
3 the CRA-2004 PABC. No changes have been made to these modeling assumptions for the CRA-
4 2009 PA. The purpose of this model is to reasonably represent the effects of fluid flow in the
5 Salado on long-term performance of the disposal system. The conceptual model is also
6 discussed in the CRA-2004, Chapter 6.0, Section 6.4.5. The Salado fluid flow model represented
7 in the CRA-2004 PABC is also used in the CRA-2009 PA (Nemer and Clayton 2008).

8 Fluid flow in the Salado is considered in the conceptual model of long-term disposal system
9 performance for several reasons. First, some liquid could move from the Salado to the repository
10 because of the considerable gradients that can form for liquid flow inward to the repository. This
11 possibility is important because such fluid can affect creep closure, gas generation, An solubility,
12 and other processes occurring in the repository. Second, gas generated in the repository is
13 thought to be capable of fracturing the Salado interbeds under certain conditions, creating
14 increased permeability channels that could be pathways for lateral transport. The lateral
15 transport pathway in intact Salado is also modeled, but it is considered unlikely to result in any
16 significant radionuclide transport to the accessible environment boundary.

17 The fundamental principle in the conceptual model for fluid flow in the Salado is that it is a
18 porous medium within which gas and brine can both be present and mobile (two-phase flow),
19 governed by conservation of energy and mass and by Darcy's Law for their fluxes (see Appendix
20 PA-2009, Sections PA-4.2). Consistent with typical concepts of two-phase flow, each phase can
21 affect the other by impeding flow because of partial saturation (relative permeability effects) and
22 by affecting pressure by capillary forces (capillary pressure effects). It was originally assumed
23 that no waste-generated gas is present before repository closure. However, during the EPA
24 completeness review of the CRA-2004, the representation of the gas-generation rate was
25 changed for the CRA-2004 PABC (Cotsworth 2005). The repository was precharged after
26 closure to represent the short-term, but initially faster, microbial gas-generation rate (see Section
27 MASS-8.0 and Leigh et al. 2005, Section 2.3). Future states are modeled as producing gas by
28 corrosion and microbial activities. Should high pressure develop over the regulatory period, it is
29 allowed to access MBs in the Salado.

30 Some variability in composition exists between different horizons of the Salado. The largest
31 differences occur between the anhydrite-rich layers called interbeds and those dominated by
32 halite. Within horizons dominated by halite, composition varies from nearly pure halite to halite
33 plus several percent other minerals, in some instances including clay (see the CCA, Chapter 2.0,
34 Section 2.1.3.4). The Salado is modeled as impure halite except for those interbeds that intersect
35 the DRZ near the repository. This conceptual model and an alternative model that explicitly
36 represented all stratigraphically distinct layers of the Salado near the repository (Christian-Frear
37 and Webb 1996) produced similar results.

38 From other modeling and theoretical considerations, flow between the Salado and the repository
39 is expected to occur primarily through interbeds that intersect the DRZ. Because of the large
40 surface areas between the interbeds and surrounding halite, the interbeds serve as conduits for
41 the flow of brine in two directions: from halite to interbeds to the repository, or, for brine
42 flowing out of the repository, from the repository into interbeds and then into halite. Because the

1 repository is modeled as a relatively porous and permeable region, brine is considered most
2 likely (but not constrained) to leave the repository through MB 139 below the repository because
3 of the effect of gravity. If repository pressures become sufficiently high, gas is modeled to exit
4 the repository via the MBs.

5 The effect of gravity may also be important in the Salado because of the slight and variable
6 natural stratigraphic dip. For long-term performance modeling, the dip in the Salado within the
7 domain is taken to be constant and 1 degree from north to south.

8 Fluid flow in the Salado is conceptualized as occurring either convergently into the repository or
9 divergently from it, as discussed in detail in the CRA-2004, Chapter 6.0, Section 6.4.2.1.
10 Because the repository is not conceptualized as homogeneous, implementing a geometry for the
11 conceptual model of convergent or divergent flow in the Salado is somewhat complicated and is
12 discussed in the CRA-2004, Chapter 6.0, Section 6.4.2.1.

13 The conceptual model for Salado fluid flow has primary interactions with three other conceptual
14 models. The interbed fracture conceptual model allows porosity and permeability of the
15 interbeds to increase as a function of pressure. The repository fluid flow model is directly
16 coupled to the Salado fluid flow model by the governing equations of flow in BRAGFLO (in the
17 governing equations of the mathematical model, they cannot be distinguished), and it differs only
18 in the region modeled and the parameters assigned to materials. The Salado model for An
19 transport is directly coupled to the conceptual model for flow in the Salado through the process
20 of advection. Additional information on the treatment of the Salado in PA is found in Appendix
21 PA-2009, Section PA-4.2.

22 **MASS-13.1 High Threshold Pressure for Halite-Rich Salado Rock Units**

23 An important parameter used to describe the effects of two-phase flow is threshold pressure,
24 which helps to determine the ease with which gas can enter a liquid-saturated rock unit. For a
25 brine-saturated rock, the threshold pressure is defined as “equal to the capillary pressure at which
26 the relative permeability to the gas phase begins to rise from its zero value, corresponding to the
27 incipient development of interconnected gas flow paths through the pore network” (Davies 1991,
28 p. 9).

29 The threshold pressure, as well as other parameters used to describe two-phase characteristics,
30 has not been measured for halite-rich rocks of the Salado. The Salado, however, is thought to be
31 similar in pore structure to rocks for which threshold pressures have been measured (Davies
32 1991). Based on this observation, Davies (1991) postulated that the threshold pressure of the
33 halite-rich rocks in the Salado could be estimated if an empirical correlation exists between rocks
34 postulated to have similar pore structure.

35 Davies developed a correlation between threshold pressure and intrinsic permeability applicable
36 to the Salado halites. A similar correlation was developed for Salado anhydrites; subsequent
37 testing confirmed that the correlation predicted threshold pressures accurately. The correlation
38 developed by Davies predicts threshold pressures in intact Salado halites on the order of 20 MPa
39 or greater (Davies 1991). This threshold pressure predicted by correlation is much higher than

1 that expected to persist in the repository, so that for all practical and predictive purposes, no gas
2 will flow into intact Salado halites (see the CRA-2004, Chapter 6.0, Section 6.4.5.1).

3 Because threshold pressure helps control the flow of gas, and because the greatest volume of
4 rock in the Salado is rich in halite, a high threshold pressure effectively limits the volume of gas
5 that can be accommodated in the pore spaces of the intact host formation. Thus, high threshold
6 pressure is considered conservative, because if gas could flow into the pore spaces of intact
7 Salado halite, repository pressures could be reduced dramatically.

8 **MASS-13.2 Historical Context of the Salado Conceptual Model**

9 See the CCA, Appendix MASS, Section MASS-13.2 for the historical information relating to the
10 CCA Salado conceptual model. The Salado conceptual model is unchanged for the CRA-2009
11 PA.

12 **MASS-13.3 The Fracture Model**

13 The fracture model assumptions have not changed from those in the CRA-2004 PABC. The
14 purpose of this model is to alter the porosity and permeability of the anhydrite interbeds and the
15 DRZ if their pressure approaches lithostatic, simulating some of the hydraulic effects of fractures
16 with the intent that unrealistically high pressures (in excess of lithostatic) do not occur in the
17 repository or disposal system. The conceptual model is also discussed in the CRA-2004, Chapter
18 6.0, Section 6.4.5.2. The fracture model assumptions have not changed from those in the CRA-
19 2004 PABC.

20 In the 1992 preliminary PA, repository pressures were shown to greatly exceed lithostatic
21 pressure if a large quantity of gas was generated. Pressures within the waste repository and
22 surrounding regions were predicted to be roughly 20 to 25 MPa. It was expected that fracturing
23 within the anhydrite MBs would occur at pressures slightly above lithostatic pressure. An expert
24 panel on fractures was convened to develop the conceptual bases for the fracturing within the
25 anhydrite MBs.

26 Two parametric behaviors must be quantified in the conceptual model. First, the change of
27 porosity with pressure in the anhydrite MBs must be specified. This is done with a relatively
28 simple equation, described in Appendix PA-2009, Section PA-4.2.4, that relates porosity change
29 to pressure change using an assumption that the fracturing can be thought of as increasing the
30 compressibility of interbeds. Parameters in the model are treated as fitting parameters and have
31 little relation to physical behavior except that they affect the porosity change. The second
32 parametric behavior is the change of permeability with pressure, which is incorporated by a
33 functional dependence on the porosity change. It is assumed that a power function is appropriate
34 for relating the magnitude of permeability increase to the magnitude of porosity increase. The
35 parameter in this power function, an exponent, is also treated as a fitting parameter and can be
36 set so that the behavior of permeability increase with porosity increase fits the desired behavior.

37 The fracture enhancement model assumes fracture propagation is uniform in the lateral direction
38 to flow within the MBs in the absence of dip. The 1-degree dip modeled in BRAGFLO may
39 affect fracture propagation direction; however, within the accuracy of the finite difference grid, a

1 fracture will develop radially outward. This would not account for fracture fingering or a
2 preferential fracturing direction; however, no existing evidence supports heterogeneous anhydrite
3 properties that would contribute to preferential fracture propagation. This evidence is discussed
4 in the CCA, Appendix MASS, Attachment 13-2.

5 The maximum enhanced fracture porosity controls the storativity within the fracture. The extent
6 of the migration of the gas front into the MB is sensitive to this storativity. The additional
7 storativity caused by porosity enhancement will mitigate gas migration within the MB. The
8 enhancement of permeability by MB fracturing will make the gas more mobile and will
9 contribute to longer gas-migration distances. Thus the effects of porosity enhancement at least
10 partially counteract the effects of permeability enhancement in affecting the gas-migration
11 distances.

12 Because intact anhydrite is partially fractured, the pressure at which porosity or permeability
13 changes are initiated is close to the initial pressure within the anhydrite. The fracture treatment
14 within the MBs will not contribute to early brine drainage from the MB because the pressures at
15 these times are below the fracture initiation pressure.

16 The input data to the interbed fracture model (see Fox 2008, Table 30, Table 31, and Table 32)
17 were chosen deterministically to produce the appropriate pressure and porosity response as
18 predicted by a linear elastic fracture mechanics model, as discussed in Mendenhall and Gerstle
19 (1993).

20 **MASS-13.4 Flow in the DRZ**

21 Modeling assumptions relating to flow in the DRZ have not changed from those in the CRA-
22 2004 PABC. The conceptual model for the DRZ around the waste disposal, operations, and
23 experimental regions has been chosen to provide a reasonably conservative estimate of fluid flow
24 between the repository and the intact halite and anhydrite MBs. The conceptual model is also
25 discussed in the CRA-2004, Chapter 6.0, Section 6.4.5.3.

26 The conceptual model implemented in the CCA PA used values for the permeability and porosity
27 of the DRZ that did not vary with time. A screening analysis examined an alternative conceptual
28 model for the DRZ in which permeability and porosity changed dynamically in response to
29 changes in pressure (Vaughn, Lord, and MacKinnon 1995e). This analysis implemented a
30 fracturing model in BRAGFLO for the DRZ. This fracturing model is used in the existing
31 anhydrite interbed model. In this model, formation permeability and porosity depend on brine
32 pressure, as described by Freeze, Larsen, and Davies (1995, pp. 2-16 through 2-19) and
33 Appendix PA-2009, Section PA-4.2.4. This model permits the representation of two important
34 formation-alteration effects. First, pressure buildup caused by gas generation and creep closure
35 within the waste will slightly increase porosity within the DRZ and offer additional fluid storage
36 with lower pressures. Second, the accompanying increase in formation permeability will enhance
37 fluid flow away from the DRZ. Because an increase in porosity tends to reduce outflow into the
38 far field, parameter values for this analysis were selected so that the DRZ alteration model
39 greatly increases permeability while only modestly increasing porosity.

1 Two basic scenarios were considered in the screening analysis by Vaughn, Lord, and
2 MacKinnon (1995e): undisturbed repository performance and disturbed repository performance.
3 Both scenarios included a 1-degree formation dip downward to the south. Intrusion event E1 is
4 considered in the disturbed scenario and consists of a borehole that penetrates the repository and
5 pressurized brine in the underlying Castile. Two variations of intrusion event E1 were
6 examined: E1 updip and E1 downdip. In the E1 updip event, the intruded panel region was
7 located on the north end of the waste disposal region, whereas in the E1 downdip event, the
8 intruded panel region was located on the south end of the disposal region. These two different
9 geometries permitted evaluation of the possibility of increased brine flow into the panel region
10 and the potential for subsequent impacts on contaminant migration. To incorporate the effects of
11 uncertainty in each case (E1 updip, E1 downdip, and undisturbed), a Latin hypercube sample
12 (LHS) size of 20 was used, for a total of 60 simulations. To assess the sensitivity of system
13 performance on formation alteration of the DRZ, conditional CCDFs of normalized
14 contaminated brine releases were constructed and compared with the corresponding baseline
15 model conditional CCDFs that were computed with constant DRZ permeability and porosity
16 values. Based on comparisons between conditional CCDFs, computed releases to the accessible
17 environment were determined to be essentially equivalent between the two treatments. Since the
18 two configurations were determined to have essentially equivalent impacts on releases, the
19 intrusion borehole was assumed to intrude in the down-dip or south side of the repository where
20 it is assumed brine would more readily accumulate (see Figure MASS-3).

21 Preliminary PAs considered alternative conceptual models that allowed for some lateral extent of
22 the DRZ into the halite surrounding the waste disposal region and for the development of a
23 transition zone between anhydrites A and B and MB 138 (WIPP Performance Assessment 1993,
24 Volume 4, Figure 4.1-2 and Figure 5.1-2; and Davies, Webb, and Gorham 1992; and Gorham et
25 al. 1992). The transition zone was envisioned as a region that had experienced some hydraulic
26 depressurization and perhaps some elastic stress relief because of the excavation, but probably no
27 irreversible rock damage and no large permeability changes. Modeling results indicated that
28 including the lateral extent of the DRZ had no significant effect on fluid flow. Communication
29 vertically to MB 138 was thought to be a potentially important process, however, and the model
30 adopted for PA assumes that the DRZ extends upward to MB 138 and permeability is sampled
31 over the same range used in the CRA PAVT. This representation continues to be used in the
32 CRA-2009 PA.

33 **MASS-13.5 Actinide Transport in the Salado**

34 The An transport modeling assumptions have not changed from those in the CRA-2004 PABC.
35 The purpose of this model, implemented in the code NUTS, is to represent the transport of
36 actinides in the Salado. This model is also discussed in the CRA-2004, Chapter 6.0, Section
37 6.4.5.4 and Appendix PA-2009, Section PA-4.3.4.

38 Actinide transport in the Salado is conceptualized as occurring only by advection, or movement
39 of material through the bulk flow of a fluid, through the porous medium described in the Salado
40 hydrology conceptual model. Advection is a direct function of fluid flow, which is discussed in
41 the conceptual model for Salado fluid flow. Other processes that might disperse actinides, such
42 as diffusion, hydrodynamic dispersion, and channeling in discrete fractures, are not included in

1 the conceptual model. Since these processes will reduce An transport, it is conservative to
2 ignore these processes.

3 To model radionuclide transport in the Salado, NUTS takes as input BRAGFLO's velocity field,
4 pressures, porosities, saturations, and other model parameters (including geometrical grid,
5 residual saturation, material map, brine compressibility, and time step) averaged over a given
6 number of time steps (20 for the CRA-2009 PA calculations). NUTS then models the transport
7 of radionuclides within all the regions for which BRAGFLO computes brine and gas flow. The
8 brine must pass through some part of the repository at some point during the 10,000-year
9 regulatory period if it is to become contaminated. Radioactive constituents of the waste in the
10 repository are assumed to dissolve into the brine while the brine is in the repository; the
11 radionuclides are then transported by advection to other regions outside the repository.
12 Consequently, the results of NUTS are subject to all the uncertainties associated with
13 BRAGFLO's conceptual model and parameterization, and are presented in Appendix PA-2009.
14 Details of the source term, which specifies the types and amounts of radionuclides that are
15 assumed to come into contact with the waste, are discussed in Appendix SOTERM-2009,
16 Section SOTERM-3.1 and Table SOTERM-6.

17 NUTS neglects molecular dispersion. For materials of interest in the WIPP repository system,
18 molecular diffusion coefficients are, at most, on the order of $4 \times 10^{-10} \text{ m}^2$ per second. Thus, the
19 simplest scaling argument using a time scale of 10,000 years leads to a molecular diffusion (that
20 is, mixing) length scale of approximately 33 ft (10 m), which is negligible compared to the
21 lateral advection length scale of roughly 7,874 ft (2,400 m) (the lateral distance from the
22 repository to the accessible environment).

23 NUTS also neglects mechanical dispersion (see the CRA-2004, Chapter 6.0, Section 6.4.5.4.2).
24 Dispersion is quantified by dispersivities, which are empirical tensor factors proportional to flow
25 velocity (to within geometrical factors related to flow direction). They account for both the
26 downstream and cross-stream spreading of local extreme values in concentration of dissolved
27 constituents. Physically, the spreading is caused by the fact that both the particle paths and
28 velocity histories of once-neighboring particles can be vastly different because of material
29 heterogeneities characterized by permeability variations. These variations arise from the
30 irregular cross-sectional areas and tortuous inhomogeneous, anisotropic connectivity between
31 pores. Because of its velocity dependence, the transverse component of mechanical dispersivity
32 tends to transport dissolved constituents from regions of relatively rapid flow (where mechanical
33 dispersion has a larger effect) to regions of slower flow (where mechanical dispersion has a
34 smaller effect). In the downstream direction, dispersivity merely spreads constituents in the flow
35 direction. Conceptually, ignoring lateral spreading assures that dissolved constituents will
36 remain in the rapid part of the flow field, which assures their transport toward the boundary.
37 Similarly, ignoring longitudinal dispersivity ignores the elongation of a feature in the flow
38 direction, which would delay the arrival of radionuclide constituents at the accessible
39 environment. However, because the EPA release limits are time-integrated measures, the exact
40 time of arrival is unimportant for constituents that arrive at the accessible environment, so long
41 as arrival occurs within the assessment period (10,000 years).

42 NUTS conservatively disregards sorptive and other retarding effects throughout the entire flow
43 region even though retardation must occur at some level within the repository, the MBs, and the

1 anhydrite interbeds, and especially in zones with clay layers or clay as accessory minerals.
2 Advection is, therefore, the only transport mechanism considered in NUTS. Because the Darcy
3 flows are given by BRAGFLO to NUTS as input, the maximum solubility limits for combined
4 dissolved and colloidal components are the most important NUTS parameters. These
5 components are described in Appendix SOTERM-2009, Section SOTERM-5.0.

1 **MASS-14.0 Geologic Units above the Salado**

2 The modeling assumptions of the geologic units above the Salado have not changed from those
3 in the CRA-2004 PABC. The model for geologic units above the Salado was developed to
4 provide a reasonable and realistic basis for simulations of fluid flow within the disposal system
5 and detailed simulations of groundwater flow and radionuclide transport in the Culebra. The
6 conceptual model for these units is also discussed in the CRA-2004, Chapter 6.0, Section 6.4.6.

7 The conceptual model used in PA for the geologic units above the Salado is based on the overall
8 concept of a groundwater basin, as introduced in the CRA-2004, Chapter 2.0, Section 2.2.1.1 and
9 in the CCA, Appendix MASS, Section MASS-14.2. The computer code SECOFL3D was
10 originally used to evaluate the effect on regional-scale fluid flow by recharge and rock properties
11 in the groundwater basin above the Salado (see the CCA, Appendix MASS, Attachment 17-2).
12 However, simpler models for this region are implemented in codes used in PA. For example, in
13 the BRAGFLO model, layer thicknesses, important material properties including porosity and
14 permeability, and hydrologic properties such as pressure and initial fluid saturation are specified,
15 but the model geometry and boundary conditions are not suited to groundwater basin modeling
16 (nor is the BRAGFLO model used to make inferences about groundwater flow in the units above
17 the Salado). In PA, the Culebra is the only subsurface pathway modeled for radionuclide
18 transport above the Salado, although the groundwater basin conceptual model includes other
19 flow interactions. The Culebra model implemented in PA includes spatial variability in
20 hydraulic conductivity and uncertainty and variability in physical and chemical transport
21 processes. Thus, the geometries and properties of units in the different models applied to the
22 units above the Salado by the DOE are chosen to be consistent with the purpose of the model.

23 The MODFLOW-2000 and SECOTP2D codes are used directly in PA to model fluid flow and
24 transport in the Culebra. The assumptions made in these codes are discussed in the CRA-2004,
25 Chapter 6.0, Section 6.4.6.2 and the CRA-2004, Appendix PA, Attachment MASS, Section
26 MASS-15.0.

27 With respect to the units above the Salado, the BRAGFLO model is used only for determination
28 of fluid fluxes between the shaft or intrusion borehole and hydrostratigraphic units. For this
29 purpose, it does not need to resolve regional or local flow characteristics.

30 The basic stratigraphy and hydrology of the units above the Salado are described in the CRA-
31 2004, Chapter 2.0, Section 2.1.3.5, Section 2.1.3.6, Section 2.1.3.7, Section 2.1.3.8, Section
32 2.1.3.9, and Section 2.1.3.10 and Section 2.2.1.4. Additional supporting information is contained
33 in the CCA, Appendices GCR, HYDRO, and SUM. Details of the conceptual model for each
34 unit are described in the CRA-2004, Chapter 6.0, Section 6.4.6.1, Section 6.4.6.2, Section
35 6.4.6.3, Section 6.4.6.4, Section 6.4.6.5, Section 6.4.6.6, and Section 6.4.6.7 and additional
36 information on units above the Salado is found in Appendix HYDRO-2009.

37 The representation of units above the Salado used in the CRA-2009 PA has not changed from
38 that used in the CRA-2004 PA.

1 **MASS-14.1 Historical Context of the Units above the Salado Model**

2 See the CCA, Appendix MASS, Section MASS-14.1 for historical information relating to the
3 conceptual models for units above the Salado for the CCA. The conceptual models for the units
4 above the Salado are unchanged for CRA-2009 PA.

5 **MASS-14.2 Groundwater-Basin Conceptual Model**

6 The groundwater-basin conceptual model and associated modeling assumptions have not
7 changed from those of the CRA-2004 PABC. For a discussion on the groundwater-basin
8 conceptual model, see the CCA, Appendix MASS, Section MASS-14.2.

1 **MASS-15.0 Flow Through the Culebra**

2 The Culebra flow modeling assumptions have not changed from those in the CRA-2004 PABC.
3 The conceptual model for groundwater flow in the Culebra (1) provides a reasonable and
4 realistic basis for simulating radionuclide transport in the Culebra and (2) allows evaluation of
5 the extent to which uncertainty about groundwater flow in the Culebra may contribute to
6 uncertainty in the estimate of cumulative radionuclide releases from the disposal system. See the
7 CRA-2004, Chapter 6.0, Section 6.4.6.2 for additional references to other relevant discussions on
8 this conceptual model.

9 The conceptual model used in PA for groundwater flow in the Culebra treats the Culebra as a
10 confined two-dimensional aquifer with constant thickness and spatially varying transmissivity
11 (see the CCA, Appendix MASS, Attachment 15-7). Flow is modeled as single-phase (liquid)
12 Darcy flow in a porous medium.

13 Basic stratigraphy and hydrology of the units above the Salado are described in the CRA-2004,
14 Chapter 2.0, Section 2.1 and Section 2.2. Additional supporting information is contained in the
15 CCA, Appendices GCR, HYDRO, and SUM.

16 The conceptual model for flow in the Culebra is discussed in the CRA-2004, Chapter 6.0,
17 Section 6.4.6.2. Details of the calibration of the T fields, based on available field data, are given
18 in Appendix TFIELD-2009, Section TFIELD-4.0. Initial and boundary conditions used in the
19 model are given in the CRA-2004, Chapter 6.0, Section 6.4.10.2. A discussion of the adequacy
20 of the two-dimensional assumption for PA calculations is included in the CCA, Appendix
21 MASS, Attachment 15-7.

22 The principal parameter used in PA to characterize flow in the Culebra is an index parameter (the
23 transmissivity index) used to select a single T field for each LHS element from a set of calibrated
24 fields (see Fox 2008, Table 1), each of which is consistent with available data.

25 **MASS-15.1 Historical Context of the Culebra Model**

26 See the CRA-2004, Appendix PA, Attachment MASS, Section MASS-15.1 for historical
27 information relating to the Culebra conceptual model. The conceptual model for this unit is
28 unchanged for CRA-2009.

29 **MASS-15.2 Dissolved Actinide Transport and Retardation in the Culebra**

30 The purpose of this model is to represent the effects of advective transport and physical and
31 chemical retardation on the movement of actinides in the Culebra. This conceptual model is also
32 discussed in the CRA-2004, Chapter 6.0, Section 6.4.6.2.1. The same model is used in the CRA-
33 2004 PABC and the CRA-2009 PA. For a historical presentation of this model, see the CRA-
34 2004, Appendix PA, Attachment MASS, Section MASS-15.2.

1 **MASS-15.3 Colloidal Actinide Transport and Retardation in the Culebra**

2 The purpose of this model is to represent the effects of colloidal An transport in the Culebra.
3 This model is also discussed in the CRA-2004, Chapter 6.0, Section 6.4.6.2.2 and the CRA-2004,
4 Appendix PA, Attachment MASS, Attachments 15-2, 15-8, and 15-9. No changes have been
5 made to this model since the CRA-2004. Additional information and historical information on
6 colloidal An transport and retardation in the Culebra can be found in the CRA-2004, Appendix
7 PA, Attachment MASS, Section MASS-15.3.

8 **MASS-15.4 Subsidence Caused by Potash Mining in the Culebra**

9 The mining-related modeling assumptions have not changed from those in the CRA-2004 PABC.
10 This model incorporates the effects of potash mining in the McNutt Potash Zone on disposal
11 system performance (see Appendix SCR-2009, FEP H13, FEP H37, and FEP H38). Provisions
12 in Part 194 provide a conceptual model and elements of a mathematical model for these effects.
13 The DOE has implemented the EPA conceptual model (40 CFR § 194.32(b), U.S. Environmental
14 Protection Agency 1996) to be consistent with EPA criteria and guidance; this model is
15 described in the CRA-2004, Chapter 6.0, Section 6.4.6.2.3. Additional information on the
16 implementation of the mining subsidence model is available in Appendix TFIELD-2009, Section
17 TFIELD-9.0; the CCA, Appendix MASS, Attachments 15-4 and 15-7; and Wallace (1996).

18 The principal parameter in this model is the range assigned to a factor by which hydraulic
19 conductivity in the Culebra is increased (see the CCA, Appendix MASS, Attachment 15-4). As
20 allowed in supplementary information to Part 194, it is the only parameter changed to account
21 for the effects of mining.

22 Mining in the McNutt has been considered in the performance of the WIPP since the original
23 siting activities. Siting criteria for both the site abandoned in 1975 and the current site included
24 setbacks from active mines. (See, for example, the CCA, Appendix MASS, Section MASS-2.0.)
25 The 1980 Final Environmental Impact Statement (FEIS) for the WIPP (U.S. Department of
26 Energy 1980, pp. 9-145 through 9-148) considered the possibility of an indirect dose arising
27 from the effects of solution mining for potash or halite.

28 Mining has been included in scenario development for the WIPP since the earliest work on this
29 topic (see U.S. Department of Energy 1980 [pp. 9-145 through 9-148], Hunter 1989, Marietta et
30 al. 1989, Guzowski 1990, Tierney 1991, and WIPP Performance Assessment 1991). These early
31 scenario developments considered both solution and room-and-pillar mining. The focus was
32 generally on effects of mining outside the disposal system. In the CCA FEPs screening, solution
33 mining was screened out during scenario development (see Appendix SCR-2009, FEP H58 and
34 FEP H59). The two primary effects of mining considered were (1) changes in the hydraulic
35 conductivity of the Culebra or other units, and (2) changes in recharge as a result of surface
36 subsidence. These mining effects were not formally incorporated into quantitative assessment of
37 repository performance in preliminary PAs.

38 The inclusion of mining in PA satisfies the requirements of section 194.32(b) to consider the
39 effects of this activity on the disposal system.

1 **MASS-16.0 Intrusion Borehole**

2 The intrusion borehole modeling assumptions have not been changed from those in the CRA-
3 2004 PABC. The inclusion of intrusion boreholes in PA adds to the number of release pathways
4 for radionuclides from the disposal system. Direct releases to the surface may occur during
5 drilling as particulate material from cuttings, cavings, and spallings are carried to the surface.
6 Also, dissolved actinides may be carried to the surface in brine during drilling. Once abandoned,
7 the borehole presents a possible long-term pathway for fluid flow, such as might occur between a
8 hypothetical Castile brine reservoir, the repository, and overlying units. This topic is also
9 addressed in the CRA-2004, Chapter 6.0, Section 6.4.7 and Appendix SCR-2009 (FEP H1 and
10 FEP H21).

11 **MASS-16.1 Cuttings, Cavings, and Spallings Releases during Drilling**

12 The cuttings, cavings, and spallings models estimate the quantity of actinides released as solids
13 directly to the surface during drilling through the repository. The releases are caused by three
14 mechanisms: the drill bit boring through the waste (cuttings); the drilling fluid eroding the walls
15 of the borehole (cavings); and high repository gas pressure causing solid material failure and
16 entrainment into the drilling fluid in the wellbore (spallings). See the CRA-2004, Chapter 6.0,
17 Section 6.4.7.1 and references to other appendices cited in that section for additional
18 information. Stochastic uncertainty in parameters relevant to these release mechanisms is
19 addressed in the CRA-2004, Chapter 6.0, Section 6.4.12. The conceptual model for cuttings,
20 cavings, and spallings is discussed in three parts because of the different processes that produce
21 the three types of material.

22 Cuttings are materials removed to the surface through drilling mud by the direct mechanical
23 action of the drill bit. The volume of waste removed to the surface is a function of the repository
24 height and the drill bit area. The principal parameter in the cuttings model is the diameter of the
25 drill bit (see Appendix DATA-2009, Attachment A).

26 Cavings are materials introduced into the drilling mud by the erosive action of circulating
27 drilling fluid on the waste in the walls of the borehole annulus. Erosion is driven solely by the
28 shearing action of the drilling fluid (or mud) as it moves up the borehole annulus. Shearing may
29 be caused by either laminar or turbulent flow. Repository-pressure effects on cavings, which are
30 negligible, are covered by the spall process. The principal parameters in the cavings model are
31 the properties of the drilling mud, drilling rates, the drill string angular velocity, and the shear
32 resistance of the waste. (See Fox 2008, Table 13 and Table 18, for details on the sampled
33 parameters used in the cavings model, the drill string angular velocity, and the effective shear
34 resistance to erosion.)

35 Spallings are solids introduced into the wellbore by the fluid pressure difference between the
36 repository and the bottom of the wellbore. If the repository pressure is sufficiently high (more
37 than about 12 MPa) relative to the well bottom hole pressure (about 8 MPa), the stress state in
38 the repository may cause repository solids to fail in the vicinity of the wellbore. In turn, these
39 solids may become entrained in the gas flowing toward the well, ultimately to be carried up to
40 the land surface and constituting a release. The principal parameters in the spallings model are
41 the gas pressure in the repository when it is penetrated and properties of the waste such as

1 permeability, tensile strength, and particle diameter. Because the release associated with spalling
2 is sensitive to gas pressure in the repository, it is strongly coupled to the BRAGFLO-calculated
3 conditions in the repository at the time of penetration.

4 **MASS-16.1.1 Historical Context of Cuttings, Cavings, and Spallings Models**

5 Cuttings and cavings releases are straightforward. The analytical equations governing erosion
6 (cavings) based on laminar and turbulent flow (Appendix PA-2009, Section PA-4.5) have been
7 implemented in the code CUTTINGS_S. Using selected input based on assumed physical
8 properties of the waste and other drilling parameters, this code calculates the final caved
9 diameter of the borehole that intersects the waste.

10 The various approaches used for spallings up to the CCA PA are documented in the CCA,
11 Appendix MASS, Section MASS-16.1.1. Since the CCA PA, the spallings model has been
12 extensively revised and has changed fundamentally from an end-state erosional model to a
13 mechanically based, coupled material failure and transport model (WIPP Performance
14 Assessment 2003a). This model is implemented in the code DRSPALL. A discussion tracing
15 the historical steps from the CCA erosional model to the current DRSPALL model can be found
16 in the CRA-2004, Appendix PA, Attachment MASS, Section MASS-16.1.1.

17 **MASS-16.1.2 Waste Mechanistic Properties**

18 Waste mechanical properties used in the CRA-2009 PA are the same as those in the CRA-2004
19 PA and the CRA-2004 PABC. Changes to the waste mechanistic properties for CRA-2004 were
20 previously documented in the CRA-2004, Appendix PA, Attachment MASS, Section MASS-
21 16.1.2. Those changes involved the development of surrogate waste materials for the WIPP
22 spallings model. Surrogate waste recipes for 50% and 100% corrosion of the Fe-based inventory
23 were fabricated from the projected inventory of waste materials. The development of each
24 surrogate product assumed extensive degradation of the modeled constituent (Hansen et al.
25 1997). Subsurface processes contributing to massive degradation of the waste taken into
26 consideration include ample brine availability; extensive microbial activity and corrosion of
27 metals; and an absence of cementation, mineral precipitation, and salt encapsulation.

28 The WIPP PA uses the parameter BOREHOLE:TAUFAIL to represent the hydrodynamic shear
29 strength of the waste in the numerical code CUTTINGS_S (see Appendix PA-2009, Section
30 PA-4.5). It is officially called the “effective shear strength for erosion,” but it is more commonly
31 known as the “waste shear strength.” The parameter is treated as a sampled value in WIPP PA
32 with a log-uniform distribution and a range of 0.05 to 77 Pa. This range of values was derived
33 by DOE from literature reviews of incipient motion of seafloor or channel bed sediments—0.05
34 Pa corresponds to a San Francisco Bay mud—and consideration of the mean particle size of the
35 WIPP waste as determined by an expert elicitation (Berglund 1996, Carlsbad Area Office
36 Technical Assistance Contractor [CTAC] 1997). The lower limit of this range of values
37 represents what is hypothesized as an extreme case of degradation of the waste and waste
38 containers.

1 **MASS-16.1.3 Mechanistic Model for Spall**

2 The CRA-2009 PA uses the same spillings model that was used in the CRA-2004 PA and the
3 CRA-2004 PABC. No changes were made to the model or implementation of the results in PA.

4 In the CRA-2004 PA, a new approach to modeling the WIPP spillings process was developed to
5 address peer review concerns during the original certification process (see the CCA, Chapter 9.0,
6 Section 9.3.1.2 and the CRA-2004, Appendix PEER-2004, Section PEER-2004 3.0). Instead of
7 focusing on the end state after penetration, as was done in the original CCA erosional model, the
8 new model sought to capture the system behavior from just before penetration through to the end
9 state. In doing so, many more phenomena were included in the model. Considered in this new
10 conceptual model was unsteady, convergent gas flow from the repository toward the wellbore
11 that caused mechanical stress and potential failure of solids near the face of the wellbore.
12 Pressure in the cavity at the point of penetration was balanced by the mud column in the
13 wellbore and the repository pressure.

14 The new spall model, DRSPALL (WIPP Performance Assessment 2003a), is based on a
15 predecessor code called GASOUT (Hansen et al. 1997, Appendix C). DRSPALL builds upon
16 GASOUT by:

- 17 1. Adding a wellbore flow model that transports mud, repository gas, and waste solids from
18 repository level to the land surface
- 19 2. Adding a fluidized bed model that evaluates the potential for failed particulate waste to
20 fluidize and become entrained in the wellbore flow

21 The wellbore flow model in DRSPALL utilizes one-dimensional geometry with a compressible,
22 viscous, isothermal, homogeneous mixture of mud, gas, and solids. Standard mass and
23 momentum balance, friction loss, and slurry viscosity equations are used. Wellbore flow model
24 results were successfully verified against those from an independent commercial code for several
25 test problems (WIPP Performance Assessment 2003b).

26 DRSPALL applies the fluidized bed theory to determine the mobilization of failed material to the
27 flow stream in the wellbore. If the escaping gas velocity exceeds the minimum fluidization
28 velocity, failed material is fluidized and entrained for transport at the land surface. If gas
29 velocity is too low to fluidize the bedded material, the cavity size is allowed to stabilize. The
30 spall volumes predicted by DRSPALL are based on the following conservative assumptions for
31 material properties and for the flow geometry within the repository:

- 32 • The particle size distribution for spillings is based on a detailed analysis (Wang 1997) of
33 data from an expert elicitation (Carlsbad Area Office Technical Assistance Contractor
34 [CTAC] 1997). This analysis considered several limiting cases in developing a conservative
35 distribution for mean particle size ranging from 1 millimeter to 10 cm (Hansen, Pfeifle, and
36 Lord 2003).
- 37 • The shape factor for fluidization of particles has a potential range from 0 to 1.0. Smaller
38 values of the shape factor denote particles that are less spherical, and, therefore, more easily

1 fluidized and transported in the flow. The shape factor is conservatively set to a value of 0.1
2 (Lord 2003).

- 3 • The tensile strength of the waste assigned for the spalling process is uncertain, ranging from
4 0.12 MPa to 0.17 MPa (Hansen, Pfeifle, and Lord 2003). Tensile strength data was measured
5 in laboratory experiments on surrogate materials chosen to conservatively represent highly
6 degraded residuals from typical wastes. The given range is felt to represent extreme, low-end
7 tensile strengths because it does not account for several strengthening mechanisms, such as
8 MgO hydration and halite precipitation/cementation (Hansen et al. 1997).
- 9 • DRSPALL uses a hemispherical geometry (one-dimensional spherical symmetry) for the
10 flow field and cavity in the waste. This conceptual model is appropriate when the drill bit
11 first penetrates the repository. But as the drill bit passes completely through the compacted
12 waste, the flow field transitions toward a cylindrically symmetric geometry. This transition
13 is important because the largest spall release volumes are predicted to occur at late times,
14 well after the drill bit has penetrated through the waste, and because the spall volumes
15 predicted for a cylindrical geometry are less than for the hemispherical geometry (Lord,
16 Rudeen, and Hansen 2003).

17 In summary, the conservative assumptions for waste properties, the waste flow geometry, and the
18 driller's actions provide very conservative spalling release volumes (see also Appendix PA-2009,
19 Section PA-4.6 for a description of the spallings model, and the CRA-2004, Appendix PEER-
20 2004, Section PEER-2004 3.0 for the results of the spallings model peer review). As stated
21 previously, the DRSPALL calculations from the CRA-2004 PABC were also used in the CRA-
22 2009 PA (see Appendix PA-2009, Section PA-6.7.4 and Section PA-8.5.2.1).

23 **MASS-16.1.4 Calculation of Cuttings, Cavings, and Spall Releases**

24 The modeling assumptions relating to the calculations of cuttings, cavings and spallings releases
25 have not changed since the CRA-2004. As detailed in Appendix PA-2009, Section PA-6.7.5,
26 cuttings and cavings releases for intrusions into CH-TRU waste are computed by multiplying the
27 volume released (calculated by the code CUTTINGS_S) by the radioactivity in three
28 independently selected waste streams, consistent with the conceptual assumption that waste
29 streams are randomly emplaced in waste stacks that are three drums high. The effect of this
30 assumption on PA results was examined in a separate PA (Hansen et al. 2003) in which cuttings
31 and cavings releases were computed by assuming that each intrusion encounters only a single
32 waste stream. The differences in repository performance (determined by comparing the mean
33 CCDFs for releases) were determined to be minor. For more details on the analysis, see the
34 CRA-2004, Appendix PA, Attachment MASS, Section MASS-21.0.

35 Because spallings may release a relatively large volume of material (exceeding 4 m³), spalling
36 releases for intrusions into CH-TRU waste are computed by multiplying the volume of spalled
37 material with the average concentration of radioactivity in the waste at the time of the intrusion.
38 A separate PA (Hansen et al. 2003) compared spalling releases computed using the average
39 concentration of radioactivity in the waste to spalling releases computed using the radioactivity
40 of a single, randomly selected waste stream. The analysis determined that the assumption had
41 only a minor effect on the mean CCDF for releases. For more details on the analysis, see the

1 CRA-2004, Appendix PA, Attachment MASS, Section MASS-21.0. During their completeness
2 review of the CRA-2004, the EPA requested additional DRSPALL vectors be used in the CRA-
3 2004 PABC. Minor changes were made to the implementation of spillings results that did not
4 change the overall modeling assumptions. These implementation changes are outlined in Leigh
5 et al. (2005, Section 7.8).

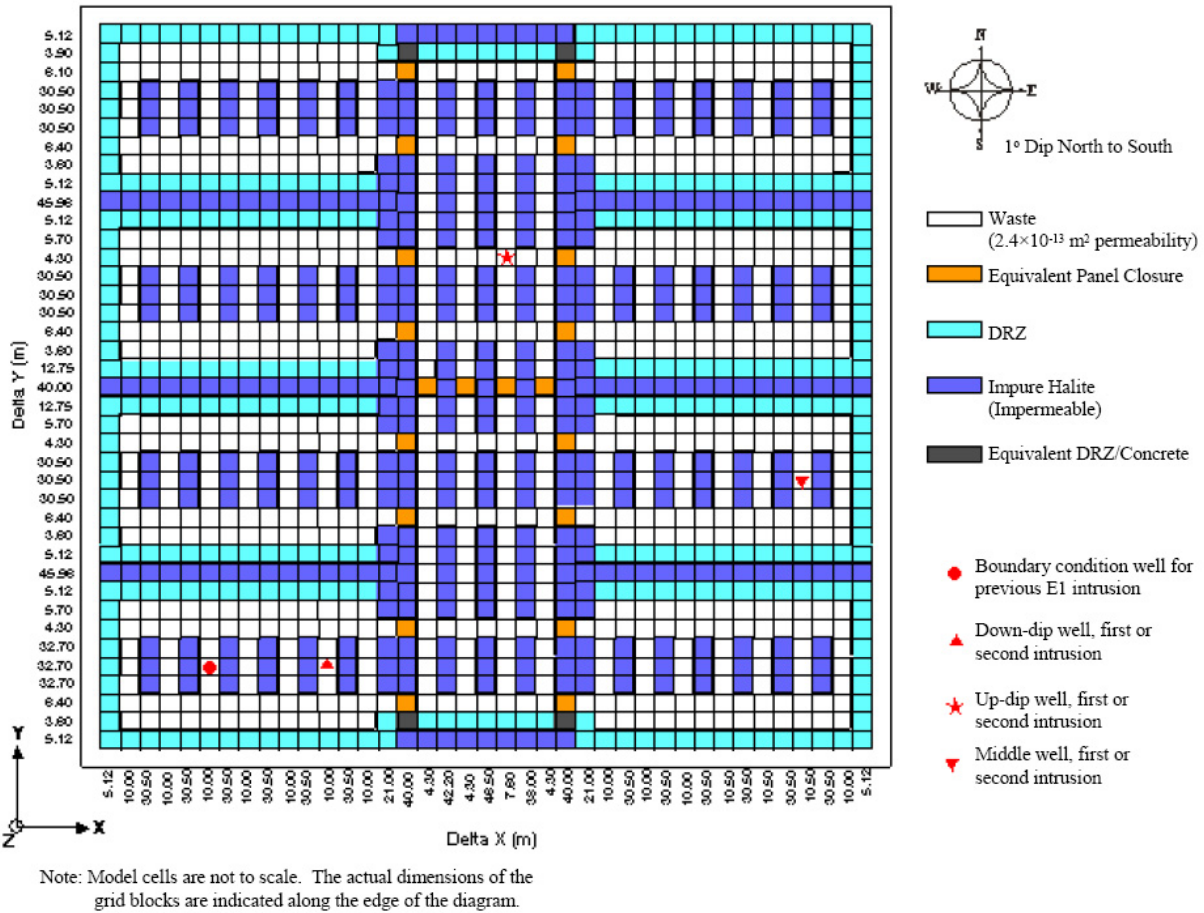
6 **MASS-16.2 Direct Brine Releases during Drilling**

7 The DBR modeling assumptions for the CRA-2004 PABC are used in the CRA-2009 PA. This
8 model provides a series of calculations to estimate the quantity of brine released directly to the
9 surface during drilling. DBRs may occur when a driller penetrates the WIPP and unknowingly
10 brings contaminated brine to the surface during drilling (these releases are not accounted for in
11 the cuttings, cavings, and spillings calculations, which model only the solids removed during
12 drilling). Appendix PA-2009, Section PA-4.7 describes the DBR model used for the CRA-2009
13 PA. The CCA, Appendix MASS, Attachment 16-2 describes the DBR model used for the CCA
14 PA. The conceptual model for DBRs is discussed in Appendix PA-2009, Section PA-4.7 and the
15 CRA-2004, Chapter 6.0, Section 6.4.7.1.1.

16 Uncertainty in the BRAGFLO DBR calculations is captured in the 10,000-year BRAGFLO
17 calculations from which the initial and boundary conditions are derived. The model parameters
18 that have the most influence on DBRs are repository pressure and brine saturation at the time of
19 intrusion. Brine saturation is influenced by many factors, including Salado and MB permeability
20 and gas-generation rates (for undisturbed scenario calculations). For E1 and E2 intrusion
21 scenarios, Castile brine-reservoir pressure and volume, and abandoned borehole permeabilities
22 influence conditions for the second and subsequent intrusions. The dip in the repository (hence
23 the location of intrusions), two-phase flow parameters (residual brine and gas saturation), time of
24 intrusion, and duration of flow have lesser impacts on brine releases.

25 To account for changes in the BRAGFLO model (see Section MASS-2.0), the implementation of
26 the DBR model was adjusted for the CRA 2004-PA. These adjustments are also used in the
27 CRA-2009 PA. Figure MASS-8 shows the DBR grid used in the CRA-2004 PA and the CRA-
28 2009 PA.

29 The grid dimensions and resolution are the same as in the CCA PA, but the material parameters
30 assigned to the panel closures were changed during the CRA-2004 to be more consistent with the
31 conceptual model for the Option D panel closures. In addition, the material parameters assigned
32 to the DRZ were changed to represent the DRZ more consistently. In the CCA PA, the pillars
33 between rooms and the halite separating panels were assigned properties consistent with the
34 DRZ material in the BRAGFLO grid. The DRZ permeability used in the CCA PA (10^{-15} m^2)
35 was low enough that brine did not flow between panels during the 11-day DBR calculations.
36 When the permeability of the DRZ was changed in the CCA PAVT (from a constant value of
37 10^{-15} m^2 to a sampled value between $10^{-19.4} \text{ m}^2$ and $10^{-12.5} \text{ m}^2$), realizations with high DRZ
38 permeability allowed brine flow between panels during the 11-day period for DBR calculations.
39 It is not reasonable to model the halite between panels as DRZ, since the DRZ would extend only
40 a few meters into the 60 m-thick pillars. Consequently, the material parameters assigned to cells
41 separating panels were changed to be representative of undisturbed halite rather than DRZ. Stein
42



1

2 **Figure MASS-8. Repository-Scale Horizontal BRAGFLO Mesh Used for DBR**
 3 **Calculations**

4 (2003a) provides details on the material parameters used in the DBR calculation and the rationale
 5 for the parameter values. Note that the CRA-2009 PA uses a different DBR maximum duration
 6 of 4.5 days, based on current drilling practices (see Appendix PA-2009, Section PA-4.7.8). This
 7 parameter change does not impact the modeling assumptions discussed above.

8 **MASS-16.3 Long-Term Properties of the Abandoned Intrusion Borehole**

9 The long-term treatment and assumptions used to represent boreholes in the CRA-2009 PA have
 10 not changed from the treatment and assumptions used in the CRA-2004 PA. See the CRA-2004,
 11 Appendix PA, Attachment MASS, Section MASS-16.3 for the borehole modeling assumptions
 12 used in the CRA-2009 PA.

1 **MASS-17.0 Climate Change**

2 The purpose of this model is to allow quantitative consideration of the extent to which
3 uncertainty about future climate may contribute to uncertainty in estimates of cumulative
4 radionuclide releases from the disposal system. This model has not changed since the CCA and
5 is used in the CRA-2009 PA. Consideration is limited to conditions that could result from
6 reasonably possible natural climatic changes. The model is not intended to provide a
7 quantitative prediction of future climate, nor is it intended to address uncertainty in system
8 properties other than estimated cumulative radionuclide releases that may be affected by climate
9 change. See the CRA-2004, Appendix PA, Attachment MASS, Section MASS-17.0 and Section
10 MASS-17.1 for current and historical information on the climate change model. The
11 implementation of this model in PA is also discussed in the CRA-2004, Chapter 6.0, Section
12 6.4.9 and Appendix PA, Section PA-2.1.4.6. See also the CCA, Appendix CLI for information
13 on expected climate variability over the 10,000-year regulatory time period.

1 **MASS-18.0 Castile Brine Reservoir**

2 The conceptual model for the hypothetical brine reservoir is included in PA to estimate the
3 extent to which uncertainty about the existence of a brine reservoir under the waste disposal
4 region may contribute to uncertainty in the estimate of cumulative radionuclide releases from the
5 disposal system. The conceptual model is not intended to provide a realistic approximation of an
6 actual brine reservoir under the waste disposal region. Data are insufficient to determine
7 whether such a brine reservoir exists.

8 The representation of the Castile brine reservoir in the CRA-2009 PA has not changed from the
9 CRA-2004 PA. However, this model is not the same as the one used in the original CCA PA.
10 The following describes the changes to the model since the 1996 CCA PA.

11 The Castile Formation is treated as an impermeable unit in PA and plays no role in the analysis
12 except to separate the Salado from the modeled brine reservoir in the BRAGFLO grid. In
13 human-intrusion scenarios, the hypothetical brine reservoir can be penetrated by an intrusion
14 borehole connecting it to the repository. The amount of brine that can enter the repository from
15 the brine reservoir is important to PA because brine is required for gas generation reactions and
16 can transport radionuclides in solution, contributing to potential releases.

17 The properties of the hypothetical brine reservoir defined for PA include: permeability, porosity,
18 pore volume, initial pressure, and various two-phase flow parameters. Values assigned for these
19 properties were chosen to either be consistent with the available data from and analyses of
20 borehole penetrations of brine reservoirs in the region, or provide a reasonable response in the
21 BRAGFLO model.

22 The treatment of the brine reservoir for the CRA-2004 PA is different than that used in the CCA
23 PA. The major changes to the brine reservoir representation were made by the EPA in the CCA
24 PAVT (U.S. Environmental Protection Agency 1998b). For the CCA PAVT, the EPA defined
25 new parameter ranges for bulk compressibility and total pore volume. The range of bulk
26 compressibility was based on a reevaluation of field test data from the WIPP-12 borehole
27 following the CCA (Beauheim 1997). Since the total volume of the grid cells used to represent
28 the brine reservoir in BRAGFLO is fixed, the range of total pore volume was set by defining a
29 range of “effective” porosity (pore volume = grid volume × effective porosity). This range of
30 porosity values is not representative of the actual host rock. It was chosen to produce a
31 reasonable response in the BRAGFLO model by providing a predefined range of total pore
32 volumes based on the field tests at WIPP-12.

33 For the CRA-2004 PA, the DOE implemented this approach by assuming that the productivity
34 ratio (PR) remains constant ($2.0051 \times 10^{-3} \text{ m}^3/\text{Pa}$). The PR is defined as:

$$PR = V \frac{C_r}{\phi},$$

35
36 where V is the grid volume of the brine reservoir ($18,462,514 \text{ m}^3$), C_r is the bulk compressibility
37 (2×10^{-11} to $1 \times 10^{-10} \text{ Pa}^{-1}$), and ϕ is the effective porosity (0.1842 to 0.9208). To maintain a
38 constant pore volume in the brine reservoir, the porosity range used in the CRA-2004 PA is

1 slightly modified from that used in the CCA PAVT because the fixed-grid volume increased
2 slightly in the CRA-2004 BRAGFLO grid from the volume assumed in the CCA BRAGFLO
3 grid. In this approach, bulk compressibility and effective porosity are directly proportional
4 (Stein 2003b). See Appendix PA-2009, Section PA-4.2.10 for the details on the implementation
5 in PA.

6 Basic geologic information about the Castile is given in the CRA-2004, Chapter 2.0, Section
7 2.1.3.3. The hydrology of the known brine reservoirs is discussed in the CRA-2004, Chapter 2.0,
8 Section 2.2.1.2.2. The treatment of the hypothetical brine reservoir in PA is discussed in the
9 CRA-2004, Chapter 6.0, Section 6.4.8.

10 **MASS-18.1 Historical Context of the Castile Brine Reservoir Model**

11 See the CCA, Appendix MASS, Attachment 18.1 for historical information on the Castile brine
12 reservoir model.

1 **MASS-19.0 Option D Panel Closure**

2 The option D panel closure assumptions have not changed from those used in the CRA-2004
3 PABC. The certification decision by the EPA (U.S. Environmental Protection Agency 1998a)
4 included several conditions that the DOE was required to meet. In the first of these conditions,
5 the EPA required the DOE to implement a specific design for the panel closure system referred
6 to as Option D and required the concrete monolith to be constructed using SMC. The DOE had
7 included four Options (A-D) for the panel closure design using standard concrete or SMC in the
8 CCA. The Option D design consisted of two components: a large monolith constructed of SMC
9 and keyed into the surrounding DRZ, and an explosion wall constructed of concrete blocks,
10 which is not keyed into the DRZ.

11 The PA calculations that supported the CCA and the subsequent CCA PAVT calculations
12 included generic panel closures in the BRAGFLO grid. These generic closures were not
13 representative of the Option D design. The generic panel closures included in the CCA PA and
14 the CCA PAVT calculations were relatively permeable and allowed gas to flow freely between
15 panels. In the CCA PA and the CCA PAVT calculations, a drilling intrusion into a single panel
16 generally caused pressures in the entire repository to decrease.

17 Following the original certification of the repository, the DOE updated the modeling of the panel
18 closures in PA so that the mandated Option D design was adequately represented. A new panel
19 closure representation was developed and presented to the Salado Flow Peer Review Panel in
20 May 2002, and again in February 2003. The peer review panel approved the new conceptual
21 models, which included the implementation of the Option D panel closures in the grid
22 (Caporuscio, Gibbons, and Oswald 2003).

23 In the CCA PA/CCA PAVT BRAGFLO grid, only two panel closures were represented. For the
24 CRA-2004 PA and the CRA-2009, however, the DOE included an additional set of panel
25 closures. Preliminary tests of the Option D panel closure representation (Hansen et al. 2002)
26 concluded that Option D panel closures were effective at impeding fluid flow between panels on
27 the order of thousands of years, but that, given enough time, pressures slowly equilibrated.
28 These results suggest that the effect of a single intrusion event on pressures in other panels
29 depends on the number of panel closures that lie between the intruded panel and the other panels.
30 Therefore, the DOE decided to divide the RoR region into two regions separated by a panel
31 closure. This panel closure represents a set of four panel closures to be located between the
32 northern and southern internal extended panels. The south RoR represents panels directly
33 adjacent to an intruded panel and the north RoR represents panels that are farther away from the
34 intruded panel (two sets of panel closures lie in between).

35 The DOE assumes that the effect of the Option D panel closures will be to impede fluid flow
36 through and around the closures. Only the concrete monolith portion of the closure system is
37 assumed to remain effective over the 10,000-year regulatory period. The explosion wall is
38 assumed to be effective for only a brief period during the operational period. The explosion wall
39 and the open drift adjacent to the monolith are represented in the BRAGFLO grid by a column of
40 grid cells with the properties of the waste area (e.g., high permeability) and include creep closure
41 effects. The monolith is represented in the BRAGFLO grid by an adjacent column of grid cells
42 with a length equal to the length of the monolith (7.9 m) multiplied by the number of panel

1 closures in series and a width equal to the width of the monolith (10 m) multiplied by the number
2 of panel closures in parallel. For instance, in Figure MASS-3, the southern panel closure in the
3 BRAGFLO grid represents a single set of two panel closures (in parallel) that separate a single
4 external panel from one of the two internal extended panels (9 and 10). The middle panel
5 closure in the BRAGFLO grid represents a single set of four panel closures (in parallel) that
6 separate the internal extended panels (9 and 10) from one another. The northern panel closure in
7 the BRAGFLO grid represents two sets (in series) of four panel closures (in parallel) that lie
8 between the northern edge of the waste region and the shafts.

9 It is assumed in the modeling that the DRZ above the concrete monolith will heal and quickly
10 attain a state of relatively low permeability. However, it is also assumed that if pressures exceed
11 the fracture initiation pressure (~ 0.2 MPa above lithostatic), the DRZ and anhydrite MB
12 materials that intersect the waste room can fracture and allow gas or brine to circumvent the
13 panel closures by flowing around the concrete monolith. This possibility is included in the
14 implementation of the panel closures in the BRAGFLO by replacing the concrete monolith
15 material with MB material everywhere the monolith intersects and cuts through the MBs. This
16 implementation is appropriate even at low pressures because the permeability range of the
17 concrete and the MBs is nearly equivalent. In addition, fracturing is considered in these grid
18 elements at high pressures, allowing fluids to flow and simulating the consequence of fractures
19 extending around the monolith.

20 The representation of panel closures used in the CRA-2004 PABC has not changed and this
21 representation continues to be used in the CRA-2009 PA (see Figure MASS-6 and Appendix PA-
22 2009, Section PA-4.2.8). Additional information on panel closure effects on repository
23 performances can be seen in the CRA-2004 BRAGFLO Analysis Package (Stein and Zelinski
24 2003a and 2003b).

1 **MASS-20.0 Summary of Clay Seam G Modeling Assumptions**

2 One of the changes to the repository design since the CCA is the raising of the repository horizon
3 in the southern half of the waste panels. Specifically, Panels 3, 4, 5, 6, and 9 will be excavated at
4 an elevation approximately 2.4 m above the level of Panels 1, 2, 7, 8, and 10 and the operations
5 and experimental areas. This change in horizon will bring the roof of the raised rooms to the
6 level of the Clay Seam G. The change is expected to improve roof conditions and enhance
7 operations and mine safety. The DOE submitted a planned change request to the EPA describing
8 the change and arguing that it would have minimal impact on long-term repository performance
9 (Triay 2000). The EPA responded to the change request in a letter (Marcinowski 2000) in which
10 they agreed with the DOE that the effects on long-term performance would be minimal. The
11 modeling assumptions used to represent this change are described in the CRA-2004, Appendix
12 PA, Attachment MASS, Section MASS-20.0. No changes were made to these assumptions since
13 the CRA-2004 PA. These assumptions have also been used in the CRA-2009 PA.

MASS-21.0 Evaluation of Waste Structural Impacts, Emplacement and Homogeneity

Waste-related modeling assumptions have not changed from those used in the CRA-2004 PABC. During the development of the CCA PA, the DOE choose to assume random placement of TRU waste in the WIPP, and developed conceptual and numerical models accordingly. The EPA reviewed these models and their results and determined that the DOE had adequately modeled random placement of waste in the disposal system. Since the CCA, additional information about the waste and its emplacement has emerged, requiring the assumption of random placement to be reevaluated. The waste inventory estimates were updated since the CCA PA (see the CRA-2004, Appendix TRU WASTE and Leigh, Trone, and Fox 2005 for the CRA-2004 PABC waste updates), resulting in different estimates of important waste components, such as CPR materials. Additionally, the CCA PA assumed that all waste could be modeled as if the waste was emplaced in 55-gallon (gal) drums. However, the DOE is emplacing waste using several different types of waste containers, including standard waste boxes and pipe overpacks. Waste has been shipped to WIPP in campaigns from the generator sites, resulting in waste emplacement that appears inconsistent with the representation of the waste as a homogeneous material. Finally, the DOE is emplacing waste types, such as supercompacted waste, that were not considered in the CCA inventory (U.S. Department of Energy 2002).

Many important waste characteristics, such as the radionuclide content and the mass of CPR materials, are directly incorporated in PA by means of waste material parameters. These parameters have been updated with the inventory updates (see Leigh and Trone 2005b, and Leigh, Trone, and Fox 2005) and thus were represented in the CRA-2004 PABC and the CRA-2009 PA. However, the PAs for compliance applications have not specifically accounted for heterogeneity in waste materials or in waste containers. At the INL, for instance, debris waste is volume-reduced by supercompaction, resulting in a very dense waste form containing a high concentration of CPR material. In addition, the Pu residues from the Rocky Flats Environmental Technology Site were packaged in pipe overpacks, which are more rigid than the typical 55-gal drum assumed in the CCA. Additionally, in accordance with the requirements of 40 CFR § 194.24(d) (U.S. Environmental Protection Agency 2004), all PAs have assumed that waste is emplaced in a random or homogeneous manner. Actual waste emplacement is determined by the availability of waste at generator sites and the shipping schedules. Pipe overpacks occupy about 43% of the containers emplaced in Panel 1, suggesting that actual emplacement will not be statistically random.

As a result of this new information and these changes, the DOE performed analyses (Hansen et al. 2003) to determine if the modeling assumptions used in PA continue to adequately represent the waste. The analysis reported in Hansen et al. (2003) focused on potential effects of supercompacted waste and waste in pipe overpacks on repository performance. Both waste types are structurally stiffer than the generic waste model used in the CCA PA, and the supercompacted waste in particular has high concentrations of CPR materials. The analysis began with a systematic reevaluation of the baseline FEPs to identify specific components of PA that could be affected by supercompacted waste. The reassessment concluded that the FEPs “screened in” were adequate to represent the variety of waste types and containers, and that none of the “screened out” FEPs should be reconsidered for implementation. The FEPs assessment

1 concluded that creep closure of the repository, chemical conditions of the waste, gas generation
2 models, and waste mechanical properties could be affected by heterogeneities in the waste
3 materials and waste containers. In addition, the DOE determined that the assumption of random
4 waste emplacement should be reevaluated.

5 Analysis of creep closure of waste-filled rooms, accounting for several types of waste materials
6 and packaging, indicated that a wider range of long-term porosities could occur than that
7 established in the CCA, given the uncertainties about the structural integrity of waste packages
8 and their spatial arrangement in the repository (Park and Hansen 2003). For this reason, the
9 analysis in Hansen et al. (2003) treated creep closure as an uncertain variable. Sensitivity
10 analysis showed that this additional uncertainty did not significantly affect the results of PA.

11 Chemical conditions were also reexamined under a range of possible waste arrangements. The
12 assessment found that, regardless of actual waste emplacement, the MgO would still be sufficient
13 to maintain desired chemical conditions. Moreover, the constituents of supercompacted waste
14 would not alter the reactions that determine chemical equilibrium and, consequently, no changes
15 to An solubilities or to the gas-generation models were warranted to account for waste
16 heterogeneity. This topic was addressed during the second recertification in response to
17 comment G-12, in which the EPA requested that the DOE address potential effects of
18 heterogeneous waste loading based on the assumption of homogeneous chemical conditions.
19 The DOE's response indicated that the chemical conditions assumptions adequately addressed
20 nonrandom waste loading (Piper 2004). This was again addressed during the evaluation of the
21 MgO excess factor change from 1.67 to 1.20 (Reyes 2008). No changes were made to the
22 chemical conditions model as a result of these investigations.

23 Supercompacted waste contains elevated amounts of CPR materials relative to other waste
24 streams, and the future arrangement of this waste in the WIPP repository is uncertain. Thus, the
25 analysis treated the spatial distribution of CPR materials as uncertain. However, sensitivity
26 analysis demonstrated that uncertainty in the spatial distribution and quantity of CPR materials
27 had little effect on PA results. This was also shown in an analysis performed during the 2004
28 recertification while responding to an EPA request for additional information (Response to
29 Comment G-12, Dunagan, Hansen, and Zelinski 2004).

30 The representation of the waste properties was also considered; however, it was determined that
31 no changes to permeability, shear strength, or tensile strength were warranted. Based on this
32 evaluation, no changes to the models for DBRs were necessary.

33 DBRs as a consequence of a drilling intrusion are calculated with the assumption of random
34 waste emplacement in the repository. In addition, releases by spallings, DBR, and long-term
35 radionuclide transport assume that radionuclides are homogeneously distributed throughout the
36 waste. A sensitivity analysis determined that PA results are not greatly affected by the
37 assumption of random waste emplacement or by the assumption that radionuclides are
38 homogeneously distributed.

39 Based on the analysis reported in Hansen et al. (2003), the DOE concluded that:

- 1 1. Explicit representation of the specific features of supercompacted waste and of waste in pipe
2 overpacks, such as structural rigidity, was not warranted in modeling, since PA results were
3 relatively insensitive to the effects of such features.
 - 4 2. PA results were not affected significantly by the assumption of nonrandom waste
5 emplacement and the representation of these waste types as a homogeneous material.
- 6 Homogeneity issues were also addressed in response to another EPA comment during the CRA-
7 2004 completeness review. The EPA questioned in comment C-23-10 whether negating
8 container-scale variability was a valid assumption for spillings calculations (Cotsworth 2004).
9 In the CRA-2004 PA, spillings releases were calculated using the average radioactivity in all
10 CH-TRU waste streams. An analysis in Vugrin (2004) compared spillings results using three
11 randomly sampled waste streams against results using the average radioactivity over all CH-TRU
12 waste streams. The analysis concluded that the calculation of spillings releases is not
13 significantly affected by waste-scale variability.
- 14 The DOE continues to assume in PA that waste is randomly emplaced in the WIPP repository.
15 The CRA-2009 PA continues to use the same waste-related modeling approaches as the CRA-
16 2004 PABC.

1 **MASS-22.0 References**

- 2 Amyx, J.W., D.M. Bass, Jr., and R.L. Whiting. 1960. *Petroleum Reservoir Engineering,*
3 *Physical Properties.* New York: McGraw.
- 4 Anderson, M.P., and W.W. Woessner. 1992. *Applied Groundwater Modeling: Simulation of*
5 *Flow and Advective Transport.* New York: Academic Press.
- 6 Bear, J. 1972. *Dynamics of Fluid in Porous Media.* New York: Elsevier.
- 7 Beauheim, R.L. 1997. Memorandum to Palmer Vaughn (Subject: Revisions to Castile Brine
8 Reservoir Parameter Packages). 16 January 1997. ERMS 244699. Sandia National
9 Laboratories, Albuquerque, NM.
- 10 Berglund, J.W. 1992. *Mechanisms Governing the Direct Removal of Wastes from the Waste*
11 *Isolation Pilot Plant Repository Caused by Exploratory Drilling.* SAND92-7295. ERMS
12 223946. Albuquerque: Sandia National Laboratories.
- 13 Berglund, J.W. 1996. Memorandum to B.M. Butcher (Subject: Effective Shear Resistance to
14 Erosion TAUFAIL). 28 October 1996. ERMS 247189. Sandia National Laboratories, Carlsbad,
15 NM.
- 16 Caporuscio, F., J. Gibbons, C. Li, and E. Oswald. 2003. *Salado Flow Conceptual Models Final*
17 *Peer Review Report* (March). ERMS 526879. Carlsbad, NM: Carlsbad Area Office.
- 18 Carlsbad Area Office Technical Assistance Contractor (CTAC). 1997. *Expert Elicitation on*
19 *WIPP Waste Particle Diameter Size Distribution(s) During the 10,000-Year Regulatory Post-*
20 *Closure Period* (Final Report, June 3). ERMS 541365. Carlsbad, NM: U.S. Department of
21 Energy.
- 22 Christian-Frear, T.L., and S.W. Webb. 1996. *The Effect of Explicit Representation of the*
23 *Stratigraphy on Brine and Gas Flow at the Waste Isolation Pilot Plant.* SAND94-3173. WPO
24 37240. Albuquerque: Sandia National Laboratories.
- 25 Clayton, D.J. 2007. Memorandum to E. Vugrin, M. Lee, and D. Kessel (Subject: Corrections to
26 Input Files for DBR PABC Calculations). 6 June 2007. ERMS 546311. U.S. Department of
27 Energy, Sandia National Laboratories, Carlsbad, NM.
- 28 Clayton, D.J. 2008. *Analysis Plan for the Performance Assessment for the 2009 Compliance*
29 *Recertification Application* (Revision 1). AP-137. ERMS 547905. Carlsbad, NM: Sandia
30 National Laboratories.
- 31 Cotsworth, E. 2004. Letter to R.P. Detwiler (1 Enclosure). 20 May 2004. ERMS 535554. U.S.
32 Environmental Protection Agency, Office of Air and Radiation Washington, DC.
- 33 Cotsworth, E. 2005. Letter to I. Triay (1 Enclosure). 4 March 2005. ERMS 538858. U.S.
34 Environmental Protection Agency, Office of Air and Radiation, Washington, DC.

- 1 Davies, P.B. 1991. *Evaluation of the Role of Threshold Pressure in Controlling Flow of Waste-*
2 *Generated Gas into Bedded Salt at the Waste Isolation Pilot Plant.* SAND90-3246. WPO
3 26169. Albuquerque: Sandia National Laboratories.
- 4 Davies, P.B., S.W. Webb, and E.D. Gorham. 1992. Memorandum to B.M. Butcher, J.
5 Schreiber, and P. Vaughn (Subject: Feedback on “PA Modeling Using BRAGFLO—1992”; 4
6 Attachments). 14 July 1992. Sandia National Laboratories, Albuquerque, NM.
- 7 Dunagan, S. 2007. *Parameter Problem Report (PPR, 2007-001* (1 Attachment). Form NP 9-2-
8 2. ERMS 545481. Carlsbad, NM: Sandia National Laboratories.
- 9 Dunagan, S., C. Hansen, and W. Zelinski. 2004. *Effects of Increasing Cellulosics, Plastics and*
10 *Rubbers on WIPP Performance Assessment.* ERMS 535941. Carlsbad, NM: Sandia National
11 Laboratories.
- 12 Fox, B. 2008. *Parameter Summary Report for CRA-2009* (Revision 0). ERMS 549747.
13 Carlsbad, NM: Sandia National Laboratories.
- 14 Freeze, G.A., K.W. Larson, and P.B. Davies. 1995. *Coupled Multiphase Flow and Closure*
15 *Analysis of Repository Response to Waste-Generated Gas at the Waste Isolation Pilot Plant*
16 *(WIPP).* SAND93-1986. ERMS 229557. Albuquerque: Sandia National Laboratories.
- 17 Garner, J., and C. Leigh. 2005. *Analysis Package for PANEL, CRA-2004 Performance*
18 *Assessment Baseline Calculation* (Revision 0). ERMS 540572. Carlsbad, NM: Sandia National
19 Laboratories.
- 20 Gorham, E., R. Beauheim, P. Davies, S. Howarth, and S. Webb. 1992. “Recommendations to
21 PA on Salado Formation Intrinsic Permeability and Pore Pressure for 40 CFR 191 Subpart B
22 Calculations, June 15, 1992.” *Preliminary Performance Assessment for the Waste Isolation Pilot*
23 *Plant, December 1993* (pp. A-49 through A-65). Volume 3, Model Parameters. SAND92-
24 0700/3. Albuquerque: Sandia National Laboratories.
- 25 Guzowski, R.V. 1990. *Preliminary Identification of Scenarios for the Waste Isolation Pilot*
26 *Plant, Southeastern New Mexico.* SAND90-7090. WPO 25771. Albuquerque: Sandia National
27 Laboratories.
- 28 Hansen, F.D., M.K. Knowles, T.W. Thompson, M. Gross, J.D. McLennan and J.F. Schatz. 1997.
29 *Description and Evaluation of a Mechanically Based Conceptual Model for Spall.* SAND97-
30 1369. Albuquerque: Sandia National Laboratories.
- 31 Hansen, C.W., C. Leigh, D. Lord, and J. Stein. 2002. *BRAGFLO Results for the Technical*
32 *Baseline Migration.* ERMS 523209. Carlsbad, NM: Sandia National Laboratories.
- 33 Hansen, C.W., L.H. Brush, M.B. Gross, F.D. Hansen, B. Park, J.S. Stein, and T.W. Thompson.
34 2003. *Effects of Supercompacted Waste and Heterogeneous Waste Emplacement on Repository*
35 *Performance* (Revision 1). ERMS 532475. Carlsbad, NM: Sandia National Laboratories.

- 1 Hansen, F.D., T.W. Pfeifle, and D.L. Lord. 2003. *Parameter Justification Report for DRSPALL*
2 (Revision 0). SAND2003-2930. Carlsbad, NM: Sandia National Laboratories.
- 3 Herrick, C.G., M. Riggins, B.Y Park, and E.D. Vugrin. 2007. *Recommendation for the Lower*
4 *Limit of the Waste Shear Strength (Parameter BOREHOLE:TAUFAIL)* (Rev. 1). ERMS 546343.
5 Carlsbad, NM: Sandia National Laboratories.
- 6 Hunter, R.L. 1989. *Events and Processes for Constructing Scenarios for the Release of*
7 *Transuranic Waste from the Waste Isolation Pilot Plant, Southeastern New Mexico*. SAND89-
8 2546. WPO 27731. Albuquerque: Sandia National Laboratories.
- 9 Ismail, A.E. 2007a. Memorandum to File (Subject: Revised Porosity Estimates for the DRZ).
10 10 April 2007. ERMS 545755. U.S. Department of Energy, Sandia National Laboratories,
11 Carlsbad, NM.
- 12 Ismail, A.E. 2007b. Memorandum to E.D. Vugrin, M.Y. Lee, and D.S. Kessel (Subject: Errors
13 in Input Files for NUTS for CRA-2004 PABC Calculations; 1 Attachment). 11 June 2007.
14 ERMS 546200. U.S. Department of Energy, Sandia National Laboratories, Carlsbad, NM.
- 15 James, S.J., and J. Stein. 2002. *Analysis Plan for the Development of a Simplified Shaft Seal*
16 *Model for the WIPP Performance Assessment*. AP-094. ERMS 524958. Carlsbad, NM: Sandia
17 National Laboratories.
- 18 James, S., and J. Stein. 2003. *Analysis Report for Development of a Simplified Shaft Seal Model*
19 *for the WIPP Performance Assessment* (Rev. 1). ERMS 525203. Carlsbad, NM: Sandia
20 National Laboratories.
- 21 Julien, P.Y. 1998. *Erosion and Sedimentation*. Cambridge: Cambridge University Press.
- 22 Kanney, J.F. 2003. *Hydrogen Gas as a Surrogate for Waste-Generated Gas Physical Properties*
23 *in BRAGFLO*. Technical Memorandum. ERMS 532900. Sandia National Laboratories,
24 Carlsbad, NM.
- 25 Kirchner, T. 2008. *Generation of the LHS Samples for the AP-137 Revision 0 (CRA-09) PA*
26 *Calculations*. ERMS 547971. Carlsbad, NM: Sandia National Laboratories.
- 27 Kirkes, R. 2007. *Evaluation of the Duration of Direct Brine Release in WIPP Performance*
28 *Assessment* (Revision 0). ERMS 545988. Carlsbad, NM: Sandia National Laboratories.
- 29 Leigh, C., J. Kanney, L. Brush, J. Garner, G. Kirkes, T. Lowery, M. Nemer, J. Stein, E. Vugrin,
30 S. Wagner, and T. Kirchner 2005. *2004 Compliance Recertification Application Baseline*
31 *Performance Assessment Calculation* (Revision 0). ERMS 541521. Carlsbad, NM: Sandia
32 National Laboratories.
- 33 Leigh, C.D., and J.R. Trone. 2005a. *Calculation of Radionuclide Inventories for Use in NUTS*
34 *in the Performance Assessment Baseline Calculation* (Revision 0). ERMS 539644. Carlsbad,
35 NM: Sandia National Laboratories.

- 1 Leigh, C., and J. Trone. 2005b. *Calculation of the Waste Unit Factor for the Performance*
2 *Assessment Baseline Calculation* (Revision 0). ERMS 539613. Carlsbad, NM: Sandia National
3 Laboratories.
- 4 Leigh, C., J. Trone, and B. Fox. (2005). *TRU Waste Inventory for the 2004 Compliance*
5 *Recertification Application Performance Assessment Baseline Calculation* (Revision 0). ERMS
6 541118. Carlsbad, NM: Sandia National Laboratories.
- 7 Long, J. 2006. *Installation of Open VMS 8.2-1 on the WIPP Alpha Cluster and Regression*
8 *Testing* (March 16). ERMS 542680. Carlsbad, NM: Sandia National Laboratories.
- 9 Lord, D.L. 2003. *Justification for Particle Diameter and Shape Factor used in DRSPALL*.
10 ERMS 531477. Carlsbad, NM: Sandia National Laboratories.
- 11 Lord, D., D. Rudeen, and C. Hansen. 2003. *Analysis Package for DRSPALL: Compliance*
12 *Recertification Application*. Part I—Calculation of Spall Volumes. ERMS 532766. Carlsbad,
13 NM: Sandia National Laboratories.
- 14 Marcinowski, F. 2000. Letter to Dr. I. Triay, Manager. 11 August 2000. U.S. Environmental
15 Protection Agency, Office of Air and Radiation, Washington, DC.
- 16 Marietta, M.G., S.G. Bertram-Howery, D.R. Anderson, K.F. Brinster, R.V. Guzowski, H.
17 Iuzzolino, and R.P. Rechard. 1989. *Performance Assessment Methodology Demonstration:*
18 *Methodology Development for Evaluating Compliance with EPA 40 CFR 191, Subpart B, for the*
19 *Waste Isolation Pilot Plant*. SAND89-2027. WPO 25952. Albuquerque: Sandia National
20 Laboratories.
- 21 Mendenhall, F.T., and W. Gerstle. 1993. Memorandum to Distribution (Subject: WIPP
22 Anhydrite Fracture Modeling). 6 December 1993. SWCF-A: W.B.S. 1.1.7.1. WPO 39830.
23 Sandia National Laboratories, Albuquerque, NM.
- 24 Monod, J. 1949. “The Growth of Bacterial Cultures.” *Annual Review of Microbiology*, vol. 3
25 (October): 371–94.
- 26 National Institute of Standards and Technology (NIST). 1992. *NIST Thermophysical Properties*
27 *of Hydrogen Mixtures Database (SUPERTRAPP) User’s Guide* (Version 1.0). Gaithersburg,
28 MD: U.S. Department of Commerce, National Institute of Standards and Technology, Standard
29 Reference Data Program.
- 30 Nemer, M.B. 2007. Memorandum to WIPP SNL Records Center (Subject: Effects of not
31 Including Emplacement Materials in CPR Inventory on Recent PA Results). 8 February 2007.
32 ERMS 545689. U.S. Department of Energy, Sandia National Laboratories, Carlsbad, NM.
- 33 Nemer, M., and D. Clayton. 2008. *Analysis Package for Salado Flow Modeling, 2009*
34 *Compliance Recertification Application Calculation*. ERMS 548607. Carlsbad, NM: Sandia
35 National Laboratories.

- 1 Parchure, T.M., and A.J. Mehta. 1985. "Erosion of Soft Sediment Deposits." *Journal of*
2 *Hydraulic Engineering*, vol. 111: 1308–26.
- 3 Park, B., and F.D. Hansen. 2003. *Analysis Report for Determination of the Porosity Surfaces of*
4 *the Disposal Room Containing Various Waste Inventories for WIPP PA (Revision 0)*. ERMS
5 533216. Albuquerque: Sandia National Laboratories.
- 6 Partheniades, E. 1965. Erosion and Deposition of Cohesive Soils. *Journal of the Hydraulics*
7 *Division, Proceedings of the American Society of Civil Engineers*, vol. 91. no. HY1: 105–39.
- 8 Piper, L.L. 2004. Letter to U.S. Environmental Protection Agency (Subject: Partial Response
9 to Environmental Protection Agency (EPA) September 2, 2004, Letter on Compliance
10 Recertification Application, 6th Response Package, Comment G-12). 23 December 2004.
11 Carlsbad Field Office, Carlsbad, NM.
- 12 Rechard, R.P., W. Beyeler, R.D. McCurley, D.K. Rudeen, J.E. Bean, and J.D. Schreiber. 1990.
13 *Parameter Sensitivity Studies of Selected Components of the Waste Isolation Pilot Plant*
14 *Repository/Shaft System*. SAND89-2030. WPO 25946. Albuquerque: Sandia National
15 Laboratories.
- 16 Reeves, M., D.S. Ward, N.D. Johns, and R.M. Cranwell. 1986. *Theory and Implementation for*
17 *SWIFT II, The Sandia Waste-Isolation Flow and Transport Model for Fractured Media, Release*
18 *484*. SAND83-1159. NUREG/CR-3328. Albuquerque: Sandia National Laboratories.
- 19 Reyes, J. 2008. Letter to D.C. Moody 5 Attachments). 11 February 2008. U.S. Environmental
20 Protection Agency, Office of Air and Radiation, Washington, DC.
- 21 Sandia National Laboratories (SNL). 2002. *Technical Baseline Reports: WBS 1.3.5.3,*
22 *Compliance Monitoring; WBS 1.3.5.4, Repository Investigations; Milestone RII30 (July 31)*.
23 ERMS 523189. Carlsbad, NM: Sandia National Laboratories.
- 24 Schreiber, J.D. 1997. *WIPP PA User's Manual for BRAGFLO (Version 4.10, May)*. ERMS
25 245238. Carlsbad, NM: Sandia National Laboratories.
- 26 Stein, J.S. 2003a. *Analysis Plan for Calculations of Direct Brine Releases : Compliance*
27 *Recertification Application*. AP-104. ERMS 528743. Carlsbad, NM: Sandia National
28 Laboratories.
- 29 Stein, J.S. 2003b. Memorandum to D. Kessel (Subject: Correlation Between Bulk
30 Compressibility and Porosity in the Castile Brine Pocket as Modeled in BRAGFLO). April 2003.
31 ERMS 527293. Sandia National Laboratories: Carlsbad, NM.
- 32 Stein, J., and W. Zelinski. 2003a. *Analysis Plan for the Testing of a Proposed BRAGFLO Grid*
33 *to be Used for the Compliance Recertification Application Performance Assessment*
34 *Calculations*. AP-106. ERMS 525236. Carlsbad, NM: Sandia National Laboratories.

- 1 Stein, J.S., and W. Zelinski. 2003b. *Analysis Report for: Testing of a Proposed BRAGFLO Grid*
2 *to be used for the Compliance Recertification Application Performance Assessment*
3 *Calculations*. ERMS 526868. Carlsbad, NM: Sandia National Laboratories.
- 4 Telander, M.R., and R.E. Westerman. 1997. *Hydrogen Generation by Metal Corrosion in*
5 *Simulated Waste Isolation Pilot Plant Environments*. SAND96-2538. Albuquerque: Sandia
6 National Laboratories.
- 7 Tierney, M.S. 1991. *Combining Scenarios in a Calculation of the Overall Probability*
8 *Distribution of Cumulative Releases of Radioactivity From the Waste Isolation Pilot Plant,*
9 *Southeastern New Mexico*. SAND90-0838. WPO 26030. Albuquerque: Sandia National
10 Laboratories.
- 11 Triay, I. 2000. Letter to Mr. F. Marcinowski, Director. June 26, 2000. U.S. Department of
12 Energy, Carlsbad Field Office, Carlsbad, NM.
- 13 U.S. Department of Energy (DOE). 1980. *Final Environmental Impact Statement, Waste*
14 *Isolation Pilot Plant* (October). 2 vols. DOE/EIS-0026. ERMS 238835 (vol. 1) and ERMS
15 238838 (vol. 2). Washington, DC: U.S. Department of Energy.
- 16 U.S. Department of Energy (DOE). 1996. *Title 40 CFR Part 191 Compliance Certification*
17 *Application for the Waste Isolation Pilot Plant* (October). 21 vols. DOE/CAO 1996-2184.
18 Carlsbad, NM: Carlsbad Area Office.
- 19 U.S. Department of Energy (DOE). 2002. *Assessment Of Impacts On Long-Term Performance*
20 *From Supercompacted Wastes Produced By The Advanced Mixed Waste Treatment Project*
21 (December 6). Carlsbad, NM: Carlsbad Area Office.
- 22 U.S. Department of Energy (DOE). 2004. *Title 40 CFR Part 191 Compliance Recertification*
23 *Application for the Waste Isolation Pilot Plant* (March). 10 vols. DOE/WIPP 2004-3231.
24 Carlsbad, NM: Carlsbad Field Office.
- 25 U.S. Environmental Protection Agency (EPA). 1993. “40 CFR Part 191: Environmental
26 Radiation Protection Standards for the Management and Disposal of Spent Nuclear Fuel, High-
27 Level and Transuranic Radioactive Wastes; Final Rule.” *Federal Register*, vol. 58 (December
28 20, 1993): 66398–416.
- 29 U.S. Environmental Protection Agency (EPA). 1996. “40 CFR Part 194: Criteria for the
30 Certification and Recertification of the Waste Isolation Pilot Plant’s Compliance with the 40
31 CFR Part 191 Disposal Regulations; Final Rule.” *Federal Register*, vol. 61 (February 9, 1996):
32 5223–45.
- 33 U.S. Environmental Protection Agency (EPA). 1998a. “40 CFR Part 194: Criteria for the
34 Certification and Recertification of the Waste Isolation Pilot Plant’s Compliance with the 40
35 CFR Part 191 Disposal Regulations: Certification Decision; Final Rule.” *Federal Register*, vol.
36 63 (May 18, 1998): 27353–406.

- 1 U.S. Environmental Protection Agency (EPA). 1998b. *Technical Support Document for 194.23:*
2 *Parameter Justification Report* (May). Washington DC: Office of Radiation and Indoor Air.
- 3 U.S. Environmental Protection Agency (EPA). 2004. “40 CFR Part 194: Criteria for the
4 Certification and Recertification of the Waste Isolation Pilot Plant’s Compliance with the
5 Disposal Regulations; Alternative Provisions” (Final Rule). *Federal Register*, vol. 69 (July 16,
6 2004): 42571–83.
- 7 U.S. Environmental Protection Agency (EPA). 2006. “40 CFR Part 194: Criteria for the
8 Certification and Recertification of the Waste Isolation Pilot Plant’s Compliance with the
9 Disposal Regulations: Recertification Decision” (Final Notice). *Federal Register*, vol. 71 (April
10 10, 2006): 18010–021.
- 11 Vaughn, P., M. Lord, and R. MacKinnon. 1995a. Memorandum to D.R. Anderson (Subject:
12 DR-6: Brine Puddling in the Repository due to Heterogeneities). 21 December 1995. SWCF-
13 A:1.1.6.3. WPO 30795. Sandia National Laboratories, Albuquerque, NM.
- 14 Vaughn, P., M. Lord, and R. MacKinnon. 1995b. Memorandum to D.R. Anderson (Subject:
15 DR-7: Permeability Varying with Porosity in Closure Regions). 21 December 1995. SWCF-
16 A:1.1.6.3. WPO 30796. Sandia National Laboratories, Albuquerque, NM.
- 17 Vaughn, P., M. Lord, and R. MacKinnon. 1995c. Memorandum to D. R. Anderson (Subject:
18 DR3: Dynamic Closure of the North End and Hallways). 28 September 1995. SWCF-
19 A:1.1.6.3. WPO 30798. Sandia National Laboratories, Albuquerque, NM.
- 20 Vaughn, P., M. Lord, and R. MacKinnon. 1995d. Memorandum to D.R. Anderson (Subject:
21 DR-2: Capillary Action [Wicking] within the Waste Materials). 21 December 1995. SWCF-
22 A:1.1.6.3. WPO 30793. Sandia National Laboratories, Albuquerque, NM.
- 23 Vaughn, P., M. Lord, and R. MacKinnon. 1995e. Memorandum to D.R. Anderson (Subject:
24 S-6: Dynamic Alteration of the DRZ/Transition Zone). 28 September 1995. WPO 30798.
25 Sandia National Laboratories, Albuquerque, NM.
- 26 Vaughn, P., M. Lord, J. Garner, and R. MacKinnon. 1995. Memorandum to D.R. Anderson
27 (Subject: FEP Screening Issue GG-1). 10 October 1995. ERMS 230791. Sandia National
28 Laboratories, Albuquerque, NM.
- 29 Vugrin, E.D. 2004. Memorandum to David Kessel (Subject: Container-Scale Variability and
30 DRSPALL in response to C-23-10, Rev 1). 15 November 2004. ERMS 537870. Sandia
31 National Laboratories, Carlsbad, NM.
- 32 Wagner, S.W. 2008. *Reassessment of MONPAR Analysis for Use in the 2009 Compliance*
33 *Recertification Application*. ERMS 548948. Carlsbad, NM: Sandia National Laboratories.
- 34 Wallace, M. 1996. “Summary Memo of Record for NS-11: Subsidence Associated with
35 Mining Inside or Outside the Controlled Area.” *Records Package for Screening Effort NS-11:*
36 *Subsidence Associated with Mining Inside or Outside the Controlled Area* (November 21) (pp.
37 1–28). ERMS 412918. Albuquerque: Sandia National Laboratories.

- 1 Wang, H.F, and M.P. Anderson. 1982. *Introduction to Groundwater Modeling: Finite*
2 *Difference and Finite Element Methods*. New York: Academic Press.
- 3 Wang, Y. 1997. Memorandum to Margaret Chu (Subject: Estimate WIPP Waste Particle Sizes
4 on Expert Elicitation Results: Revision 1). 5 August 1997. ERMS 246936. Albuquerque:
5 Sandia National Laboratories.
- 6 Webb, S. 1995. Memorandum to D.R. Anderson (Subject: DR-1:3D Room Flow Model with
7 Dip). 30 May 1995. SWCF-A:1.1.6.3. WPO 22494. Albuquerque: Sandia National
8 Laboratories.
- 9 WIPP Performance Assessment. 1991. *Preliminary Comparison with 40 CFR Part 191,*
10 *Subpart B, for the Waste Isolation Pilot Plant, December 1991*. 4 vol. SAND91-0893/1-4.
11 Albuquerque: Sandia National Laboratories.
- 12 WIPP Performance Assessment. 1993. *Preliminary Performance Assessment for the Waste*
13 *Isolation Pilot Plant, December 1992*. Volume 4: Uncertainty and Sensitivity Analyses for 40
14 CFR 191, Subpart B. SAND92-0700/4. ERMS 223528. Albuquerque: Sandia National
15 Laboratories.
- 16 WIPP Performance Assessment. 2003a. *Design Document for DRSPALL Version 1.00* (Version
17 1.10, September). ERMS 529878. Carlsbad, NM: Sandia National Laboratories.
- 18 WIPP Performance Assessment. 2003b. *Verification and Validation Plan and Validation*
19 *Document for DRSPALL Version 1.00* (Version 1.00, September). ERMS 524782. Carlsbad,
20 NM: Sandia National Laboratories.